

# **HYDROTHERMAL SYNTHESIS OF SOLID STATE MATERIALS AND CRYSTALLOGRAPHY**

**By**

**Bahar ÖZMEN**

**A Dissertation Submitted to the  
Graduate School in Partial Fulfillment of the  
Requirements for the Degree of**

**MASTER OF SCIENCE**

**Department: Chemistry  
Major: Chemistry**

**İzmir Institute of Technology  
İzmir, Turkey**

**July, 2004**

We approve the thesis of Bahar **ÖZMEN**

**Date of Signature**

-----  
Assist.Prof.Dr. Mehtap EANES  
Supervisor  
Department of Chemistry

23.07.2004

-----  
Assist.Prof.Dr. Talal SHAHWAN  
Department of Chemistry

23.07.2004

-----  
Assist.Prof.Dr. Sedat **ÇELEB**□  
Department of Chemistry, E.U.

23.07.2004

-----  
Prof.Dr. Levent ARTOK  
Head of Chemistry Department

23.07.2004

## ACKNOWLEDGEMENTS

I would like to extend special appreciation to my research advisor, Asst. Prof. Mehtap Eanes, for her support, patience and guidance throughout my master research program.

I would like to thank to TÜBİTAK and İYTE Research Fund for their financial support to our Solid State Chemistry Laboratory. I also thank to Jim A. Ibers for sending the chemicals from Northwestern University and Don Van Derveer from Clemson University for his help in crystallography.

Finally, I wish to express my thanks to all of my friends in İYTE for their help and also special thanks to my father, M. Ali Özmen and my mother Ismahan Özmen for their patience, support and endless love to me during my thesis and all of my life.

## ABSTRACT

The structure solution of the new polyoxovanadate compound ( $[\text{V}_{16}\text{O}_{31}(\text{OH})_7]\text{Cl} \cdot 15\text{H}_2\text{O}$ ), has been done by the SHELX crystal solution software. The compound was synthesized solvothermally at  $170^\circ\text{C}$  in the Northwestern University. The compound crystallizes in the space group  $\text{C}_{2/c}$  of the monoclinic system with eight formula units in a cell of dimensions  $a = 18.070(2) \text{ \AA}$ ,  $b = 17.414(2) \text{ \AA}$ ,  $c = 15.1154(18) \text{ \AA}$ ,  $\beta = 97.696(2)^\circ$ ,  $V = 4713.8(10) \text{ \AA}^3$  ( $T = 153 \text{ K}$ ). The structure is composed of vanadium-oxygen clusters encapsulating  $\text{Cl}^-$  anion. Each of the V centers has square pyramidal geometry coordinated by five O atoms. The 16 ( $\text{VO}_5$ ) units are fused together through common edges to form ( $\text{V}_{16}\text{O}_{38}$ ) cage with  $\text{Cl}^-$  anion in the middle.

The single crystals of the  $[\text{Ni}(\text{en})_3(\text{VO}_3)_2]$  compound was synthesized by hydrothermal method.  $[\text{Ni}(\text{en})_3(\text{VO}_3)_2]$  compound is in the crystal system of hexagonal and in the space group  $\text{P6}_1$ . The unit cell parameters are  $a = 8.9940(13) \text{ \AA}$ ,  $b = 8.9940(13) \text{ \AA}$ ,  $c = 34.001(7) \text{ \AA}$  and  $\alpha = 90^\circ$ ,  $\beta = 90^\circ$ ,  $\gamma = 120^\circ$ . The structure is composed of  $\text{VO}_4$  tetrahedras which are joined with others by sharing corners into infinite chains running along the c axis. The complex cation  $[\text{Ni}(\text{en})_3]^{2+}$  are located between the chains. The chain in the compound has a repetitive sequence of 12-nuclear corner-sharing tetrahedras. The compound was synthesized at  $160^\circ\text{C}$  for 3 days in the steel reaction autoclaves which have PTFE (Polytetrafluoroethylene) cups in them.

By the reaction of the reactants  $\text{NH}_4\text{VO}_3$ ,  $\text{Ni}(\text{NO}_3)_2 \cdot 6\text{H}_2\text{O}$ ,  $\text{H}_3\text{BO}_3$  with  $\text{H}_2\text{O}$  the orange crystals of  $\text{NH}_4(\text{V}_3\text{O}_8)$  and the green unknown crystals were obtained at  $160^\circ\text{C}$  in 3 days..

By the reaction of the reactants  $\text{NaVO}_3$ ,  $\text{Ni}(\text{NO}_3)_2 \cdot 6\text{H}_2\text{O}$ ,  $\text{H}_3\text{BO}_3$ ,  $\text{NH}_2\text{CH}_2\text{CH}_2\text{NH}_2$ , with the solvents  $\text{H}_3\text{PO}_4$  and  $\text{H}_2\text{O}$  the green bulk unknown crystals were obtained at  $160^\circ\text{C}$  in 3 days.

By the reaction of the reactants  $\text{B}_4\text{K}_2\text{O}_7 \cdot \text{H}_2\text{O}$ ,  $\text{KVO}_3$  with  $\text{H}_2\text{O}$  and  $\text{NH}_2\text{CH}_2\text{CH}_2\text{NH}_2$  brown unknown crystals were obtained at  $170^\circ\text{C}$  in 5 days.

We have also done some crystal growth studies in our laboratory. There are several known compounds as  $\text{CoV}_2\text{O}_6(\text{H}_2\text{O})_2$ ,  $\text{Co}(\text{VO})_2(\text{PO}_4)_2(\text{H}_2\text{O})_4$ , which were also synthesized in our laboratory with good yields. These crystals were synthesized with other methods and characterized. However we were able to grow their crystals in good shape and size by using hydrothermal method.  $\text{CoV}_2\text{O}_6(\text{H}_2\text{O})_2$  was obtained from the

reaction of  $\text{NH}_4\text{VO}_3$ ,  $\text{Co}(\text{NO}_3)_2 \cdot 6\text{H}_2\text{O}$  and  $\text{H}_3\text{BO}_3$ . The compound crystallizes in the space group  $P_{nma}$  (62) of the orthorhombic system in a cell of dimensions,  $a = 5.572 \text{ \AA}$ ,  $b = 10.70 \text{ \AA}$ ,  $c = 11.860 \text{ \AA}$ ,  $\alpha = \beta = \gamma = 90^\circ$ ,  $V = 707.69 \text{ \AA}^3$ .  $\text{CoV}_2\text{O}_6(\text{H}_2\text{O})_2$  was prepared in a steel autoclave by using ultra pure water as the solvent and heated at  $160^\circ\text{C}$  for 3 days. Red prism shaped crystals of the reported materials were obtained with the orange plates in a red-orange crystalline powder. The single crystal XRD results showed that the orange plates have the formula of  $\text{NH}_4(\text{V}_3\text{O}_8)$  which crystallizes in the space group  $P_{21/m}$  (11) of the monoclinic system in a cell of dimensions  $a = 4.999 \text{ \AA}$ ,  $b = 8.423 \text{ \AA}$ ,  $c = 7.849 \text{ \AA}$ ,  $\alpha = 96.426^\circ$ ,  $V = 328.44 \text{ \AA}^3$ . It has been shown that  $\text{CoV}_2\text{O}_6(\text{H}_2\text{O})_2$  compound can also be synthesized by the reaction of  $\text{NaVO}_3$ ,  $\text{GeO}_2$ ,  $\text{H}_3\text{BO}_3$ ,  $\text{CoCl}_2 \cdot 6\text{H}_2\text{O}$  with  $\text{H}_2\text{O}$  as the solvent.

The green crystals of the compound  $\text{Co}(\text{VO})_2(\text{PO}_4)_2(\text{H}_2\text{O})_4$  were synthesized from the reaction of  $\text{V}_2\text{O}_5$ ,  $\text{H}_2\text{C}_2\text{O}_4 \cdot 2\text{H}_2\text{O}$ ,  $\text{CoCl}_2 \cdot 6\text{H}_2\text{O}$  with the solvents  $\text{H}_3\text{PO}_4$  and  $\text{H}_2\text{O}$  at  $160^\circ\text{C}$  for 3 days. The compound crystallizes in the space group  $I_{4/mmm}$  (139) of the tetragonal system in a cell of dimensions  $a = 6.264 \text{ \AA}$ ,  $c = 13.428 \text{ \AA}$ ,  $\alpha = \beta = \gamma = 90^\circ$ ,  $V = 526.88 \text{ \AA}^3$ .

## ÖZ

Yeni bir poliokzovanadat bileşiği,  $([V_{16}O_{31}(OH)_7]Cl \cdot 15H_2O)$ 'nin yapı çözümü SHELX kristal çözüm programı ile yapılmıştır. Bileşik, solvotermal olarak Northwestern Üniversitesi'nde  $170\text{ }^{\circ}C$  'de sentezlenmiştir. Bileşik, monoklinik sistemde,  $C_{2/c}$  space grubunda,  $a = 18.070 (2)\text{ \AA}$ ,  $b = 17.414 (2)\text{ \AA}$ ,  $c = 15.1154 (18)\text{ \AA}$ ,  $\beta = 97.696 (2)^{\circ}$ ,  $V = 4713.8 (10)\text{ \AA}^3$  ( $T = 153\text{ K}$ ) hücre boyutlarında sekiz formül birimindedir. Yapı içinde  $Cl^{-}$  anyonu olan vanadium-oksijen kürelerinden oluşmaktadır. Her vanadium merkezi beş oksijen atomu tarafından çevrelenen kare piramit geometrisine sahiptir. 16  $(VO_5)$  birimleri birbirine ortak köşelerinden ortada  $Cl^{-}$  anyonu olan  $(V_{16}O_{38})$  kafesi oluşturacak şekilde bağlanmaktadır.

$[Ni(en)_3(VO_3)_2]$  bileşiminin tek kristalleri hidrotermal metotla sentezlenmiştir.  $[Ni(en)_3(VO_3)_2]$  bileşiği hegzagonal kristal sisteminde ve  $P6_1$  space grubundadır. Birim hücre boyutları  $a = 8.9940 (13)\text{ \AA}$ ,  $b = 8.9940 (13)\text{ \AA}$ ,  $c = 34.001 (7)\text{ \AA}$  and  $\alpha = 90^{\circ}$ ,  $\beta = 90^{\circ}$ ,  $\gamma = 120^{\circ}$ 'dir. Yapı c eksenini boyunca sonsuz zincirler halinde köşelerini paylaşarak diğerleriyle birleşen  $VO_4$  tetrahedrelerinden oluşmuştur.  $[Ni(en)_3]^{2+}$  kompleks katyonu zincirler arasında yerleşmiştir. Bileşikteki zincir, 12 köşe-paylaşan tetrahedra'lerden oluşmuştur. Bileşik  $160\text{ }^{\circ}C$ ' de, 3 günde içinde PTFE (Politetrafloroetilen) kaplar olan çelik reaksiyon otoklavlarında sentezlenmiştir.

$NH_4VO_3$ ,  $Ni(NO_3)_2 \cdot 6H_2O$ ,  $H_3BO_3$  reaktantları  $H_2O$  ile reaksiyonundan  $NH_4(V_3O_8)$ 'in turuncu kristalleri ve bilinmeyen yeşil kristaller  $160\text{ }^{\circ}C$ ' de 3 günde elde edildi.

$NaVO_3$ ,  $Ni(NO_3)_2 \cdot 6H_2O$ ,  $H_3BO_3$ ,  $NH_2CH_2CH_2NH_2$  reaktantları  $H_3PO_4$  ve  $H_2O$  çözümleri ile reaksiyonundan yansıyan halindeki bilinmeyen yeşil kristaller  $160\text{ }^{\circ}C$ ' de 3 günde elde edildi.

$B_4K_2O_7 \cdot H_2O$ ,  $KVO_3$  reaktantları  $H_2O$  ve  $NH_2CH_2CH_2NH_2$  çözümleri ile reaksiyonundan bilinmeyen kahverengi kristaller  $170\text{ }^{\circ}C$ ' de 5 günde elde edildi.

Ayrıca laboratuvarımızda kristal büyütme çalışmaları da yapılmıştır. Laboratuvarımızda da iyi verimlerde sentezlenmiş olan  $CoV_2O_6(H_2O)_2$ ,  $Co(VO)_2(PO_4)_2(H_2O)_4$  gibi birçok bilinen bileşik vardır. Bu kristaller diğer yöntemlerle sentezlenmiş ve karakterize edilmiştir. Yine de biz, hidrotermal metotla bunları

kristallerini iyi çekil ve boyutlarda büyütebildik.  $\text{NH}_4\text{VO}_3$ ,  $\text{Co}(\text{NO}_3)_2 \cdot 6\text{H}_2\text{O}$  ve  $\text{H}_3\text{BO}_3$ 'in reaksiyonundan  $\text{CoV}_2\text{O}_6(\text{H}_2\text{O})_2$  elde edilmiştir. Bileşik, birim hücre boyutları  $a = 5.572 \text{ \AA}$ ,  $b = 10.70 \text{ \AA}$ ,  $c = 11.860 \text{ \AA}$ ,  $\alpha = \beta = \gamma = 90^\circ$ ,  $V = 707.69 \text{ \AA}^3$  olan ortorombik sistemin  $P_{nma}$  (62) space grubunda kristallenir.  $\text{CoV}_2\text{O}_6(\text{H}_2\text{O})_2$ , çözgen olarak ultra saf su kullanılarak ve  $160^\circ\text{C}$ 'de 3 gün sütilerak çelik bir otoklavda hazırlanmıştır. Turuncu-kırmızı kristallin toz içinde turuncu tabakalar yanında bildirilen bileşimin kırmızı prizmatik şekilli kristalleri elde edilmiştir. Tek kristal XRD sonuçları turuncu tabakaların monoklinik sistemde  $P_{21/m}$  (11) space grubunda kristallenen, hücre boyutları  $a = 4.999 \text{ \AA}$ ,  $b = 8.423 \text{ \AA}$ ,  $c = 7.849 \text{ \AA}$ ,  $\alpha = 96.426^\circ$ ,  $V = 328.44 \text{ \AA}^3$  olan  $\text{NH}_4(\text{V}_3\text{O}_8)$  formülünde olduğunu gösterdi.  $\text{CoV}_2\text{O}_6(\text{H}_2\text{O})_2$ 'in,  $\text{NaVO}_3$ ,  $\text{GeO}_2$ ,  $\text{H}_3\text{BO}_3$ ,  $\text{CoCl}_2 \cdot 6\text{H}_2\text{O}$ 'ların reaksiyonu ve su çözgeni ile de sentezlenebileceği gösterildi.

$\text{Co}(\text{VO})_2(\text{PO}_4)_2(\text{H}_2\text{O})_4$  bileşiminin yeşil kristalleri,  $\text{V}_2\text{O}_5$ ,  $\text{H}_2\text{C}_2\text{O}_4 \cdot 2\text{H}_2\text{O}$ ,  $\text{CoCl}_2 \cdot 6\text{H}_2\text{O}$ 'nin reaksiyonunda çözgen olarak  $\text{H}_3\text{PO}_4$  ve  $\text{H}_2\text{O}$  kullanılarak  $160^\circ\text{C}$ 'de 3 günde sentezlendi. Bileşik, hücre boyutları  $a = 6.264 \text{ \AA}$ ,  $c = 13.428 \text{ \AA}$ ,  $\alpha = \beta = \gamma = 90^\circ$ ,  $V = 526.88 \text{ \AA}^3$  olan tetragonal sistemin  $I_{4/mmm}$  (139) space grubunda kristallenir.

# TABLE OF CONTENTS

LIST OF FIGURES .....	x
LIST OF TABLES.....	xii
CHAPTER 1 INTRODUCTION .....	1
1.1 Crystal Growth.....	11
1.1.1 Solid Growth Techniques .....	14
1.1.2 Vapor Phase Growth.....	14
1.1.3 Solution Growth .....	14
1.1.3.1 Growth of single crystals by Hydrothermal Method .....	15
CHAPTER 2 EXPERIMENTAL METHOD .....	17
2.1 The Physical Analyzing Methods of Solids.....	17
2.1.1 Diffraction Techniques .....	18
2.1.1.1 X-ray Powder Diffraction .....	18
2.1.1.2 Single Crystal X-ray Diffraction.....	20
2.1.2. Microscopic Techniques.....	21
2.1.2.1. Electron Microscopy.....	21
2.2 Experimental Procedure.....	23
2.2.1 Reaction Autoclaves .....	23
2.2.2 Sample Selection .....	25
2.2.3 Hydrothermal Procedure.....	25
CHAPTER 3 POLYOXOMETALATES (POM's) .....	27
3.1 Introduction.....	27
3.2 Application Areas of Polyoxometalates .....	28
3.3 Magnetism of Polyoxometalates.....	29
3.4 Experimental .....	30
3.4.1 Synthesis .....	30
3.4.2 Crystallography.....	31
3.4.3 Results and Discussion .....	31
CHAPTER 4 VANADIUM COMPOUNDS .....	38
4.1. Introduction.....	38
4.1.1 Influences of Organic Compounds on Vanadium Oxide Structures .....	43
4.2 Most Synthesized Metal Oxides .....	47



4.3 Synthesis and Characterization of $[\text{Ni}(\text{en})_3(\text{VO}_3)_2]$ .....	47
4.3.1 Introduction .....	47
4.3.2 Experimental Procedure .....	48
4.3.2.1 Synthesis .....	48
4.3.2.2 X-Ray Crystallographic Analyses.....	51
4.4 Some Other Synthesized Vanadium Compounds.....	56
4.5 Crystal Growth Experiments .....	66
CHAPTER 5 CONCLUSION .....	70
REFERENCES .....	73

## LIST OF FIGURES

<b>Figure 1.1</b> Phase Diagram of Water.....	5
Figure 1.2 Volume (density) / temperature dependence of water.....	6
Figure 1.3 Pressure / temperature dependence of water for different degrees of filling of the reaction vessel.....	7
Figure 1.4 A grown single crystal of octahedron.....	12
Figure 1.5 A grown single crystal of rhomboidal dodecahedron.....	13
Figure 1.6 Schematic hydrothermal bomb used for crystal growth.....	16
Figure 2.1 Diagram of an X-ray Diffractometer. Various parts .....	19
Figure 2.2 An acid digestion bomb, its parts and a PTFE cup with its cover.....	24
Figure 2.3 Carbolite CWF 1100 oven.....	26
Figure 2.4 A mounted single crystal to a capillary with epoxy .....	26
Figure 3.1 Scheme of the bridges most commonly found in polyoxovanadates (IV).30	30
Figure 3.2. Unit cell picture of $[(V_{16}O_{31}(OH)_7)Cl.15H_2O]$ ,.....	33
Figure 3.3 $(V_{16}O_{38})$ cage and its polyhedral view.....	34
Figure 4.1 Coordination polyhedra adopted by V (V)- and V (IV)- oxo species ....	39
Figure 4.2 Polyhedral representations of the structures of the $[V_2O_7]^{4-}$ and $[V_4O_{12}]^{4-}$ clusters; ball and stick and polyhedral views of the structure of $[V_{10}O_{28}]^{4-}$ .....	40
Figure 4.3 Views of the one-dimensional vanadate chains of (a) $KVO_3$ and (b) $\square$ $NaVO_3$ .....	41
Figure 4.4 The network structure of $V_2O_5$ .....	42
Figure 4.5 The structure of $VO_2$ .....	42
Figure 4.6 Schematic representations of various modes of involvement of organonitrogen components in vanadium oxide materials .....	46
Figure 4.7 A single crystal of $[Ni(en)_3(VO_3)_2]$ .....	49
Figure 4.8 SEM EDAX graph of the $[Ni(en)_3(VO_3)_2]$ compound.....	50
Figure 4.9 The X-ray powder of the $[Ni(en)_3(VO_3)_2]$ compound.....	50
Figure 4.10 Unit cell picture of $[Ni(en)_3(VO_3)_2]$ .....	55
Figure 4.11 $[Ni(en)_3]^{2+}$ complex between vanadium chains.....	56
Figure 4.12 Yellow rod shaped crystals.....	57
Figure 4.13 SEM EDX graph of the yellow rod crystals.....	58

<b>Figure 4.14</b> The X-ray powder peaks of the rod shaped yellow crystals.....	58
Figure 4.15 Two different views of the green octahedral shaped crystals.....	60
Figure 4.16 SEM EDX graph of the green octahedral shaped crystals .....	61
Figure 4.17 XRD peaks of the green octahedral shaped crystals .....	61
Figure 4.18 A bulk of dark green crystals together in a light green pure powder ...	62
Figure 4.19 The SEM EDX peaks of the bulk of dark green crystals .....	63
Figure 4.20 The X-ray powder peaks of the bulk of dark green crystals.....	64
Figure 4.21 Two different views of the brown octahedral shaped single crystals...	65
Figure 4.22 The SEM EDX results of the brown octahedral shaped crystals.....	66
Figure 4.23 Red prism shaped crystals .....	68
Figure 4.24 Orange plate shaped crystals .....	68
Figure 4.25 A green square shaped crystal .....	69

## LIST OF TABLES

<b>Table 1.1</b> Critical Temperatures and Boiling Points for Selected Solvents .....	8
Table 1.2 Applications for $\alpha$ -quartz .....	15
Table 3.1 Crystal Data and Structure Refinements for $[V_{16}O_{31}(OH)_7]Cl$ .....	35
Table 3.2 Selected Bond Distances .....	35
Table 3.3 Atomic Parameters and Isotropic Displacement Parameters .....	36
Table 3.4 Bond Valences .....	37
Table 4.1 Selected examples and applications of inorganic oxides [38] .....	45
Table 4.2 Crystallographic Data for $[Ni(en)_3(VO_3)_2]$ .....	52
Table 4.3 Bond lengths [ $\text{\AA}$ ] and angles [ $^\circ$ ] for $[Ni(en)_3(VO_3)_2]$ .....	53
Table 4.4 Atomic coordinates ( $\times 10^4$ ) and equivalent isotropic displacement parameters for $[Ni(en)_3(VO_3)_2]$ .....	54

# CHAPTER 1

## INTRODUCTION

Most of the inorganic solids are prepared by the reaction of a solid with another solid, a liquid (melt) or a gas, usually at high temperatures. Many “solid/solid” reactions are actually “solid / liquid” reactions, because at the high reaction temperature one of the solid can melt to form liquid phase. Therefore it is sometimes difficult to determine what physical phases are involved in a given reaction.

In synthesizing multicomponent solid materials the oldest and the most common method is the direct reaction of solid components at high temperatures which is called the “Ceramic Method”. Because solids do not react with each other at room temperature, high temperatures are required to reach the suitable reaction rates. Under high reaction temperatures (between 600 °C and 1500 °C) of traditional solid state synthesis most of the inorganic phases are unstable [1].

The reason for using high temperature mainly is that if there is a large difference between the structure of the starting material and the product, all bonds in the starting material must be broken, and atoms must migrate before new bonds can be formed [2]. This diffusion makes the reactions impossibly slow unless very high temperatures are used. As a rule of thumb two-thirds of the melting temperature of one component are enough to activate diffusion sufficiently and hence to enable the solid state reaction [1]. Most compounds made at high temperature are very thermodynamically stable. Because thermodynamically stable known phases cannot be avoided, the synthesis of new materials becomes difficult at high temperatures [3]. However synthesis of new kinetically stable or metastable compounds can be possible if the proper reaction conditions can be found. Preparation of kinetically stabilized compounds requires relatively lower temperatures because the desired compounds are not thermodynamically stable.

It is clear that the reaction between two solids may not occur even if thermodynamic considerations favor product formation. There are three important factors that influence the rate of reaction between solids, the area of contact between the

reacting solids and hence their surface areas, the rate of nucleation of the product phase, rates of diffusion of ions through the various phases, and especially through the product phase.

When applying the ceramic method first the starting compounds should be fine-grained in order to maximize surface areas and hence reaction rates. The powder is pressed into a pellet to provide an intimate contact between grains which are the single crystals in a polycrystalline aggregate.

Carbonates, nitrates and other oxy salts that decompose at high temperatures are often employed in traditional solid state reactions. The heating program depends very much on the form and reactivity of the reactants.

For solid state reactions in general, it is necessary to take some caution in choosing a suitable container material which is chemically inert to the reactants at high temperatures. For the synthesis of metal oxides generally platinum, silica, stabilized zirconia and alumina containers are used, while graphite containers are preferred for sulfides and other chalcogenides or pnictides. If one of the components is volatile or sensitive to the atmosphere, the reaction is carried out in sealed evacuated capsules.

The advantages of solid state reactions are availability of the precursors and low cost for powder production on the industrial scale. Ceramic method has several disadvantages; i.e. undesirable phases may be formed, such as  $\text{BaTi}_2\text{O}_5$  during the synthesis of  $\text{BaTiO}_3$ ; the homogeneous distribution of dopants is sometimes difficult to achieve and there are only limited possibilities for an in-situ monitoring of the progress of the reaction. Instead physical measurements such as X-ray diffraction are periodically carried out. Because of this difficulty, mixtures of reactants and products are frequently obtained. Separation of the desired product from these mixtures is generally difficult, if not impossible. In many systems the reaction temperature cannot be raised as high as necessary for reasonable reaction rates, because one or more components of the reacting mixture may volatilize. In order to overcome some of these problems, particularly to reduce the reaction times and to increase the diffusion rates, it is necessary to optimize the critical parameters such as decreasing particle sizes and increasing surface area by grinding, performing the solid-state reactions in molten fluxes or high temperature solvents [1].

There are a number of ways in order to prepare new kinetically stable solid state compounds at low temperatures. The most common techniques are chemical vapor

transport (CVT), or the use of molten salts (or flux growth) to dissolve reactants at a relatively low temperature [2, 3].

In the CVT method the reactants are basically held in a silica tube and kept under an atmosphere of a gaseous transporting agent. Reactants are placed at one end of the tube which is sealed and then put inside a furnace so that a temperature gradient exists inside the tube. Reactant and gases combine forming products which subsequently decompose at the other end of the tube, yielding crystalline deposits. This method is very convenient for the growth of a single crystal or the purification of a compound. Chemical vapor transport works well for binary compounds, but is not very efficient for more complex systems.

Flux growth is a promising technique for preparation of more complicated systems. The most used molten salts are metal halides, metal chalcogenides and alkali metal polychalcogenides. Melts are high temperature liquids, thus some solubilization of solid starting materials occurs and recrystallization takes place on subsequent cooling of the melt.

The term “hydrothermal” means any reaction done in water above 100 °C whereas the reactions done above the critical values of water (374 °C and 221 bar) are known as “supercritical” [4].

During and after the World War II (WW II) a major turning point occurred by the synthesis of ultrapure single crystals of  $\alpha$ -quartz. There were growing demands for large amounts of materials of increasing purity, so the natural supplies would not be sufficient after the war. For quartz demands grew because of the very low dielectric loss route for microwave applications [4]. Due to these reasons large single crystals of  $\alpha$ -quartz were grown in the laboratory [5]. It was found that  $\alpha$ -quartz was only stable below the temperature 580 °C, and silicate melts were so viscous that they formed glasses before crystallization. Then controlled growth of  $\alpha$ -quartz under hydrothermal conditions was tried. After WW II in the Bell labs single crystals up to 1 kg in mass were grown successfully [6]. Then several companies started to grow  $\alpha$ -quartz commercially over 500,000 kg each year.

The first man-made hydrothermal chemical reaction was performed by Bunsen in 1830s. He succeeded the growth of barium carbonate from superheated water in a thick walled glass tube.

During the 19th century scientists developed two important things. The first was the Morey vessel which can be hydrothermally treated. The autoclaves were lined with inert metals as silver, gold or platinum in the pressures up to 800 bar [4]. The second was the Bridgeman seal invented by Percy Bridgeman. It allowed solutions at higher pressures up to 7 kbar.

The other important types of crystals grown commercially by using hydrothermal techniques are  $\text{AlPO}_4$ ,  $\text{KTiOPO}_4$  and emeralds [4]. Crystal growth of these known materials was done because of their important electronic applications.

The most interesting supercritical solvent is water which has 374 °C and 221 bar of critical values (Fig. 1.1). As water comes near its critical point, its dielectric constant and viscosity decrease where its mobility increases. The low viscosity and high mobility of supercritical water allows it to be excellent reaction media for the synthesis of unique metastable phases and the growth of good quality single crystals for analysis. Superheated water has the ability to solvate reagents and is a good reaction media for better transport and for intermixing of reagents. It also leads to well-crystallized solids. However water is a bit polar that most metal oxoanions are soluble in higher than 1 %. The hydrothermal reactions are done between the temperatures 100 °C and 374 °C however at this interval water carries its characteristics as the same as its supercritical state.

Hydrothermal synthesis has a number of advantages over conventional synthetic methods. For example it allows synthesis of compounds with elements in oxidation states which are often difficult to achieve, and the formation of low temperature, metastable compounds [7].



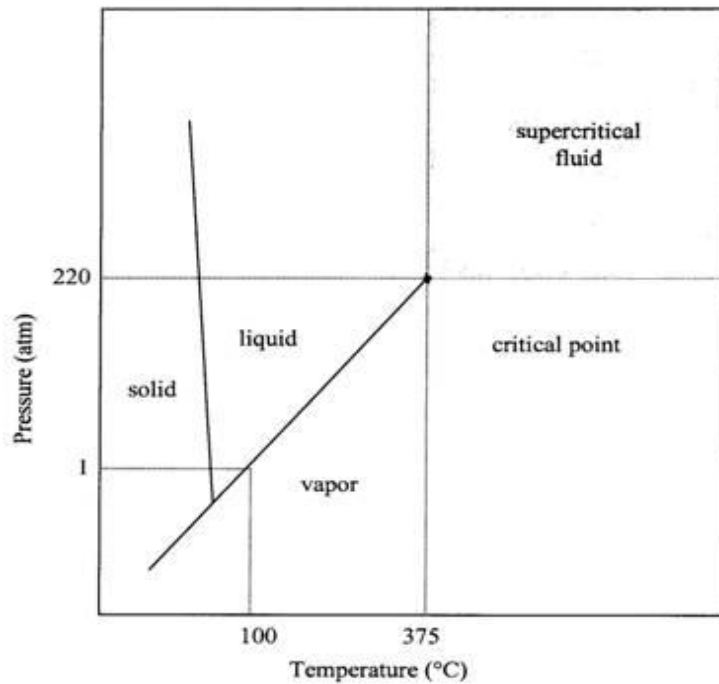


**Figure 1.1** Phase Diagram of Water

Water has a critical role in the natural mineral synthesis. Many silicates, aluminates, phosphates, carbonates, oxides and sulfosalts were formed in the form of hydrothermal fluid [4]. There are many examples of crystals that are synthesized by hydrothermal method like quartz variants such as amethyst, citrine, smoky quartz, ruby, sapphire and emerald [1].

Water is the most used solvent in solvothermal processes, because it is a pressure transmitting medium. Therefore the P-V-T diagram of water at high temperatures and pressures are important (Fig 1.2, Fig 1.3). By increasing the temperature, the viscosity and the polarity i.e. the dielectric constant of water decreases but these properties increase with higher pressures.

Because the hydrothermal reactions are carried out in closed vessels, the P-T relations of water at constant volume are very important.

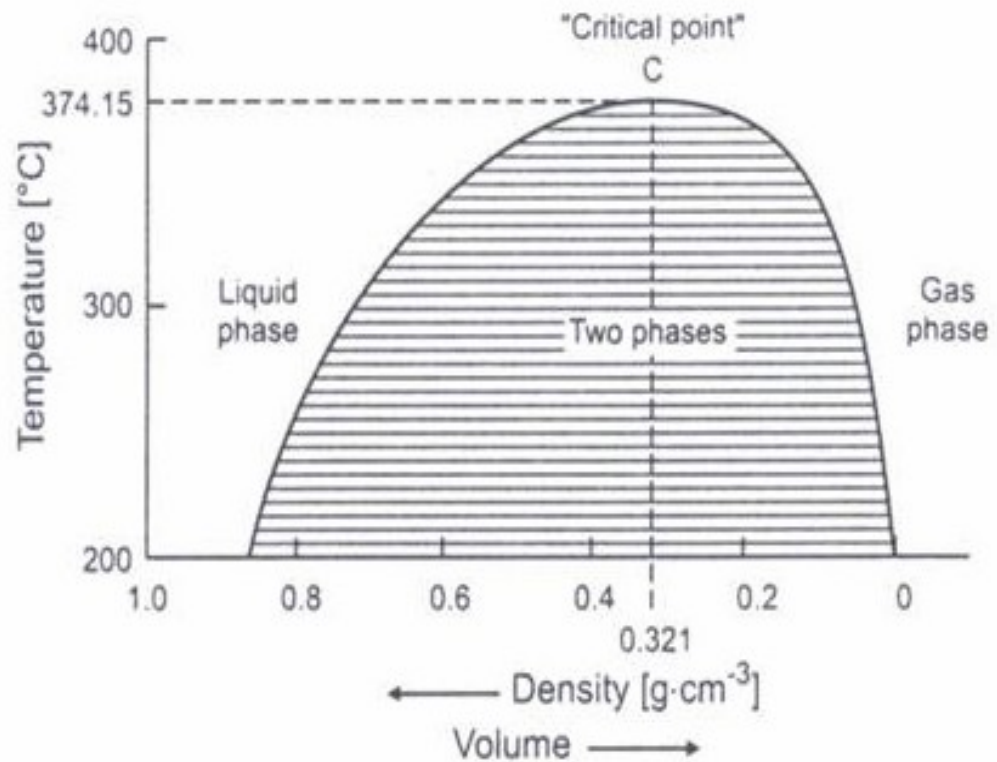


**Figure 1.2** Volume (density) / temperature dependence of water

In the two phase region, the liquid and vapor phases coexist in equilibrium. With increasing temperature, the density of the liquid phase decreases while the density of gas phase increases. At the critical point C (with critical temperature of 374.15 °C and a critical density of 0.321 g cm<sup>-3</sup>) the densities and other properties of both phases are the same. Above the critical temperature only one phase exists which is supercritical or fluid phase.

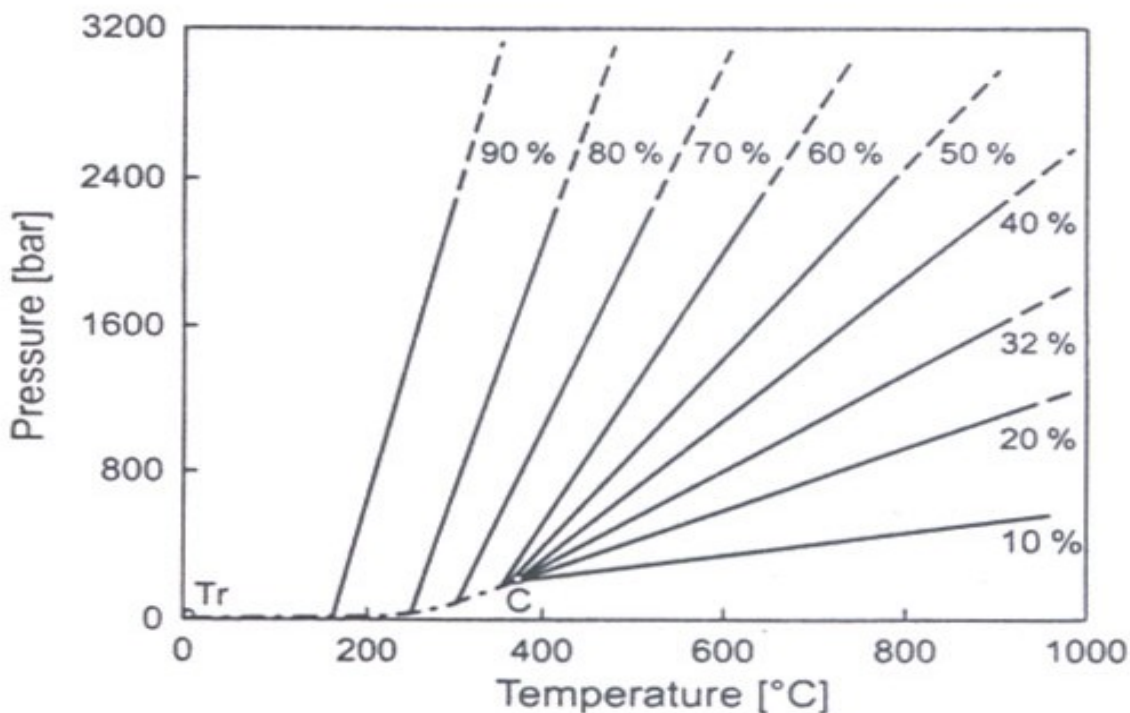


**Figure 1.3** Pressure / temperature dependence of water for different degrees of filling of the reaction vessel

At the triple point (Tr) solid, liquid and gas phases coexist in equilibrium. The curve between Tr and C represents the saturated steam curve at which liquid and gaseous phase coexist. At pressures below this curve liquid water is absent and the vapor phase is not saturated. Above this curve liquid water is under compression and the vapor phase is absent.

Hydrothermal crystallization is performed with degrees of filling of 32 % and more successfully above 65 % with pressures of 200-3000 bar.

For most hydrothermal synthesis moderate temperature range of 100-300 °C at the corresponding low solution vapor pressures are applied. The solution consisting of oxides, hydroxides and salts of the corresponding metal is placed into an autoclave. Reaction mixture is then heated at the desired temperature, the starting materials react or transform through dissolution and precipitate to the stable compound. After cooling the autoclave the product can be isolated by filtration and after washing several times with water and acetone to obtain the pure product [1]. Several parameters such as the stoichiometries of reactants, pH of the reaction media, temperature, reaction time and

the types of coligands in the reaction media play important role in the application of hydrothermal method [8].

In addition to water, there are great number of nonaqueous solvents that can be used as superheated fluids (Table 1.1) [9]. Solvothermal processes occur above the boiling point and 1 bar in liquid media. Water and ammonia are the most common solvothermal reaction liquids used in hydrothermal synthesis and ammonothermal synthesis respectively. Nature is a model for solvothermal methods, many geologically important minerals are grown by this way. Crystallization by solvothermal synthesis is directly an isothermal equilibrium reaction. The insoluble compounds under ambient conditions are dissolved and after hydrothermal treatment a stable crystalline phase is formed [1].

Table 1.1 Critical Temperatures and Boiling Points for Selected Solvents

Solvent	T <sub>c</sub> (°C)	bp (°C)
Water	374.1	100
Ammonia	132.3	-33.5
Ethylenediamine	320	116.9
Chlorine	144	-34.6
Hydrogenchloride	51.4	-85.05
Carbon dioxide	31.3	-78.5
Sulfur dioxide	157.8	-10
Carbon disulfide	279	46.5
Hydrogen sulfide	100.4	-60.2
Ethanol	243	78.3
Methylamine	156.9	48
Methanol	240	65

Ammonia is a good medium for inorganic synthesis in high pressure fluids. It can solubilize many inorganic reagents even though it is less polar and less protic than water. Use of ammonia as solvent is an advantage for a chemist due to its access to

compounds that are unstable in water. Ammonia is mostly an undeveloped area for chemists. It is a gas in room temperature and creates extremely higher pressures than water at high temperatures and fill ratios. Its critical values are lower than water's  $T_c = 132\text{ }^{\circ}\text{C}$ ,  $P_c = 113.5\text{ bar}$ . At higher temperatures the use of acidic  $\text{NH}_3$  is an unexplored area. [4].

Methanol is another solvent which has its critical point at  $240\text{ }^{\circ}\text{C}$  and  $81\text{ bar}$ . Although its polarity is smaller than water, it can solubilize most inorganic compounds. Also it does not attack quartz under basic conditions as water does.

$\text{CO}_2$  is an effective medium for the synthesis of several inorganic and organometallic complexes.  $\text{CO}_2$  is used as a solvent for inorganic aerogels [10]. Because  $\text{CO}_2$  is very nonpolar, it can not solubilize many inorganic compounds. However  $\text{CO}_2$  /water mixture is an effective solvent, because this combination forms carbonic acid which is polar enough to solve inorganic solids. Several metal carbonates have been prepared by this method [4, 11].

Strong hydrohalic acids (5-15 M) are used as solvents by Rabenau and co-workers as solvents [4]. They are able to solve and recrystallize gold, silver and platinum [12] as pure elements. They are very useful because quartz is unattacked by these acids up to  $500\text{ }^{\circ}\text{C}$ .

As it is proved that in the synthesis of inorganic substances solvothermal methods have great potential. Although most geochemists and crystal growers concentrated on known compounds, the optoelectronic and microporous properties of inorganic compounds took their effort to search for new ones.

The ability of supercritical fluids (SCF's) to solubilize and transport low concentrations of reactive intermediates leads to a large number of exciting novel compounds. Acidity, concentration, relative stoichiometry, solvent polarity, reaction time and temperature effect the route of the reactions in SCF's.

As SCF's themselves do not solubilize reactants very well compared to the liquid state and the solvent properties of pure water is not sufficient to dissolve substances for crystallization and also the density of the fluid is lower than the ambient liquid "mineralizers" are required [4]. A mineralizer is any compound which is added to the aqueous solution to speed up crystallization, and to increase the solubility of solute by forming soluble species [1]. It is a small, ionic, soluble molecule that attacks the starting material. The important thing is that they are not needed in high concentrations.

One or two percent is enough to observe the reactivity. The mobility of small species and precipitation of the product dissolve more reactants.

In the syntheses of inorganic compounds by solvothermal method the type and concentration of the mineralizer are very important. Widely used mineralizers are hydroxides, halides, sulfides and chlorides of alkali metals, polychalcogenides, carbonates and bicarbonates, alkali salts of weak acids e.g.  $\text{Na}_2\text{CO}_3$ ,  $\text{Na}_3\text{BO}_3$ ,  $\text{Na}_2\text{S}$  [4].

Polyoxometalates are the polyoxoanions of the early transition elements, usually vanadium, molybdenum, and tungsten. They were first investigated in the last third of 19<sup>th</sup> century. However within the last four or five decades modern experimental techniques have begun to reveal the range of structure and reactivity of these substances. There are some unanswered questions about the limits to composition, size and structure, metal incorporation, mechanisms of synthesis and reactivity of polyoxometalates. Although there are much research activities including practical applications of polyoxometalates, especially in heterogeneous and homogeneous catalysis, and in medicine, it is a pity to say that their potential in these and other areas remains poorly developed [13].

Two kinds of polyoxoanions are known today. The first one is the silicates, and oxoanions of neighbouring main-group elements and the second one is the early transition elements of groups 5 and 6. The polyoxoanion-forming elements are V, Nb, Ta (5 B group), Cr, Mo, W (6 B group), B, Si, Ge, P, As, Sb, S, Se, Te, and I. Although both types of polyoxoanions are in the structure of linked  $\text{MO}_n$  polyhedra ( $n = 4-6$ ), polyoxometalates are characterized by  $\text{MO}_6$  octahedra with short “terminal”  $\text{M} = \text{O}$  ( $d \sigma$ - $p \sigma$ ) bonds that tend to result in “closed” discrete structures with such bonds directed outwards. In contrast, the main group elements, especially phosphates and silicates, show open (cyclic) or polymeric structures based on linked  $\text{MO}_4$  tetrahedra [13].

The polyoxometalates have an extensive solution chemistry in both aqueous and nonaqueous solvents because of low surface charge densities resulting in weak anion-cation attractions (lattice energies) relative to cation solvation energies. Generally polyoxometalate anion surfaces contain both terminal ( $\text{M} = \text{O}$ ) and bridging ( $\text{M}-\text{O}-\text{M}$ ) oxygen atoms. According to the experiments and recent density functional calculations the bridging oxygens carry a greater negative charge and are protonated in preference to terminal oxygens [13-14].

One of the most important problems in the contemporary chemistry is the deliberate especially synthon-based synthesis of multifunctional compounds and materials with desirable or predictable properties such as mesoporosity (well defined cavities and channels), electronic and ionic transport, ferro- as well as ferrimagnetism, luminescence, and catalytic activity. Transition metal oxide-based compounds are of special interest in that respect. For example, the deeply colored, mixed-valence hydrogen molybdenum bronzes with their unusual property of high conductivity and wide range of composition-play an important role in technology, industrial chemical processes, and materials science. Their fields of application range from electrochemical elements, hydrogenation and dehydrogenation catalysts, superconductors, passive electrochromic display devices, to “smart” windows. Therefore the synthesis of such compounds or solids from pre-organized linkable building blocks (synthons) with well-defined geometries and well-defined chemical properties are of special interest [13].

## 1.1 Crystal Growth

The crystal growth is important for producing suitable single crystals for X-ray diffraction measurements. It has been kept general because growing crystals is very much an art, and for any particular substance the method to be chosen and the variations in its use must usually be decided on the basis of exploratory experiments. While initial attempts to grow crystals may be disappointing, it should not be surprising that a number of compounds that at first seemed incapable of producing satisfactory crystals did yield them when the proper conditions were found.

If a crystal is to be satisfactory for collecting X-ray diffraction data, the crystal must possess uniform internal structure and must be of proper size and shape. To fulfill the uniform internal structure, a crystal must be pure at the molecular, ionic or atomic level. It must be a single crystal in the usual sense, that is it should not be twinned [15] or composed of microscopic subcrystals. It should not be grossly fractured, bent or otherwise physically distorted. It need not, however, have particularly uniform or well-formed external faces [16].

The important application of the hydrothermal method began with the artificial production of bulk single crystals of quartz and with the synthesis of zeolites during late 1930s and 1940s. The hydrothermal method of crystal growth has several advantages. It

has critical importance for the technological efficiency in developing bigger, purer, and dislocation-free single crystals (Fig. 1.4, Fig. 1.5). The method has been widely accepted since 1960s and practically all inorganic species, starting from native elements to the most complex oxides, silicates, germanates, phosphates, chalcogenides, carbonates, and so on, have been obtained by this method. The technique is being employed on a large scale to prepare piezoelectric, magnetic, optic, ceramic and a host of other materials both as single crystals and polycrystalline materials. The hydrothermal technique, in contrast to other conventional techniques, offers several advantages:

- i. Compounds with elements in oxidation states that are difficult to obtain, especially important for transition metal compounds, can be obtained in a closed system by the hydrothermal method [e.g., ferromagnetic chromium (IV) oxide]
- ii. The hydrothermal method is also useful for the so-called low temperature phases, e.g.,  $\alpha$ -quartz,  $\alpha$ -berlinite, and others
- iii. For the synthesis of metastable compounds, such as subiodides of tellurium,  $\text{Te}_2\text{I}$ , the hydrothermal method is unique [17].

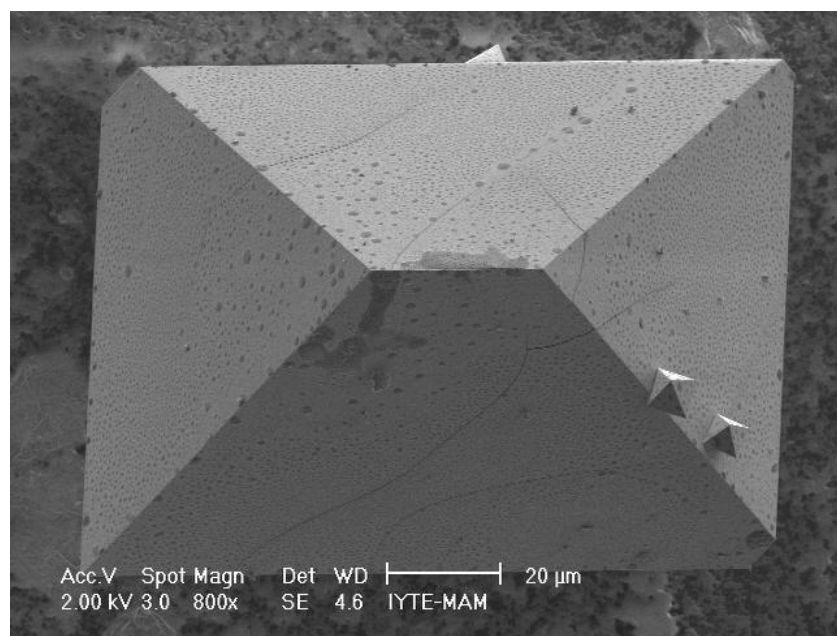


**Figure 1.4** A grown single crystal of octahedron



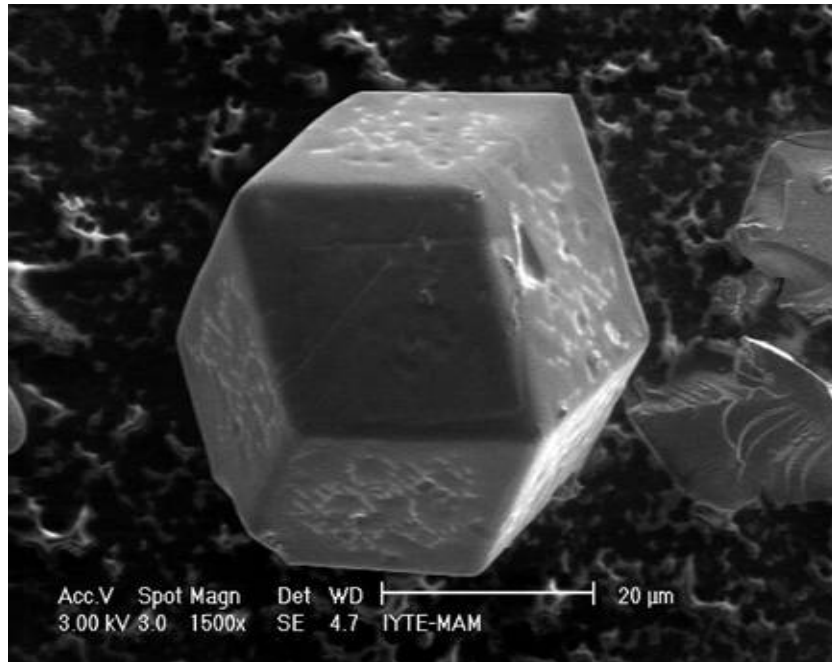


**Figure 1.5** A grown single crystal of rhomboidal dodecahedron

Commercial production of quartz and zeolites began during 1940s. In the passing years scientists began to search the crystallization of new phases which do not have the natural analogues. Moreover the search for the growth of some most complex inorganic single crystals which did not have analogues in nature began. During 1960s, there was a question about the search and growth of unknown compounds of photo-semiconductors, ferromagnets, lasers, piezo- and ferrielectrics, so the hydrothermal method gained greater attention. A large number of groups appeared in Europe, Asia and North America, and also the number of crystals obtained by hydrothermal method increased exponentially [17].

Crystals may be grown from solid, liquid (melt), vapor and solution phases although, usually, only the vapor and liquid phases give crystals of sufficient size to be used in applications or for property measurements. Main categories of crystal growth methods are, growth from the solid: S-S process involving solid-solid phase transition, growth from the melt: L-S process involving liquid-solid phase transition, growth from the vapor: V-S process involving vapor-solid phase transition and growth from solution.

### 1.1.1 Solid Growth Techniques

Require atomic diffusion. At normal temperatures such diffusion is usually very slow (except in the case of superionic materials where the small cation is quite mobile). Annealing and sintering - hot pressing are two important solid growth techniques.

### 1.1.2 Vapor Phase Growth

This method depends on the existence of reversible equilibrium between reactant A, transporting agent B, and gaseous product AB.



### 1.1.3 Solution Growth

In contrast to the other methods in which melts solidify to give crystals that have the same composition as the melt, precipitation from solution methods involve the growth of crystals from a solvent of different composition to the crystals. The major advantages of solution method are that it permits crystal growth at a temperature well below the melting point and isothermal conditions with slow growth rates give quality crystals of low defect concentration. The disadvantages of this method are its slow growth rate and contamination by the container or flux. The other types of this method are gel growth, flux growth, molten metal solution growth, organic solution growth, thermal freezing method (Bridgman-Stockbarger), zone melting method, flame fusion method (Verneuil method), Czochralski's method, flux pulling (top seeded solution growth-TSSG) and the aqueous solution growth methods (hydrothermal method) [18].

### 1.1.3.1 Growth of single crystals by Hydrothermal Method

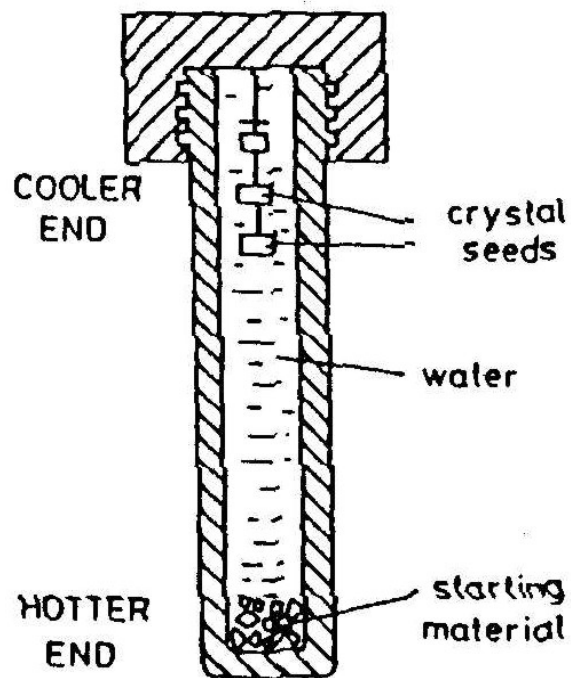
The hydrothermal technique has produced a wide variety of minerals and crystals, both in nature and in laboratory. In fact it is the only technique to synthesize some compounds as quartz, berlinite ( $\text{AlPO}_4$ ) and so on. However the method has some limitations as far as the size is concerned. Although berlinite, gallium berlinite and lithium tetraborate show many superior piezoelectric properties compared to  $\alpha$ -quartz, it is not possible to obtain them as large as  $\alpha$ -quartz crystals. Among the various crystalline forms of quartz  $\alpha$ -quartz which is stable below  $573^\circ\text{C}$  at atmospheric pressure, is the most popular and technologically very important (Table 1.2) [18].

Table 1.2 Applications for  $\alpha$ -quartz

Industrial equipment	Precision oscillators, optical fibers, dielectric materials, radio and cable communications, electronic applications, measurement equipment, pagers, security systems (alarms)...
Consumer equipment	Electronic hand calculators, watches, clocks, timers, cable TV's, color TV's, video recorders, RF converters, traneivers, radio equipment, microphones, electronic appliances, microcomputer and computer terminals, TV-game machines, telephones, copy machines...

The crucial point in the growth of single crystals by hydrothermal methods is adding a mineralizer. A mineralizer speeds up the crystallization of the solution. It mostly operates by increasing the solubility of the solute through the formation of soluble species that would not usually be present in the water. For instance the solubility of quartz in water at  $400^\circ\text{C}$  and 2 kbar is too small to permit the recrystallization of quartz. By adding a NaOH mineralizer, large quartz crystals may be grown (Fig 1.6). Quartz dissolves in the hottest part of the reaction vessel, is transported throughout the vessel and precipitated in cooler parts of the vessel where its solubility in water is lower. Quartz single crystals are used in many devices in radar and sonar as piezoelectric transducers, as monochromators in X-ray diffraction, etc. Annual world

production of quartz single crystals using both hydrothermal and other methods is currently 600 tons. The other substances produced by this method are corundum ( $\text{Al}_2\text{O}_3$ ) and ruby ( $\text{Al}_2\text{O}_3$  doped with  $\text{Cr}^{3+}$ ).



**Figure 1.6** Schematic hydrothermal bomb used for crystal growth

## CHAPTER 2

### EXPERIMENTAL METHOD

#### 2.1 The Physical Analyzing Methods of Solids

The structures of materials are readily studied by diffraction methods. Structural properties are often responsible for several physical and chemical properties such as electrical conductivity, chemical stability, toughness and others [18].

X-ray diffraction methods are some of the most powerful characterization tools known by scientists. In chemistry concerning solids, the two primary pieces of information most often sought are the structure of the material and its reactivity. X-ray diffraction methods can be used to study single crystals, powders and other forms of solids [19].

X-ray diffraction is used for structural characterization of solid state materials. All crystalline solids have their own characteristic X-ray powder diffraction patterns which are used as their 'fingerprinting'. However powder diffraction has many other applications besides phase identification, for example the study of polymorphism, phase transitions and solid solutions, determination of accurate unit cell parameters, particle size measurement and phase diagram determination [8].

There are many forms of crystalline solids such as a single crystal that is pure and free from defects, a single crystal whose structure can be modified by defects and specific impurities, a powder, i.e. a large number of small crystals, a polycrystalline solid piece, e.g. a pellet or a ceramic tube in which a large number of crystals are present in various orientations or a thin film [20].

The noncrystalline solid materials can be amorphous or glass. Noncrystalline solids may be prepared in various forms as tubes, pellets or thin films [18].

The methods used to find what an inorganic substance is, are divided into 2 main categories. It depends on whether the substance is molecular or non-molecular. If the substance is molecular, the identification can be carried out by combination of

spectroscopic methods and chemical analysis. If the substance is nonmolecular and crystalline, identification is carried out by X-ray powder diffraction and chemical analysis.

The characteristic powder patterns of most known inorganic solids can usually be identified rapidly. The next stage is to determine its structure, if it is not known already.

For molecular materials the molecular geometry can be obtained by further spectroscopic measurements. If the substance is crystalline, X-ray crystallography may be used.

There are 3 main categories of physical techniques which may be used to characterize solids, they are diffraction, microscopic and spectroscopic techniques.

## **2.1.1 Diffraction Techniques**

### **2.1.1.1 X-ray Powder Diffraction**

X-ray powder diffraction methods can be used to study the degree of crystallinity of a material, to determine the basic structure of the material, and to elucidate the degree of purity and crystallinity of the sample under interest. A diagram of an X-ray powder diffractometer is given in Fig 2.1. X-rays are produced in the X-ray tube and are collimated onto a sample. In most cases Cu K $\alpha$  radiation is used for studies of powders. The sample is usually moved at angles between  $2\theta = 5-60$  degrees or larger. A proportional counter is used as a detector and the intensities of the diffraction peaks are recorded on a chart recorder or stored on a computer.

X-ray powder diffraction method can be used also for quantitative determination of the mineralogical components in a mixture, provided that appropriate standards are used. The detection limit of X-ray powder diffraction method is typically around 5%.

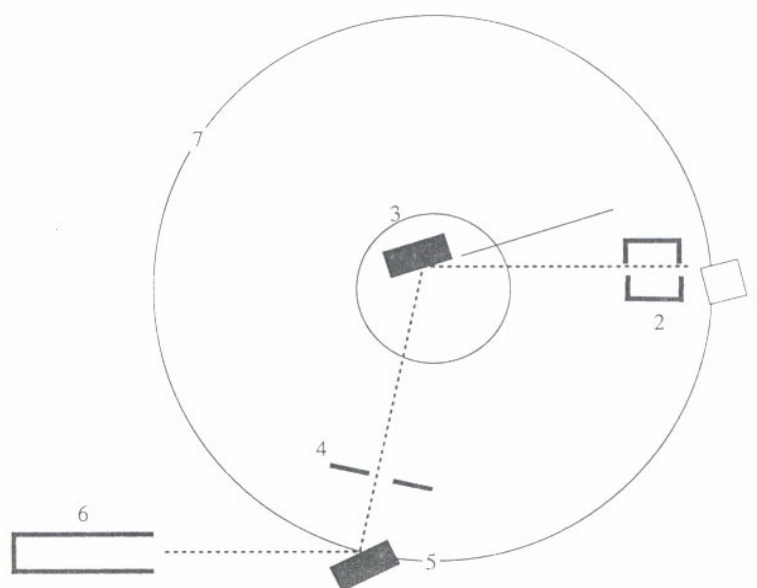


**Figure 2.1** Diagram of an X-ray Diffractometer. Various parts: 1= X-ray Source, 2= Collimator, 3= Sample, 4= Slits, 5= Monochromator, 6= Detector, 7= Focus circle.

A random orientation of the powder is needed in order to observe all of the diffraction peaks. Once the  $2\theta$  values are collected they can be converted to  $\theta$  and by using Bragg's law values of the  $d$  spacings can be obtained. If the substance is a common type then the experimental X-ray powder diffraction pattern can be compared to known published patterns such as those found in the ASTM (American Society for Testing and Materials) tables [19]. Standard patterns of crystalline substances are given in the Powder Diffraction File, JCPDS (Joint Committee on Powder Diffraction Standards) or ASTM File. The file now contains 35000 entries and is increasing at a rate of about 2000 per year [18]. If a powder pattern has never been collected before, analogies to known structural types can be made.

Thin films, wires, fibers and other similar forms of materials can also be studied with the X-ray powder diffraction method. Usually the powder or other sample form is attached to a glass slide by some noncrystalline material such as vaseline. It is important to press the sample onto such a slide because a random orientation is necessary in order to observe all of the different planes. During the analysis it is important to compare the peak positions, relative intensities and the general shape of the background signal [19].

An X-ray powder diffraction pattern is a set of lines or peaks each of which are in different intensity and position (d-spacing or Bragg angle,  $\theta$ ) on a strip of photographic film or chart paper. For a given substance the line positions are fixed and characteristic for that substance. The intensities may vary from sample to sample depending on the method of sample preparation and the instrument conditions.

In the X-ray powder diffraction average crystal size in a powdered sample provided and the average diameter is less than 2000 Å. The lines in a powder diffraction pattern are of finite breadth but if the particles are very small the lines are broader than usual. The broadening increases with decreasing particle size. The limit particle size to be seen is about 20 to 100 Å [18].

Crystalline solids give diffraction patterns that have a number of sharp lines. Noncrystalline solids like glasses, gels give diffraction patterns that have a small number of very broad lines with low intensity.

The thermal motion of atoms which is inevitably present in all substances above absolute zero, causes a reduction in peak intensities and an increase in the background radiation. This is mostly noticeable at high temperatures and as the melting point of the sample is approached.

Our X-ray powder diffraction patterns of compounds were obtained using a Philips X'pert Pro powder diffractometer. Samples were ground and placed on a zero background single crystalline silicon sample holder. Data were collected using  $\text{CuK}\alpha$  radiation at settings of -45 kv and 40 mA for 27 minutes. The scan rate was highly dependent on the amount and quality of sample and the data were typically collected for  $2\theta$  values of  $4^\circ$  to  $70^\circ$  [18].

### **2.1.1.2 Single Crystal X-ray Diffraction**

There are several single X-ray diffraction techniques. One of the most used one is the diffraction cameras and the results are the patterns of spots on photographic films.

With a single crystal the first step is to mount a crystal on a goniometer which is usually to rotate the crystal in space with two mutually perpendicular arcs. In addition the goniometer can be rotated about a spindle axis. In many cases a precession photograph is taken and the crystal is moved in space until the crystallographic axes are



aligned with the photographic detector which is behind the X-ray source and the sample. Usually Mo K $\alpha$  radiation is used in single crystal studies.

Data are then collected on the different diffraction peaks and the intensities are counted in a systematic fashion. Bond lengths and distances are calculated and compared to other materials with similar composition and structure [19].

The crystal system of a crystal, i.e. cubic, tetragonal, monoclinic, etc. may be determined from single crystal X-ray photographs. Basically by looking for a symmetrical arrangement of spots, one can find the symmetry of the unit cell.

Once the unit cell has been determined, the next stage is to determine the space group. This is done by looking for patterns of absent spots in the X-ray photographs. For instance alternate spots in a row or perhaps entire row may be absent. From the systematic absences, it is possible to determine the lattice type, face centered, body centered, etc. And whether or not the crystal has elements of space symmetry i.e. screw axes or glide planes [18].

### **2.1.2. Microscopic Techniques**

Various kinds of microscope are available and they can be divided into 2 groups: optical and electron. With optical microscopes, particles down to a few micrometers in diameter may be seen under high magnification. The lower limit is reached when the particle size approaches the wavelength of visible light, 0.4 to 0.7  $\mu\text{m}$ . For submicrometer sized particles it is essential to use electron microscopy. By this way one can image diameters in a few Angstroms.

#### **2.1.2.1. Electron Microscopy**

Electron Microscopy is a very versatile technique capable of providing structural information over a wide range of modification. The scanning electron microscope (SEM) studies the texture topography and surface features of powders or solid pieces. Features up to tens of micrometers in size can be seen because of the depth of focus of

SEM instruments. The resulting pictures have a definite three-dimensional quality. The resolution of SEM is approximately between 100 Å and 10 µm [18].

Our SEM / EDX results of the searched compounds were analyzed with a Philips XL 30S FEG Scanning Electron Microscope. Although the conditions change from sample to sample approximately accelerating voltage, was 5 kV, spot was 3, magnification was 1200, the detector type was Secondary Electron (SE) or Through the Lens (TLD) and the working distance was 4.5-6 mm. In the SEM / EDX analyses of our samples, we can obtain the data only in 1-2 µm distance from the surface. For the elements staying deeper, results may not be very reliable. The results of EDX analysis are usually presented as a spectrum. In this graphical representation the X -axis represents the energy level - and therefore identifies the elements, and the Y-axis provides the number of counts of each element detected.

A common error equates peak height to the quantity of each element present. In order to provide an accurate determination of the quantity of a particular element there are a number of factors, which must be applied to the number of counts. These corrections are performed where the quantities as presented below are normalized to 100 % and displayed as weight % (wt %).

The results obtainable through a modern ‘Quantitative Standardless Analysis’ package offer a very accurate representation of the composition of the material (with the exception, generally, of trace elements below the 1000 ppm detection level). Nevertheless, the figures provided in the weight % need to be considered according to the guidelines provided below:

Results in weight %	100-20	20-5	5-1	1-0.2
Relative % i.e.	5	10	20	50-100

(the error could be up to)

It should be noted that the ideal specimen for EDX microanalysis is perfectly flat and polished. Although the our software does take a limited amount of surface roughness into account it is safe to assume that greater surface roughness will mean less reliable and consistent results.

## 2.2 Experimental Procedure

### 2.2.1 Reaction Autoclaves

Acid digestion bombs made of steel (Fig 2.2 a,b) are used as reaction vessels which of their inner parts are made from PTFE (Polytetrafluoroethylene) (Fig 2.2 c). PTFE lined digestion bombs are used because teflon is an inert material so it does not react with reactants, it provides a convenient medium for dissolving samples rapidly in strong acids or alkalines, it has high temperature usefulness. PTFE has two characteristics which make it less than perfect for its application:

1- PTFE has a tendency to creep or flow under pressure or load. This is present even at room temperature and emphasized at higher temperatures. At temperatures higher than 150 °C the creep effect becomes more pronounced that makes it difficult to maintain tight seals that results in deformation and shorter life for PTFE components. The creep effect is proportional to maximum operating temperature.

2- PTFE is a porous material. There can be vapor migration across the cover seal and through the wall of the liner itself. Amount of solute lost in this manner during a normal digestion is negligible, but vapor migration will occur and frequently it will produce discoloration on the inner metal walls of the bomb body and the screw cap.



(a) An acid digestion bomb



(b) PTFE cup with cover , acid digestion bomb body, screw cap, pressure plate (upper), pressure plate (lower), corrosion and rupture discs, spring.[from left to right]



(c) PTFE cup with its cover

Figure 2.2 An acid digestion bomb, its parts and a PTFE cup with its cover

These bombs can be used safely and routinely for treating a great variety of samples with different digestion media under a wide range of operating conditions. The pressure generated within bombs, filling level and the amount of heat applied to promote the reactions are dependent upon the nature of materials being treated.

### **2.2.2 Sample Selection**

In a 23 mL bomb, most inorganic digestions proceed smoothly using not more than 1 gram of sample. In all reactions, the bomb must never be completely filled there must be vapor space above the surface of the charge. When working with inorganic materials, the total volume of the charge must never exceed two-thirds (66 %) of the capacity of the cup.

### **2.2.3 Hydrothermal Procedure**

The first step is the preparation of 23 ml teflon bombs by loading the starting materials into each bomb. The second step is filling the bombs with the reaction solutions such as water, salt solutions or other solvents, then placing the bombs into an oven (Fig 2.3) for several days at 100-200 °C. In the end of the reaction, the oven is led to cool down to room temperature. The product, then washed several times with pure water and acetone to remove the traces of the solvent from the crystals. After selecting a single crystal in the mineral oil from the product under the J.P. Selecta Zoom Stereo Microscope, it is mounted with epoxy in a capillary in order to analyze with a X-ray single crystal diffractometer (Fig. 2.4).



**Figure 2.3** Carbolite CWF 1100 oven



**Figure 2.4** A mounted single crystal to a capillary with epoxy

## CHAPTER 3

### POLYOXOMETALATES (POM's)

#### 3.1 Introduction

Hydrothermal reactions are very useful in preparing low-density open-framework solids in crystalline form [8]. In addition this method is widely used in synthesizing many hybrid vanadium oxides templated or coordinated by transition metal complexes or fragments [21].

Recently a number of polyvanadates that contain 3 to 34 vanadium atoms has been synthesized and characterized [20, 22, 23]. These interesting metal oxides contain various kinds of metal atoms fused together with oxide ligands presented in some bridging modes [24]. Most of the polyoxometalates are stable in air at room and also at elevated temperatures. Their preparation is inexpensive and efficient in synthetic laboratories [21].

Vanadium oxide clusters are composed of vanadium chains and layers [8, 13, 20, 22, 23]. In these compounds vanadium atoms take different oxidation states and coordination numbers in combinations of  $[\text{VO}_x]$  ( $x = 4, 5, 6$ ) polyhedra but mostly observed structure is  $[\text{VO}_4]$  tetrahedral unit which is similar to  $[\text{MO}_4]$  [ $\text{M} = \text{Si}, \text{Al}$ ] tetrahedra [8, 25, 26, 27].

Almost all elements form different compounds with oxygen except the noble gases. There are many structural characterizations of oxides as discrete binuclear molecular species and polymeric species seen as chains, layers and three dimensional network structures [28].

There is a considerable attention in the chemistry of soluble metal oxides or polyoxometalates [25]. Many transition elements form large polynuclear metal-oxoanions,  $\text{M}_x\text{O}_y^n$  where M can be V (V), Nb (V), Ta (V), Mo (VI) or W (VI) which contain up to 200 atoms or more.

POM's are suitable and attractive as active counterions for new radical cation salts, because of their several characteristics as below: [29]

1. They are soluble in aqueous, nonaqueous solutions and they can maintain their structures as in solid state.

2. They can take versatile charges, shapes and sizes that can induce new organic packings and so new band structures.

3. They are good electron acceptors. This property provides the formation of hybrid materials by delocalized electrons which coexist in both organic network and the inorganic clusters.

4. They are also ligands so they incorporate more than one magnetically active transition metal ions at special sites of the polyoxoanions.

POM's are anionic-types of  $[MO_x]$  building blocks. M is a d-block element in high oxidation state [25].

The basic structures of polyoxovanadates, molybdates and tungstates are the same. In these structures each metal atom occupies an  $[MO_x]$  coordination polyhedron, in which the metal atom is displaced, as a result of M-O  $\pi$  bonding toward those polyhedral vertexes that form the surface of the structure [20].

The structures of POM's depend on the different basic polyhedras, as  $[MO_4]$ ,  $[MO_5]$  and  $[MO_6]$  where  $[O = MO_4]$  (M = V, Mo, W) polyhedra forms cluster shells or cages, similar to fullerenes and the layers of  $V_2O_5$  [23, 30].

Vanadates show more structural flexibility compared to tungstates based on their structural variety of  $[VO_x]$  polyhedra,  $x = 4, 5, 6$  [20].

As a basic rule while increasing the size of POM's, the overall charge should be increased however the charge density on the anion must be kept constant. This is required to keep the anion in growth as a soluble, nonhydrolyzing component in solution.

### 3.2 Application Areas of Polyoxometalates

The application areas of polyoxometalates are analytical chemistry, materials science and catalysis, nanotechnology, chemical sensing, environmental decontamination, biochemical and geochemical processes and medicine [21, 24, 31].

The applications of POM's which are known as "value adding properties" are summarized below: [17] metal oxide like; stable ( $H_2O$  / air, T): processing advantage; large size (diameter, 6-25 Å); discrete size / discrete structure (confined geometric



factors); anions (charge from -3 to -14); high ionic weight (103–104); fully oxidized compounds / reducible; variable oxidation numbers for the addenda atoms; color of oxidized forms different from color of reduced forms; photoreducible; arrhenius acids ( $pK_a < 0$ ); incorporate over 70 elements and form large number of structures: processing advantage; acid forms very soluble in  $H_2O$  and other oxygen carrying solvents (ethers, alcohols, ketones); also soluble or transferable into nonpolar solvents: processing advantage; hydrolyzable to form deficient structures: processing advantage

The applications of POM's can be listed as below according to their redox properties, photochemical response, ionic charge, conductivity and ionic weights [21]. Categories of applications for POMs (derived from Patent Literature; Excluding Catalysis and Medicine) are in coatings, analytical chemistry, processing radioactive waste, separations, sorbents of gases, membranes, sensors, dyes / pigments, electrooptics, electrochemistry/electrodes, capacitors, dopants in nonconductive polymers, dopants in conductive polymers, dopants in sol-gel matrixes, cation exchangers, flammability control, bleaching of paper pulp, clinical analysis, food chemistry.

### **3.3 Magnetism of Polyoxometalates**

POM's which have  $d^0$  ions are not important structures to have magnetic properties. However the POM's which have  $d^1$  centers have interesting magnetic properties such as polyoxovanadates (IV) [20]. Also some can encapsulate small clusters of magnetic metal ions like cobalt (II), nickel (II) etc. These large metal ion clusters show different magnetic interactions of which behave as tiny magnets.

Another important magnetic property of POM's is their mixed-valence feature with localized and delocalized possibilities [20]. Heteropoly anions can be reduced to mixed-valence species where excess electrons can be fully or partially delocalized by forming delocalized-delocalized, delocalized-localized and localized-localized interactions [25]. POM's can also encapsulate magnetic metal centers to form magnetic clusters [20].

Magnetic POM's are used as anions of organic charge-transfer systems in order to research the interaction between moving electrons in the organic backbone and

localized magnetic electrons in the POM's. By this way new classes of molecular materials are obtained [32].

Polyoxovanadates are an important class of magnetic POM's. The building blocks of the clusters are shown in Fig 3.1

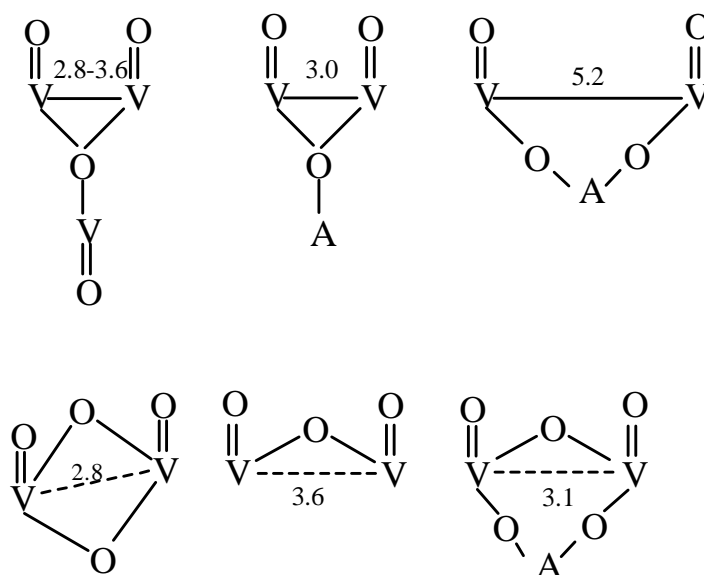


**Figure 3.1** Scheme of the bridges most commonly found in polyoxovanadates (IV).

## 3.4 Experimental

### 3.4.1 Synthesis

Synthesis of the  $([V_{16}O_{31}(OH)_7]Cl \cdot 15H_2O)$  was done in Northwestern University Chemistry Laboratory from the reaction of  $NaVO_3$  (0.027 g, 0.22 mmol),  $Sb_2S_3$  (0.038 g, 0.11 mmol) and  $Na_2S$  (0.017 g, 0.22 mmol). The following reagents were used as obtained:  $NaVO_3$  (99.9 %) and  $Sb_2S_3$  (99.6 %).  $Na_2S$  was prepared by the stoichiometric reactions of the elements in liquid  $NH_3$ .

A reaction mixture was loaded into a fused-silica tube under an Ar atmosphere in a glove box. Then 0.4 mL of 5M  $NH_4Cl$  was added via syringe. The tube was frozen, evacuated to  $\sim 10^{-3}$  Torr, flame-sealed, and thawed. It was then loaded into a high-

pressure autoclave along with 1700 mL of H<sub>2</sub>O to counter the pressure. The autoclave was heated at 170 °C for 3 days and then cooled to room temperature. The solid products were recovered by suction filtration and washed with water. Black columns of the reported materials were obtained in 30-40 % yield. Examination of these columns with an EDX-equipped Hitachi S-3500 SEM gave results consistent with the stated compositions.

### 3.4.2 Crystallography

Data collection of the title compound were done in Northwestern. single crystal X-ray diffraction data were collected with the use of the program SMART on Bruker Smart 1000 CCD diffractometer [33] at 153 K. Monochromatized MoK $\alpha$  radiation ( $\lambda$ = 0.71073 Å) was employed. The diffracted intensities generated by a scan of 0.3° in  $\omega$  were recorded on three sets of 606 frames at  $\omega$  settings of 0°, 120°, and 240°. The exposure times were 15 s / frame. Cell refinement and data reduction were carried out with the use of the program SAINT [33]. Face-indexed absorption corrections were made with the program XPREP [34]. Then the program SADABS was employed to make incident beam and decay corrections [33]. In our laboratory the structures were solved by direct methods with the program SHELXS and refined by full-matrix least-squares techniques with the program SHELXL in the SHELXTL-97 suite [34]. Further crystallographic details are given in Table 3.1, selected bond distances are given in Table 3.2 and final values of the atomic parameters and isotropic displacement parameters are given in Table 3.3.

### 3.4.3 Results and Discussion

The extended structure of crystals of ([V<sub>16</sub>O<sub>31</sub>(OH)<sub>7</sub>]Cl 15H<sub>2</sub>O) involves the unit cell view of vanadium oxide in Fig 3.2. This new polyoxovanadate exhibits an original three dimensional structure whose framework is composed of vanadium-oxygen clusters encapsulated Cl<sup>-</sup> anion, OH<sup>-</sup> anion, and water molecules. The structure consist of ([V<sub>16</sub>O<sub>31</sub>(OH)<sub>7</sub>]Cl) clusters and water molecules linked to each other by means of a net of hydrogen bonds between the hydrogen atoms and the apical oxygen atoms of the

polyoxovanadates units, generating a three dimensional network of  $[(V_{16}O_{31}(OH)_7)Cl] \cdots \mu\text{-H}_2\text{O} \cdots [(V_{16}O_{31}(OH)_7)Cl]$  arrays. The constituent  $(V_{16}O_{31}(OH)_7)Cl$  cluster is constructed from the  $(V_{16}O_{38})$  cage encapsulating a  $Cl^-$  anion which interacts with the 16 V centers of the cage (Fig. 3.3 a, b). The average distance between  $Cl^-$  and vanadium is 3.60 (15) Å very close to the value found by Müller [35] and Ganne [36].

The 16  $(VO_5)$  units of the  $(V_{16}O_{31}(OH)_7)Cl$  core in the title compound are fused with each other through common edges and linked with central  $Cl^-$  anion. The square pyramidal geometry around each vanadium in the 16  $(VO_5)$  units is defined by an apical  $\mu$ -oxygen group (1.606 (6)-1.652 (6) Å) and four basal oxygens of the cage (1.884 (5)-2.027 (6) Å).

The cation  $[V_{16}O_{31}(OH)_7]^+$  (see Fig.3.3) has an ellipsoidal shape of  $S_4$  with a 4-fold axis passing through the atoms O 19 and O 19 A. All the V-O and O $\cdots$ H distances are given in Table 3.3. From these data it seems clear that cations establish hydrogen bonding (O-H $\cdots$ O between 2 and 2 Å) with oxygens from the water molecule.

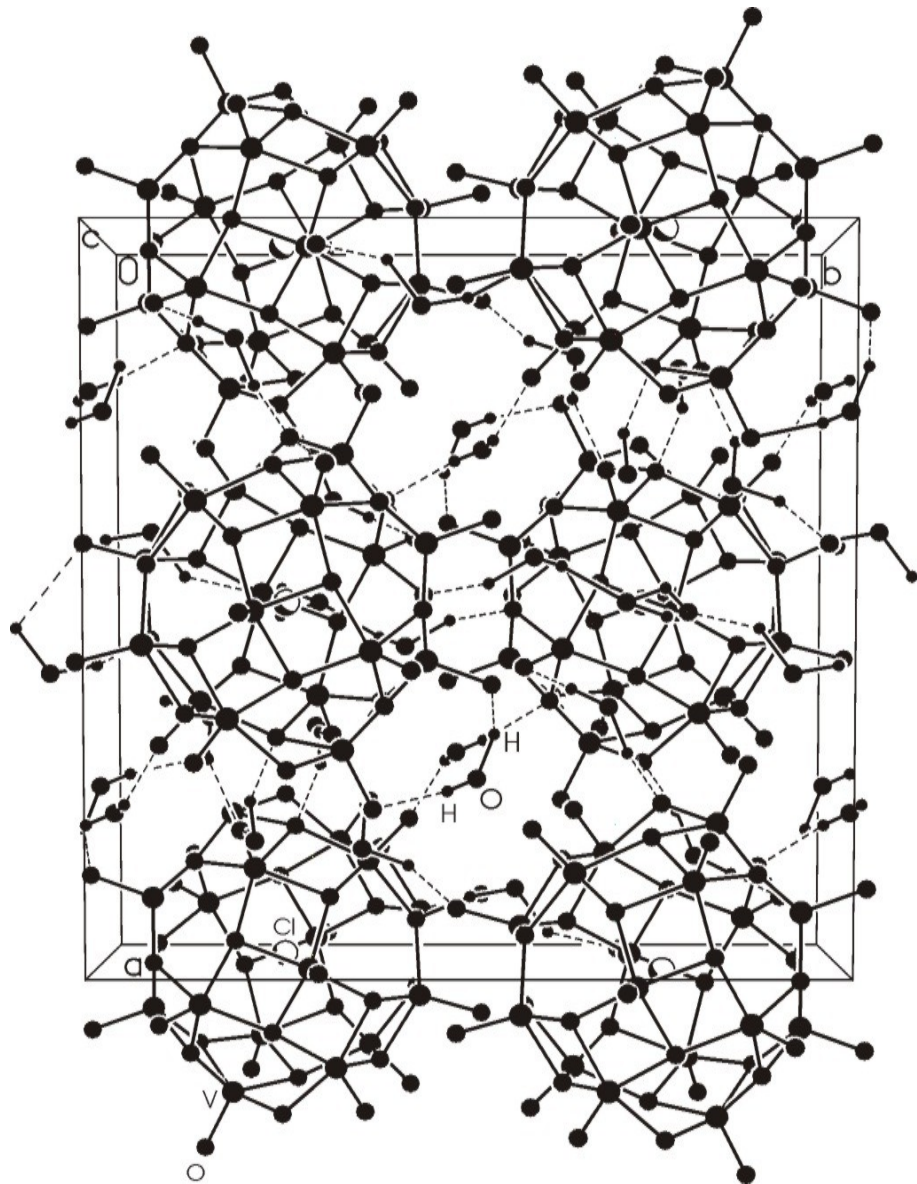
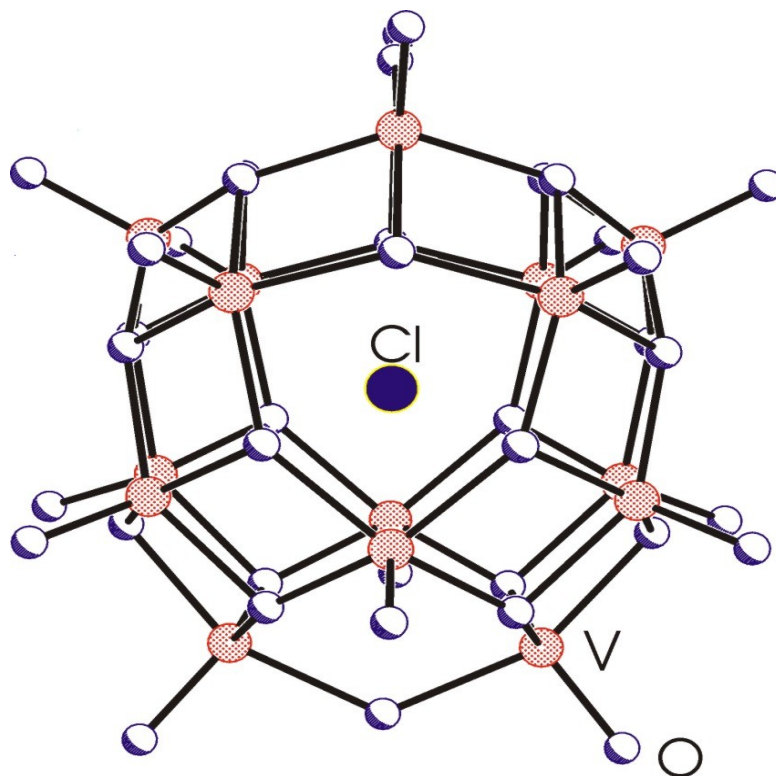
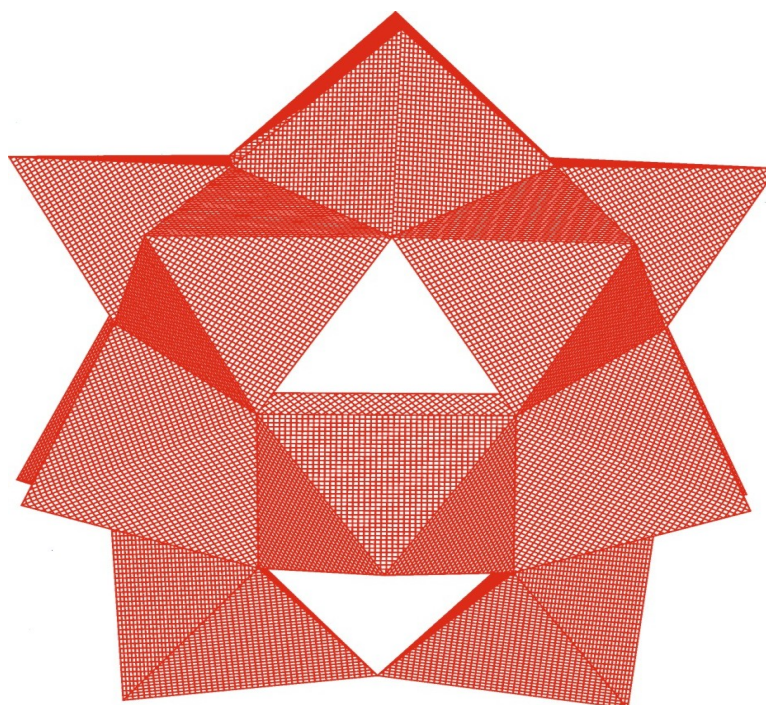


**Figure 3.2.** Unit cell picture of  $[V_{16}O_{31}(OH)_7]Cl \cdot 15H_2O$ , big solid circles are vanadium atoms, small solid circles are oxygen atoms, shaded circles are chlorine atom.



(a)  $(V_{16}O_{38})$  cage encapsulating a  $Cl^-$  anion



(b) the polyhedral view of the  $(V_{16}O_{38})$  cage

Figure 3.3  $(V_{16}O_{38})$  cage and its polyhedral view

**Table 3.1** Crystal Data and Structure Refinements for  $[V_{16}O_{31}(OH)_7]Cl$ 

Compound	$[V_{16}O_{31}(OH)_7]Cl$
a (Å)	18.070(2)
b (Å)	17.414(2)
c (Å)	15.1154(18)
$\alpha$ (deg)	97.696(2)
V, (Å <sup>3</sup> )	4713.8(10)
Z	8
$\rho$ (Å)	0.71073
T, (K)	153
$\rho_c$ , (gcm <sup>-3</sup> )	2.436
R	0.0696
R <sub>w</sub>	0.1275

**Table 3.2** Selected Bond Distances

V1-O1 1.652(6)	V5-O5 1.604(6)	O20-H20A ··· O18	1.843
V1-O10 1.925(6)	V5-O10 1.928(6)	O20-H20A ··· O8	2.469
V1-O12 1.930(6)	V5-O17 1.928(5)	O20-H20B ··· O1	1.754
V1-O11 1.938(6)	V5-O12 1.963(6)	O21-H21A ··· O2	2.156
V1-O9 1.942(6)	V5-O19 2.027(6)	O21-H21B ··· O14	1.818
V2-O2 1.632(5)	V6-O6 1.613(6)	O21-H21B ··· O8	2.547
V2-O13 1.902(6)	V6-O10 1.939(6)	O22-H22A ··· O6	1.872
V2-O11 1.934(6)	V6-O11 1.972(6)	O22-H22B ··· O19	1.537
V2-O14 1.935(6)	V6-O16 1.976(6)	O23-H23A ··· O8	2.174
V2-O9 1.958(6)	V6-O15 1.978(5)	O23-H23B ··· O15	2.147
V3-O3 1.621(6)	V7-O7 1.627(6)	O24-H24A ··· O4	1.611
V3-O13 1.884(6)	V7-O15 1.919(5)	O24-H24B ··· O2	1.996
V3-O16 1.905(6)	V7-O14 1.923(6)	O25-H25A ··· O27	2.164
V3-O15 1.940(6)	V7-O13 1.951(6)	O25-H25B ··· O16	1.675
V3-O16 1.946(5)	V7-O19 1.999(6)	O26-H26A ··· O3	2.083
V4-O4 1.613(6)	V8-O8 1.617(6)	O26-H26A ··· O6	2.493
V4-O12 1.926(6)	V8-O18 1.951(6)	O26-H26B ··· O7	2.162
V4-O18 1.929(6)	V8-O9 1.955(6)	O27-H27A ··· O1	2.092
V4-O18 1.957(6)	V8-O17 1.961(6)		
V4-O17 1.969(6)	V8-O14 1.973(6)		

**Table 3.3** Atomic Parameters and Isotropic Displacement Parameters

Atom	x	y	z	Ueq
V1	0.48849(8)	0.21912(8)	0.51913(10)	0.0141(4)
V2	0.62725(8)	0.29576(8)	0.59819(10)	0.0126(4)
V3	0.42071(8)	0.44336(8)	0.75294(10)	0.0145(4)
V4	0.44289(8)	0.06870(8)	0.67259(10)	0.0137(4)
V5	0.34514(8)	0.18393(9)	0.57737(10)	0.0143(4)
V6	0.43513(8)	0.37179(8)	0.57334(10)	0.0140(4)
V7	0.69955(8)	0.33174(9)	0.77140(10)	0.0147(4)
V8	0.63562(8)	0.14006(8)	0.68470(10)	0.0136(4)
Cl1	0.5000	0.25803(19)	0.7500	0.0276(9)
O1	0.4864(3)	0.2045(4)	0.4108(4)	0.0214(15)
O2	0.6826(3)	0.3136(3)	0.5237(4)	0.0153(14)
O3	0.3887(3)	0.5300(3)	0.7575(4)	0.0219(16)
O4	0.4200(3)	-0.0172(3)	0.6396(4)	0.0191(15)
O5	0.2881(3)	0.1428(3)	0.5016(4)	0.0183(15)
O6	0.4101(3)	0.4253(3)	0.4874(4)	0.0195(15)
O7	0.7799(3)	0.3716(3)	0.7639(4)	0.0191(15)
O8	0.6956(3)	0.0832(3)	0.6484(4)	0.0199(15)
O9	0.5873(3)	0.1919(3)	0.5776(4)	0.0138(14)
O10	0.3975(3)	0.2709(3)	0.5367(4)	0.0153(14)
O11	0.5270(3)	0.3217(3)	0.5451(4)	0.0144(14)
O12	0.4408(3)	0.1330(3)	0.5686(4)	0.0135(13)
O13	0.6338(3)	0.3821(3)	0.6759(4)	0.0163(14)
O14	0.6836(3)	0.2420(3)	0.6972(4)	0.0149(14)
O15	0.6388(3)	0.3886(3)	0.8433(4)	0.0159(14)
O16	0.4898(3)	0.4394(3)	0.6648(4)	0.0141(14)
O17	0.3502(3)	0.1245(3)	0.6857(4)	0.0121(13)
O18	0.5503(3)	0.0742(3)	0.6973(4)	0.0161(14)
O19	0.5977(5)	-0.0640(5)	0.6168(6)	0.055(2)
O21	0.6735(4)	0.2883(5)	0.3440(6)	0.028(2)
O22	0.1426(4)	0.1875(5)	0.6545(5)	0.045(2)
O23	0.7913(5)	0.0178(6)	0.5451(6)	0.031(2)
O24	0.6599(4)	0.1451(5)	0.4348(5)	0.047(2)
O25	0.5615(4)	0.4123(5)	0.4042(6)	0.045(2)
O26	0.2413(5)	0.0103(5)	0.6427(6)	0.049(2).
O27	0.5000	0.2911(7)	0.2500	0.041(3).



The formula of the structure was first found as  $(V_{16}O_{38})Cl \cdot 15H_2O$ , however based on the valence bond calculation formula was corrected as  $[V_{16}O_{31}(OH)_7]Cl \cdot 15H_2O$ . Individual valence of each vanadium cation has been estimated from calculations of bond valence sums by using the formula of Brown Altermatt [37]. These results as well as the average values are given in Table 3.4. Taking into account the refined crystallographic formula, the average vanadium valence is estimated to be about 4.4. Based on this information the cluster cation charge is balanced by  $OH^-$  anion to form 1+ charged cluster cation, and the remaining lattice volume is occupied by water.

Polyoxovanadate with vanadium in the oxidation states +IV and +V seems to be much more diverse than in the case of polyoxomolybdates or polyoxotungstates. By changing starting materials or pH of the reaction, new materials can be obtained with vanadium.

Table 3.4 Bond Valences

V atom	Valency	V atom	Valency
V1	4.3	V5	4.3
V2	4.4	V6	4.3
V3	4.6	V7	4.3
V4	4.4	V8	4.2

## CHAPTER 4

### VANADIUM COMPOUNDS

#### 4.1. Introduction

The vanadium oxide part of the hybrid materials is mostly in the  $V_xO_y^{n-}$  formula. In the mineral chemistry vanadium takes three oxidation states V (III), V (IV) and V (V). Tetravalent vanadium with electronic configuration  $3s^2 3p^6 3d^1$  shows five or six coordination however pentavalent vanadium shows 4-, 5- or 6- coordination. In both structures there are short V = O bond lengths (1.57-1.68 Å) [38].

The coordination geometry of V (IV) can be square pyramidal and distorted octahedral or square bipyramidal. The square pyramidal geometry described 4 + 1, has 1 short vanadyl bond in the axial position and 4 longer equilateral bonds (1.80-2.12 Å). The six-coordinate geometry is known as 4 + 1 + 1, that has 4 intermediate equatorial bonds (1.86-2.16 Å), one axial vanadyl bond and a long axial bond (2.20-2.32 Å) (Fig. 4.1).

The five-coordinate geometry V (V) exhibits tetrahedral, square pyramidal, distorted trigonal bipyramidal and distorted octahedral or square bipyramidal geometries. In the tetrahedral structure there are short (1.6 to 1.7 Å) and longer distances (1.8 to 2.0 Å) depending on the terminal and bridging nature of the V-O bond.

Geometry of the five-coordinate V (V) changes depending on the number of vanadyl group. When there is a single V = O bond, the 4 + 1 square pyramidal geometry is observed, if there are two short V = O bonds, distorted trigonal bipyramidal, 3 + 2 geometry, is observed with the short vanadyl bonds occupying two equilateral positions and the longer bonds occupying one equatorial and two axial positions.

The six-coordinate geometry V (VI) exhibits 4 + 1 + 1 or 2 + 2 + 2 bonds depending on the presence of one or two short vanadyl bonds, respectively. The 4 + 1 + 1 geometry is similar to that is for tetravalent vanadium. The 2 + 2 + 2 geometry has

two short vanadyl bonds in a cis position, two long bonds (2.1-2.3 Å) trans to the vanadyl groups and two intermediate bond lengths (1.85-2.05 Å) cis to the V = O bonds. The multiply bonded vanadyl groups are located in cis position in both 2 + 3 and 2 + 2 + 2 polyhedra to maximize  $\pi$  bonding to  $t_{2g}$  orbitals (Fig 4.1).

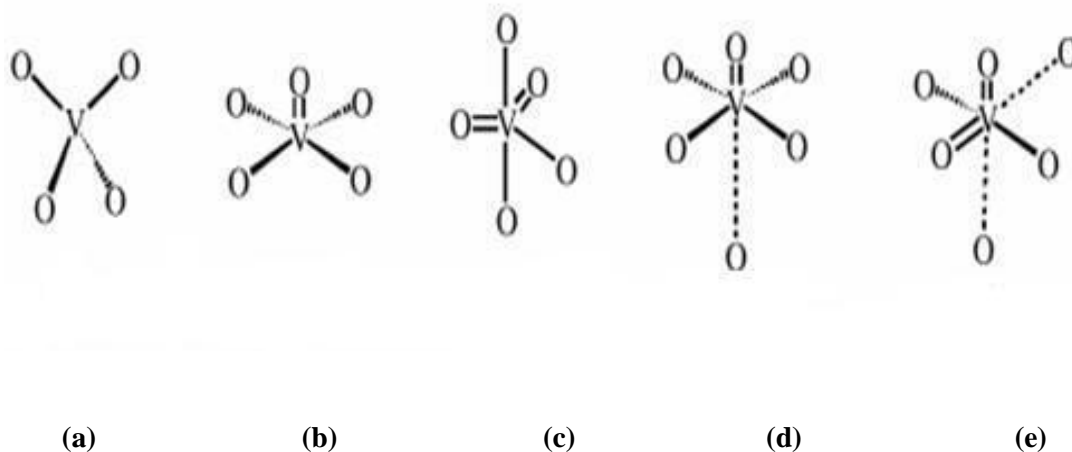


**Figure 4.1** Coordination polyhedra adopted by V (V)- and V (IV)- oxo species: tetrahedral, “4 + 1” square pyramidal, “3 + 2” trigonal bipyramidal, “4 + 1 + 1” octahedral, and “2 + 2 + 2” octahedral.

Vanadium oxide chemistry has several characteristic families as binary oxides, bronzes and molecular polyanions. The chemistry of polyanions has been reviewed recently [22, 38, 39]. Representative examples of vanadate cluster chemistry shows divanadate ( $V_2O_7$ )<sup>4-</sup> [40], tetravanadate ( $V_4O_{12}$ )<sup>4-</sup> [41] and decavanadate ( $V_{10}O_{28}$ )<sup>6-</sup> [42] in Fig 4.2, ( $V_4O_{12}$ )<sup>4-</sup> structure is a ring of corner-sharing V (V) tetrahedra and the decavanadate is constructed from edge-sharing V (V) octahedra. Vanadium polyhedra can have edge-, corner- and face-sharing types.

Metavanadates have the empirical formula  $VO_3^-$  as shown in the structure of  $KVO_3$  and  $\square NaVO_3$  (shown in Fig. 4.3). In the  $KVO_3$  structure there is a chain of corner-sharing tetrahedras [38]. In contrast the  $\square NaVO_3$  structure has a double chain of edge-sharing trigonal pyramids (2 + 3 geometry) formed by two corner-sharing tetrahedral chains.

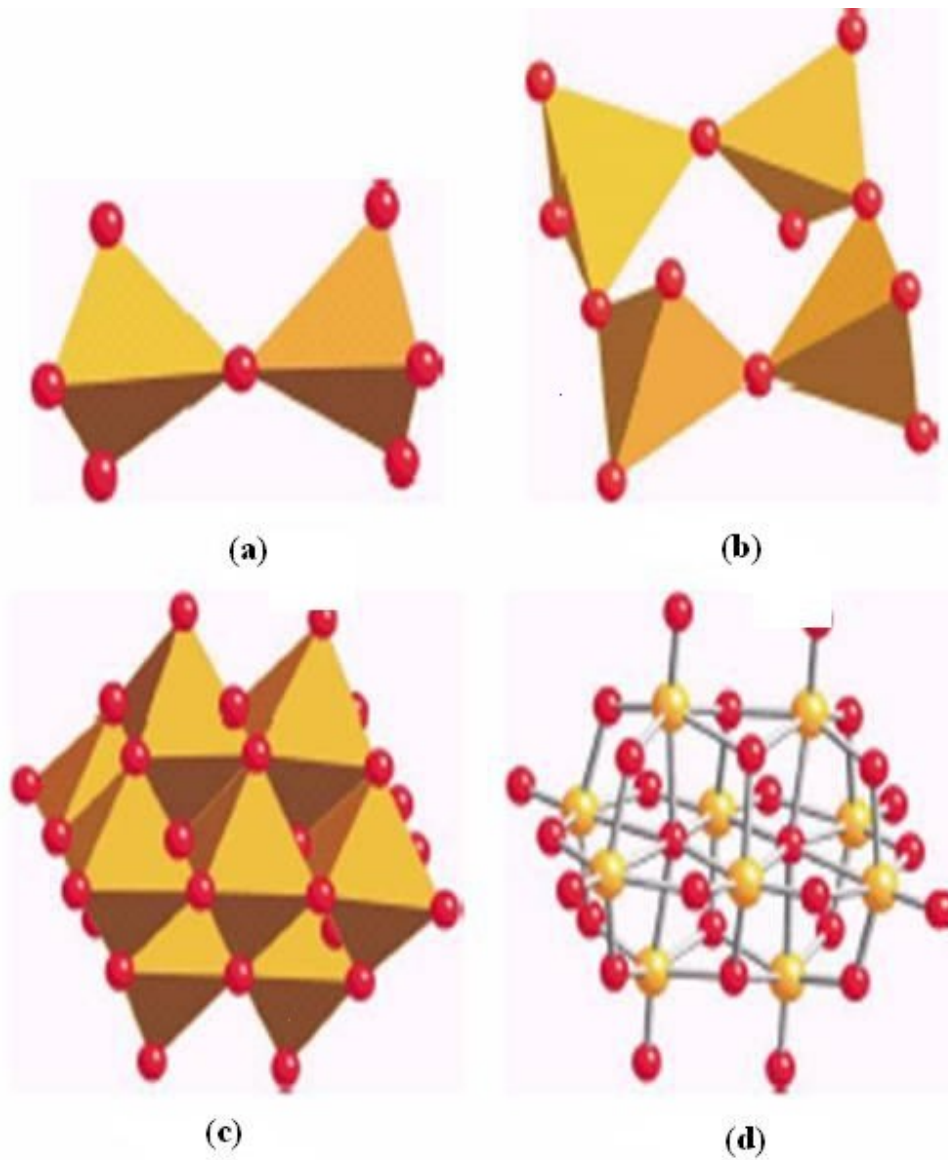
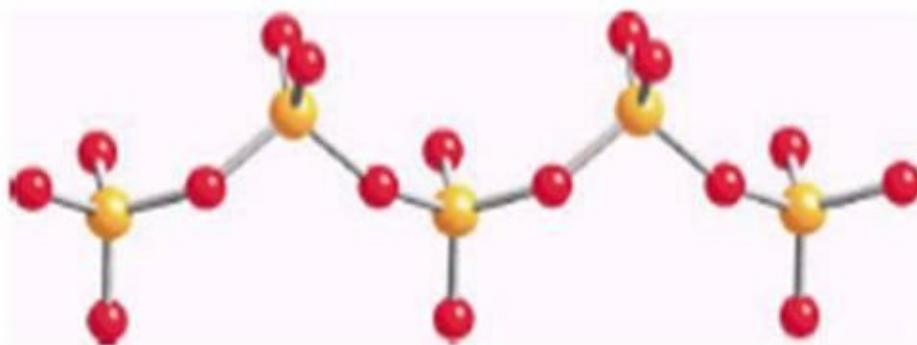
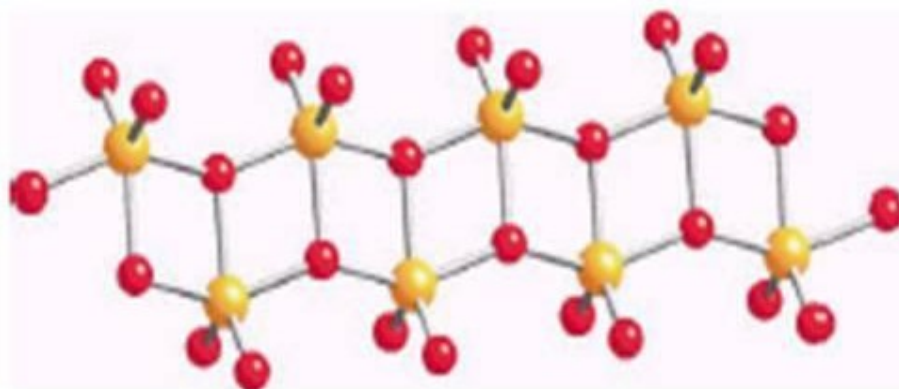


**Figure 4.2** Polyhedral representations of the structures of the  $[\text{V}_2\text{O}_7]^{4-}$  and  $[\text{V}_4\text{O}_{12}]^{4-}$  clusters; ball and stick and polyhedral views of the structure of  $[\text{V}_{10}\text{O}_{28}]^{4-}$



(a)



(b)

**Figure 4.3** Views of the one-dimensional vanadate chains of (a)  $\text{KVO}_3$  and (b)  $\square\text{-NaVO}_3$ .

Another vanadium oxide cluster is  $\text{V}_2\text{O}_5$  which shows two-dimensional vanadium oxides [38]. As shown in Fig. 4.4 the structure consists of both edge and corner-sharing of  $[\text{VO}_5]$  square pyramids. The double chains of edge-sharing polyhedra consist of a chain with the apical oxo group directed above the plane of network while the second chain shows oxo groups directed below the plane

The V (IV) oxides show a complex structural chemistry for example  $\text{VO}_2$  exhibits a rutile structure [43] shown in Fig. 4.5. The structure of  $\text{VO}_2$  is constructed from strands of edge-sharing  $[\text{VO}_6]$  octahedra linked through corner-sharing interactions between strands into a three-dimensional framework.

Mixed valenced vanadium complexes V (IV) / V (V) show rich and complex crystal chemistry [38].

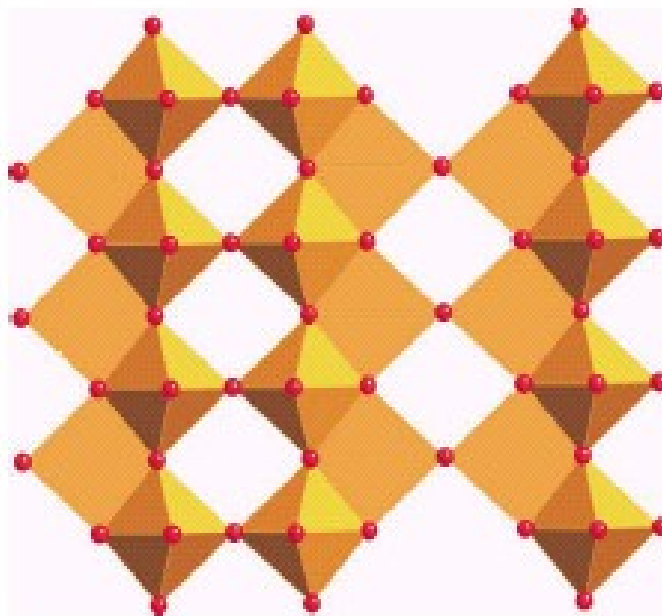


**Figure 4.4** The network structure of  $V_2O_5$ .

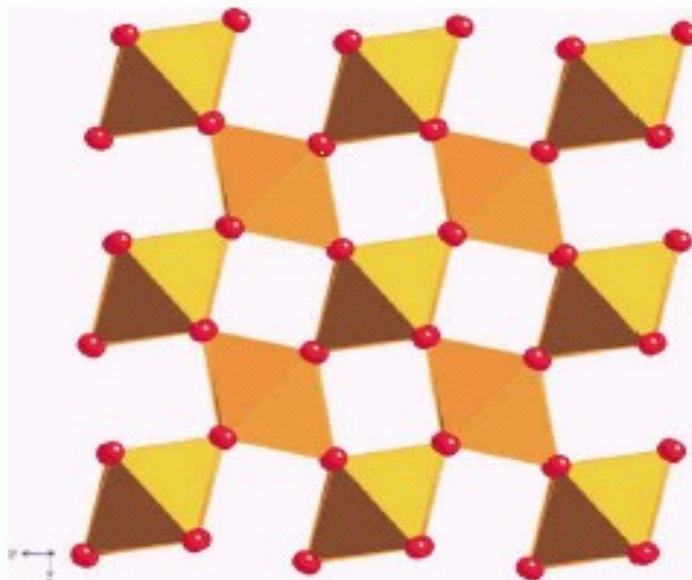


**Figure 4.5** The structure of  $VO_2$

#### 4.1.1 Influences of Organic Compounds on Vanadium Oxide Structures

Oxygen is the most abundant element on earth and also it is highly reactive. Oxygen makes bonds with most of the elements except for radon and the lighter noble gases [38].

The examples of solid state oxides are ores, gems but also bones, shells, teeth and wood used in biomineralization [44, 45].

Table 4.1 summarizes the examples and applications of inorganic oxides [38]. In the applications of vanadium oxides there are potential uses as secondary cathode materials for lithium batteries [38], in industrial oxidative catalysis [46]. Binary vanadium oxides show a metal-insulator transition used in electronic systems [47].

In nature there are many substances that contain the mixtures of inorganic oxides coexisting with organic molecules. This proves us that the organic components effect the microstructures of inorganic oxides [48].

From the synergism between organic and inorganic components organic ones change inorganic oxide microstructures. Above 1000 °C of solid-solid interaction temperatures the structural properties of organic components will not be the same. Low temperature techniques should be used in order to work with organic components.

The hydrothermal method brings many advantages in the combining organic components with inorganic structures. The first one is the decreasing viscosity of water that makes diffusion faster, so the solvent extraction of solids and the crystal growth from solution continues well [38]. The second one is the minimized solubility problems that bring many simple precursors to the media like organic and inorganic agents which are in suitable size and shape. The third one is the metastable kinetic phases under nonequilibrium conditions rather than thermodynamic phases that are isolated [49].

The organonitrogen compounds like  $R_3NH^+$  or  $H_2NCH_2CH_2NH_2$  that are used as organic components have roles as charge-compensating, space-filling and structure-directing cations [38]. The first characterized example of an oxovanadium array consists of an organic compound was reported by Jacobson in 1991 [50]. Since 1995 there have been many novel compounds described, to make a classification according to the role of the organic component there are 4 classes of vanadium oxides with organic components (Fig. 4.6):

- a) Materials where the organic component serves as an isolated cation,
- b) Phases where the organic component acts as a ligand to a vanadium site of the oxide array,
- c) Compounds where the organic ligand is bound to a secondary metal site  $M'$  as part of a coordination complex cation,
- d) Bimetallic oxide phases where the organic component is bound to a secondary metal  $M'$  which is linked to the  $V_xO_y^{n-}$  structure through oxo-bridging groups.

In type a, there are 2 subclasses, in the first one the oxide layer exhibits simple binary composition  $V_xO_y^{n-}$  and in the second one a secondary metal is incorporated into the  $M'V_xO_y^{n-}$  substructure. In type d, the subclasses are defined according to the overall dimensionality of the material: Type 1, 2 or 3 for one-, two- and three- dimensional oxide materials respectively.

The investigations have proven that the alkali and alkaline earth metals, as well as rare earth, europium and ytterbium, dissolve in liquid ammonia under normal conditions. Solubility of inorganic compounds is lower in ammonia than water because of lower dielectric constant. That's why products obtained from liquid ammonia is microcrystalline or even amorphous. High dielectric constant increase the solubility of mainly ionic solid compounds, when the energy of solution is higher than lattice energy. Dielectric constant is very dependent on temperature and density. It increases until critical temperature, at the critical temperature dielectric constant starts to decrease, because density of solvent decreases in SCF. There is a direct relationship between density and dielectric constant. Ammonia is less suitable for inorganic compounds because it has lower dielectric constant than water. Density of ammonia decreases extremely with rising temperature.



**Table 4.1** Selected examples and applications of inorganic oxides [38]

<b>Metal class</b>	<b>Examples</b>	<b>Applications</b>
Magnetic oxides	CrO <sub>2</sub> , ferrites, spinels	Magnetic tapes, transformer cores, computer memories
Oxide sensors	BaTiO <sub>3</sub> , PbZrO <sub>3</sub>	Temperature sensors, piezo speakers
Phosphors	Doped Zn <sub>2</sub> SiO <sub>4</sub> , Y <sub>2</sub> O <sub>3</sub>	Oscilloscope tubes
Electronic materials	BaTiO <sub>3</sub> , ZnO	Surge protectors, high T semiconductors
Ceramics	Al <sub>2</sub> O <sub>3</sub> , PbZr <sub>1-x</sub> Ti <sub>x</sub> O <sub>3</sub>	Ferroelectrics
Catalysts	(VO) <sub>2</sub> P <sub>2</sub> O <sub>7</sub> , Bi <sub>2</sub> Mo <sub>2</sub> O <sub>9</sub> , V <sub>2</sub> O <sub>5</sub> / TiO <sub>2</sub> , SiO <sub>2</sub> WO <sub>3</sub>	Selective oxidations, polymerization, oxidative dehydrogenation, cracking, alkylation
Ion exchange	NASICON, zeolites	Fast ion conductors, detergents
Molecular sieves	Zeolites	Separating agents
Biomaterials	Organoapatites	Artificial bone
Optical materials	LiNbO <sub>3</sub> , KTiOPO <sub>4</sub> , Nd: YAG, Cr-doped Al <sub>2</sub> O <sub>3</sub>	Harmonic generators, frequency mixers, lasers
Construction oxides	CaO	Concrete, trap for desulfurization
High temperature materials	Vitreous silica	1000–1300 °C containers

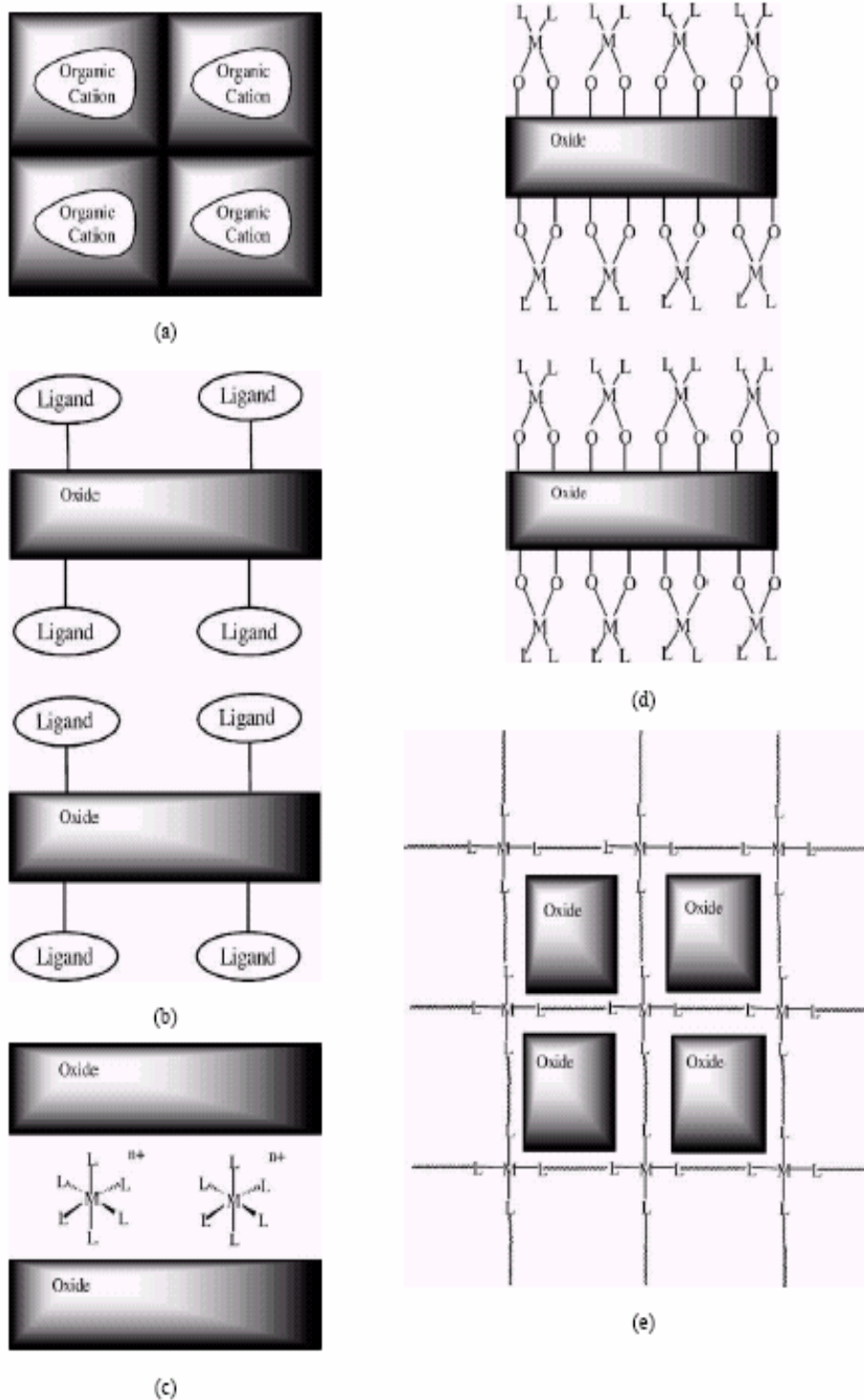


**Figure 4.6** Schematic representations of various modes of involvement of organonitrogen components in vanadium oxide materials: (a) as a counter cation, (b) as a ligand to the  $V_xO_y^{n-}$  substructure, (c) as a ligand to a secondary metal  $M$  in a coordination complex cation, (d) as a ligand to a secondary metal  $M$  which is incorporated into a bimetallic oxide substructure, and (e) as a ligand and a bridging unit in a secondary metal–ligand network.

## 4.2 Most Synthesized Metal Oxides

The most studied chemical reaction under hydrothermal conditions is the crystal growth of  $\alpha$ -quartz. Each year over half a million kilograms of high quality single crystals of quartz are prepared. It is used mostly in the cellular phones [4]. The other well-prepared metal oxides are  $\text{Al}_2\text{O}_3$  and  $\text{ZnO}$ . These reactions need hydroxide as a mineralizer, temperatures around  $400\text{ }^\circ\text{C}$ , temperature gradient of  $40\text{-}80\text{ }^\circ\text{C}$  and a degree of fill between 60 and 80 %. These fills form pressures about 700-800 bar.

Transition metal oxides have very interesting magnetic and electronic properties, so they are produced hydrothermally. Some examples are iron oxides, as magnetite and hematite [51], barium ferrites which have applications as memory devices [52-54],  $\text{AgFeO}_2$  [54], several alkali iron titanium bronzes [55], manganese oxides [56], garnets which have optical and magnetic applications [57, 58]. Hydrothermal syntheses of other magnetic oxides have been reviewed in detail [4]. Oxides of d-block metals were also grown hydrothermally [59].

Laboratory synthesis of gems also attracted great interest. The synthesis of a gem called ruby in aqueous base above  $425\text{ }^\circ\text{C}$  is another example [60]. In cultured gem synthesis hydrothermal fluids are most used for quartz-based gems such as topaz, citrine and amethyst. Another gem synthesized by this method commercially is emerald prepared by Lechleitner first in about 1960.

Because of the cost of the technique and the decreased value of synthetic gems to natural ones, their hydrothermal syntheses are not economical.

The most important hydrothermal synthesis of gems is the synthesis of diamond from graphite in SC  $\text{H}_2\text{O}$  at  $800\text{ }^\circ\text{C}$  and 1700 bar [4].

## 4.3 Synthesis and Characterization of $[\text{Ni}(\text{en})_3(\text{VO}_3)_2]$

### 4.3.1 Introduction

In our laboratory amines such as ethylenediamine (en) have been used as solvents. Ethylenediamine has a critical temperature of ( $T_c$ )  $320\text{ }^\circ\text{C}$  and a boiling point (bp) of  $116.9\text{ }^\circ\text{C}$ . Because its critical temperature is not very high we did the synthesis

in the temperature of 160 °C. The compound [Ni (en)<sub>3</sub>(VO<sub>3</sub>)<sub>2</sub>] was synthesized and the structure solution of this compound was done by the SHELX software in our laboratory.

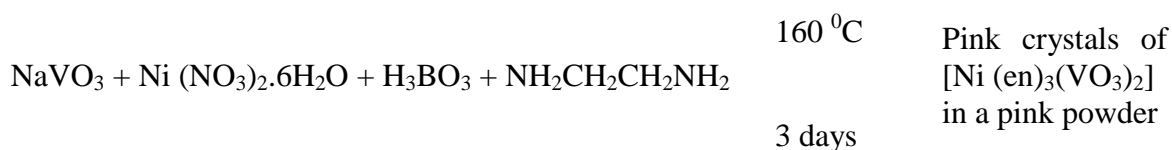
## 4.3.2 Experimental Procedure

### 4.3.2.1 Synthesis

Pink hexagonal shaped single crystals of [Ni (en)<sub>3</sub>(VO<sub>3</sub>)<sub>2</sub>] were obtained from the reaction of NaVO<sub>3</sub> (0.1219 g, 0.001 mole), Ni(NO<sub>3</sub>)<sub>2</sub>.6H<sub>2</sub>O (0.2908 g, 0.001 mole), H<sub>3</sub>BO<sub>3</sub> (0.1237 g, 0.002 mole). The following reagents were used as obtained: NaVO<sub>3</sub> (Fluka, >98 %), Ni (NO<sub>3</sub>)<sub>2</sub>.6H<sub>2</sub>O (Panreac, 98 %), H<sub>3</sub>BO<sub>3</sub> (Carlo Erba, 99.5-100.5 %) and NH<sub>2</sub>CH<sub>2</sub>CH<sub>2</sub>NH<sub>2</sub> (Merck, 0.9 kg/L, 99 %).

A reaction mixture was loaded into a 23 mL autoclave. Then 5 M, 9 mL (66% fill) of ethylenediamine (en) was added to the starting solids. The autoclave was then sealed and heated at 160 °C for 3 days; a purple solution was obtained after cooling to room temperature slowly. The products were filtered then washed with ultra pure water and acetone several times in order to clean the solid product from ethylenediamine contamination. The single crystals of the compound [Ni (en)<sub>3</sub>(VO<sub>3</sub>)<sub>2</sub>] (Fig. 4.7) were selected from the pink powder by a needle. They were then kept in the mineral oil. The reaction occurred as below:

The reactants are in the (1: 1: 2: 45) mole ratio. (5 M, 9 mL en is added)



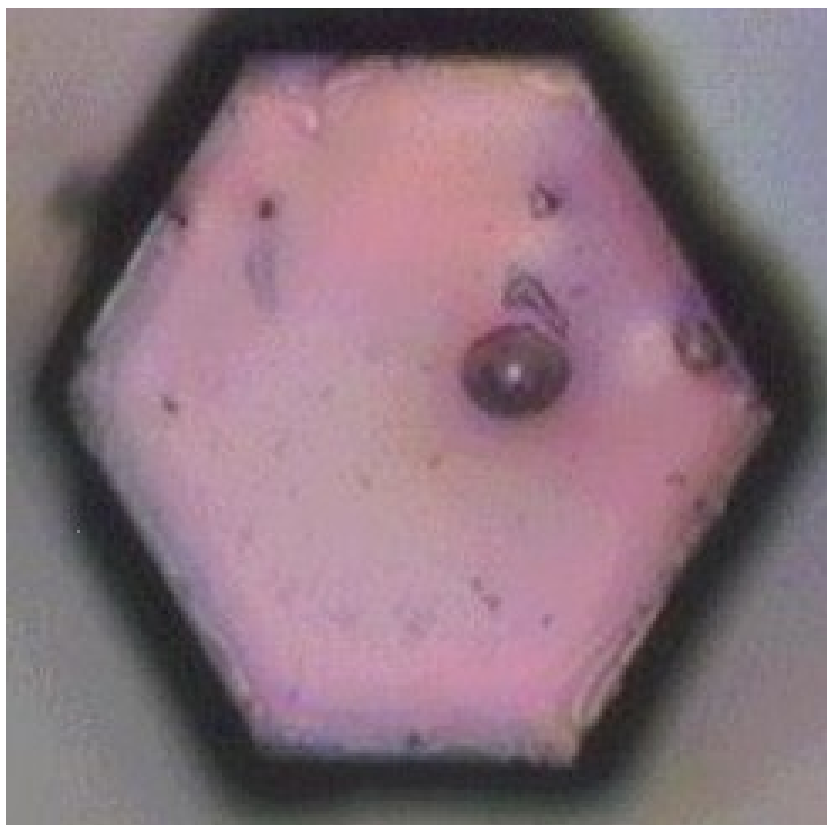
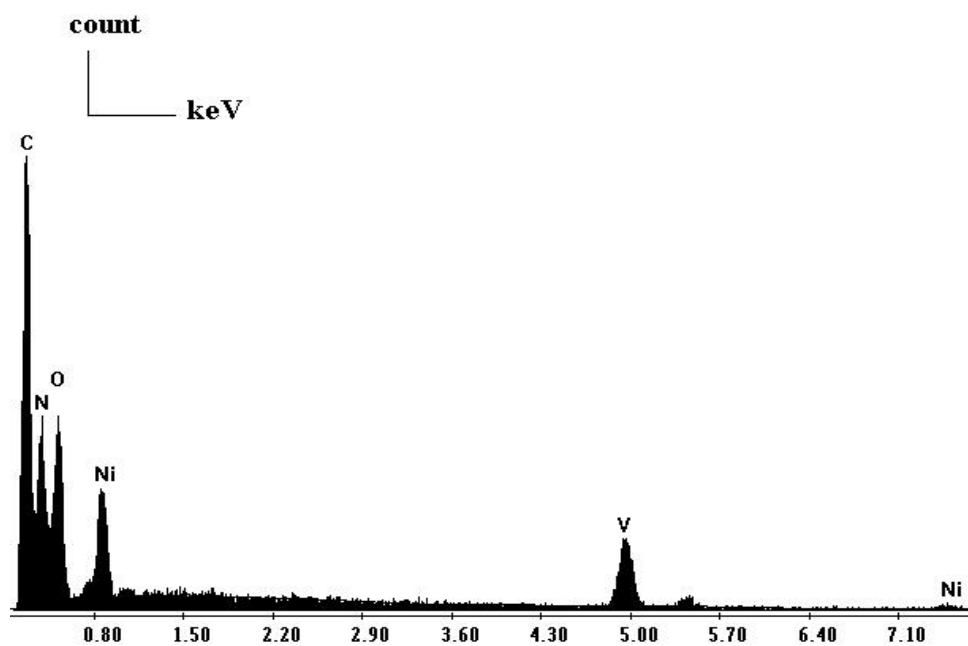


**Figure 4.7** A single crystal of  $[\text{Ni}(\text{en})_3(\text{VO}_3)_2]$

In order to obtain good quality and strict shaped of single crystals we had changed the ratios of the reagents such as (1: 2: 2), (1: 2: 1), (2: 1: 1). The result of the (1: 2: 2) ratio of the reaction was the dark pink bulks in a pinky powder. The crystal forms were observed from the reactions of remaining ratios. From the ratio of (1: 2: 1) we obtained more pink crystals. After the reaction of the ratio (1: 1: 2) an orange solution was filtered to get the crystals. We obtained pink crystals in the size of approximately 0.5-1 mm and in the 30 % yield.

The SEM EDX results of the pink hexagonal shaped crystals are shown in Fig. 4.8 These results show that in this compound we have carbon, nitrogen, oxygen, vanadium and nickel elements in the atomic percentages of 38.66 %, 33.36 %, 22.61 %, 4.09 %, and 1.28 % respectively. The X-ray powder peaks of the  $[\text{Ni}(\text{en})_3(\text{VO}_3)_2]$  compound are shown in Fig. 4.9



Wt % C K: 29.45, N K: 29.64, O K: 22.94, V K: 13.20, NiK: 4.78

At % C K: 38.66, N K: 33.36, O K: 22.61, V K: 4.09, NiK: 1.28

Figure 4.8 SEM EDAX graph of the [Ni(en)<sub>3</sub>(VO<sub>3</sub>)<sub>2</sub>] compound

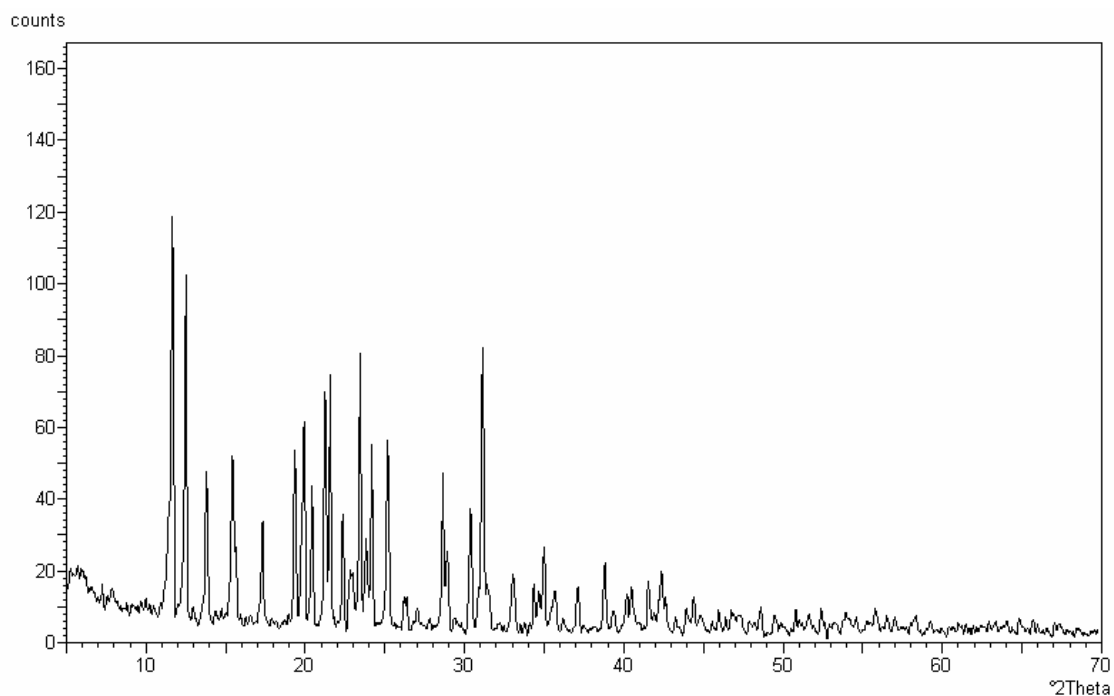


Figure 4.9 The X-ray powder of the [Ni(en)<sub>3</sub>(VO<sub>3</sub>)<sub>2</sub>] compound

### 4.3.2.2 X-Ray Crystallographic Analyses

A crystal of  $[\text{Ni}(\text{en})_3(\text{VO}_3)_2]$  was mounted on a glass fiber with epoxy glue and centered on the four-circle Rigaku AFC8 diffractometer equipped with a Mercury CCD area detector. Data were collected at room temperature ( $\sim 300\text{K}$ ) using graphite monochromated Mo  $K\alpha$  ( $\lambda = 0.71073 \text{ \AA}$ ) radiation. The crystal-to-detector distance was approximately 30 mm. The Crystal Clear software by MSC was used to collect a Ewald hemisphere of data up to a reciprocal resolution of  $(\sin\theta / \lambda)_{\text{max}} = 0.69 \text{ \AA}^{-1}$ . Each frame was recorded as a  $\omega$  scan of  $1^\circ$  with an X-ray exposure time of 30s for every compound. A separate scan was recorded to cover a blind area of the reciprocal space close to the spindle axis of the first scan. A total of 240 frames were recorded for each compound. Each frame was recorded twice to eliminate ‘zinger’ spots from cosmic radiation. The data acquisition took approximately 4h.

The unit cell parameters and the orientation matrix were initially determined from a set of seven screening frames taken at equal intervals of  $30^\circ$  in  $\omega$  using a 1D Fourier algorithm. Reflection indexing, Lorentz-polarization correction, peak integration and background determination were performed using the Crystal Clear software. A box size of  $15 \times 15$  pixels (each pixel corresponds to about  $140 \mu\text{m}$ ) was used for the integration of all reflections. Unit cell parameters were refined after integration using all observed reflections to yield the following values:  $a = 8.9940 (13) \text{ \AA}$ ,  $b = 8.9940 (13) \text{ \AA}$ ,  $c = 34.001 (7) \text{ \AA}$ ,  $\alpha = 90^\circ$ ,  $\beta = 120^\circ$  and  $\gamma = 90^\circ$  for  $\text{Ni}(\text{en})_3(\text{VO}_3)_2$ .

An empirical absorption correction was applied using a REQABA routine in the Crystal Clear software package. The data were merged and averaged in Laue group 6 yielding an internal agreement factor of  $R_m = 0.1408$  for  $\text{Ni}(\text{en})_3(\text{VO}_3)_2$ . A total of 19169 reflections were used for structure elucidation. Of these 3246 reflections were independent with  $I > 2\sigma(I)$  were used in the refinement. The structure was solved by direct methods SIR-92 and refined on  $f$  by full matrix, least squares techniques with TEXSAN [61] and SHELXTL-PLUS [62]. All atomic thermal parameters were refined anisotropically. Crystallographic data are given in Table 4.2. All bond distances and angles are given in Table 4.3. Atomic coordinates and equivalent isotropic displacement parameters are given in Table 4.4.

**Table 4.2** Crystallographic Data for [Ni(en)<sub>3</sub>(VO<sub>3</sub>)<sub>2</sub>]

Empirical formula	[Ni(en) <sub>3</sub> (VO <sub>3</sub> ) <sub>2</sub> ]
Formula weight	436.90
Temperature	293 (2) K
Wavelength	0.71073 Å
Crystal system, space group	Hexagonal, P6 <sub>1</sub>
Unit cell dimensions	a = 8.9940 (13) Å $\alpha = 90^\circ$ b = 8.9940 (13) Å $\beta = 90^\circ$ c = 34.001 (7) Å $\gamma = 120^\circ$
Volume	2381.9 (7) Å <sup>3</sup>
Z, Calculated density	17, 1.807 Mg / m <sup>3</sup>
Absorption coefficient	0.932 mm <sup>-1</sup>
F (000)	1260
Theta range for data collection	2.61 to 26.37 <sup>0</sup>
Limiting indices	-11 ≤ h ≤ 11, -11 ≤ k ≤ 10, -42 ≤ l ≤ 42
Reflections collected / unique	19169 / 3246 [R(int) = 0.1408]
Completeness to theta	26.37    99.9 %
Refinement method	Full-matrix least-squares on F <sup>2</sup>
Data / restraints / parameters	3246 / 1 / 86
Goodness-of-fit on F <sup>2</sup>	1.284
Final R indices [I > 2σ(I)]	R1 = 0.0882, wR2 = 0.2009
R indices (all data)	R1 = 0.1057, wR2 = 0.2097
Extinction coefficient	0.014 (3)
Largest diffraction peak and hole	1.197 and -0.811 e. Å <sup>-3</sup>



**Table 4.3** Bond lengths [ $\text{\AA}$ ] and angles [ $^\circ$ ] for  $[\text{Ni}(\text{en})_3(\text{VO}_3)_2]$ 

Ni1-N5	1.86 (3)	V1-O14	1.01 (2)
Ni1-N12	1.97 (4)	V1-O15	1.74 (3)
Ni1-N8	1.87 (10)	V1-O17	1.90 (6)
Ni1-N9	2.30 (4)	V1-O13	2.06 (5)
Ni1-N1	2.37 (3)	V2-O18	1.42 (6)
Ni1-N4	2.69 (10)	V2-O15	1.81 (4)
		V2-O17	1.86 (6)
		V2-O16	2.15 (2)

N1-Ni1-N4	78.6 (12)	O14-V1-O15	108 (2)
N5-Ni1-N12	87 (2)	O14-V1-O17	106 (2)
N5-Ni1-N8	72 (3)	O15-V1-O17	107.6 (18)
N12-Ni1-N8	107.4 (14)	O14-V1-O13	104.4 (18)
N-Ni1-N9	102.6 (18)	O15-V1-O13	102.0 (19)
N12-Ni1-N9	66 (2)	O17-V1-O13	127.4 (15)
N8-Ni1-N9	172 (2)	O18-V2-O15	100 (2)
N5-Ni1-N1	95.4 (19)	O18-V2-O17	136 (3)
N12-Ni1-N1	154.2 (9)	O15-V2-O17	113 (2)
N8-Ni1-N1	97.8 (15)	O18-V2-O16	104 (3)
N9-Ni1-N1	89 (2)	O15-V2-O16	97 (2)
N5-Ni1-N4	162.1 (16)	O17-V2-O16	99 (2)
N12-Ni1-N4	105.4 (15)		
N8-Ni1-N4	92 (3)		
N9-Ni1-N4	94.2 (16)		

**Table 4.4** Atomic coordinates ( $\times 10^4$ ) and equivalent isotropic displacement parameters ( $\text{\AA}^2 \times 10^3$ ) for  $[\text{Ni}(\text{en})_3(\text{VO}_3)_2]$

	x	y	z	Ueq
Ni1	0.37417	0.92573	0.01797	0.02370
N1	0.43016	0.84026	-0.03529	0.04073
C2	0.43906	0.68434	-0.02698	0.05498
C3	0.52705	0.70643	0.01313	0.05503
N4	0.43087	0.74366	0.04276	0.03391
N5	0.35267	1.12156	-0.01173	0.03788
C6	0.52779	1.26725	-0.01872	0.04065
C7	0.63691	1.29215	0.01724	0.03952
N8	0.62987	1.12930	0.02653	0.03092
N9	0.10347	0.74410	0.01411	0.03640
C10	0.01558	0.78507	0.04559	0.03978
C11	0.12502	0.83296	0.08240	0.03860
N12	0.30073	0.97693	0.07370	0.02964
V1	-0.01289	0.21797	-0.04561	0.02651
V2	0.07876	0.26277	0.05239	0.02372
O13	0.02585	0.41478	-0.05014	0.06231
O14	-0.21386	0.09190	-0.05567	0.05604
O15	0.02926	0.17673	0.00336	0.04421
O16	0.27171	0.30198	0.06340	0.04699
O17	-0.06736	0.10941	0.08636	0.05712
O18	0.07459	0.44003	0.05501	0.04109

#### 4.3.3 Results and Discussion

Unit cell structure of  $[\text{Ni}(\text{en})_3(\text{VO}_3)_2]$  composed of  $\text{VO}_4$  tetrahedra which are joined with others by sharing corners into infinite chains running along the c axis. The complex cation  $[\text{Ni}(\text{en})_3]^{2+}$  are located between the chains as shown in Figure 4.10. The chain in the compound has a repetitive sequence of 12-nuclear corner-sharing tetrahedra. The bridging oxygen atoms between two adjacent  $\text{VO}_4$  tetrahedras have V-O bond lengths ranging from 1.74 and 1.81  $\text{\AA}$ . There are also terminal oxygen atoms that have shorter V-O bonds ranging from 1.01 and 2.15  $\text{\AA}$ . Geometry around two unique vanadium atoms are distorted tetrahedra. O-V1-O bond angles ranges from 102 to 127.4 $^\circ$  and O-V2-O bond angles ranges from 97.00 to 136 $^\circ$ . Expected bond angles for tetrahedron is 109.5 $^\circ$

Figure 4.11 shows  $[\text{Ni}(\text{en})_3]^{2+}$  complex has a distorted octahedral geometry. Ni-N bond distances range from 1.86 to 2.69 Å. Bond angles are from 66 to 162.1°. These complexes reside between vanadium chains. There are only electrostatic interactions and hydrogen bonding between the vanadium oxide chains and  $[\text{Ni}(\text{en})_3]^{2+}$  complexes.

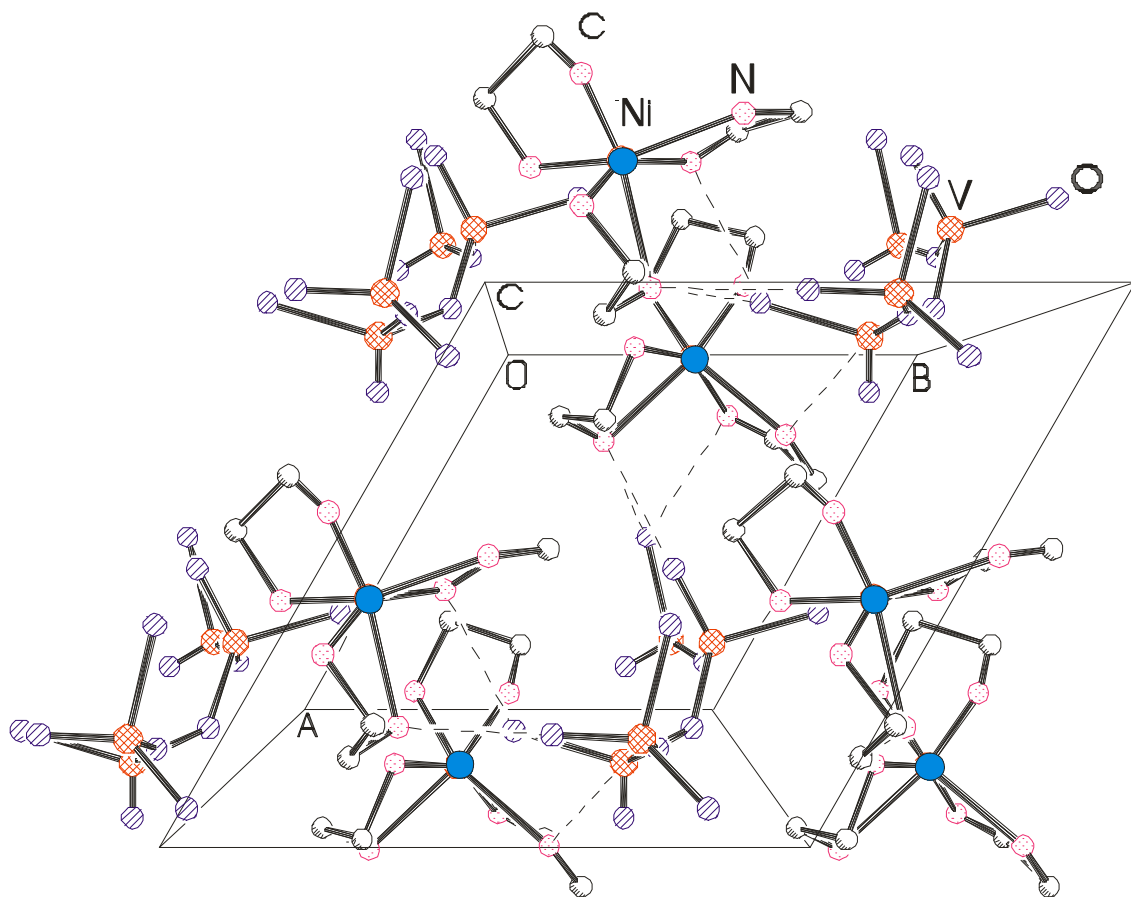


**Figure 4.10** Unit cell picture of  $[\text{Ni}(\text{en})_3(\text{VO}_3)_2]$

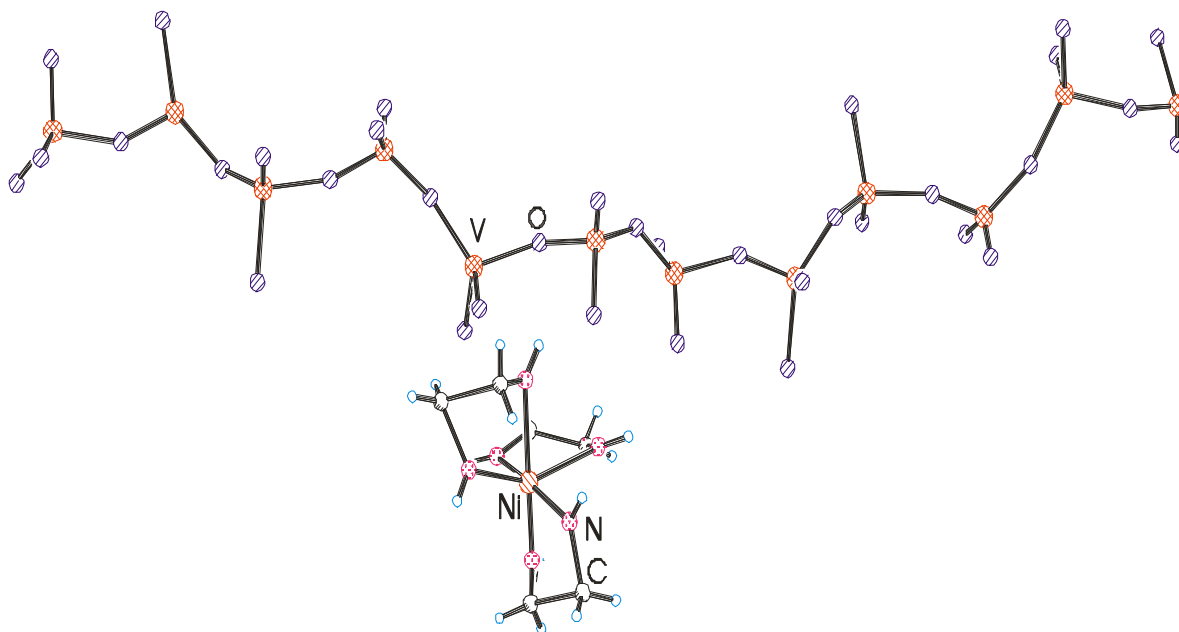


**Figure 4.11**  $[\text{Ni}(\text{en})_3]^{2+}$  complex between vanadium chains

#### 4.4 Some Other Synthesized Vanadium Compounds

-Yellow rod shaped crystals-

The red prisms of  $\text{CoV}_2\text{O}_6(\text{H}_2\text{O})_2$  were obtained from the reaction of  $\text{NaVO}_3$  (0.1219 g, 0.001 mole),  $\text{GeO}_2$  (0.1046 g, 0.001 mole),  $\text{H}_3\text{BO}_3$  (0.0618 g, 0.001 mole),  $\text{CoCl}_2 \cdot 6\text{H}_2\text{O}$  (0.238 g) with yellow rod shaped (Fig. 4.12) crystals in a red powder. The following reagents were used as obtained:  $\text{NaVO}_3$  (Fluka, >98 %),  $\text{GeO}_2$  (ABCR, 99.98 %),  $\text{H}_3\text{BO}_3$  (Carlo Erba, 99.5-100.5 %) and  $\text{CoCl}_2 \cdot 6\text{H}_2\text{O}$  (Riedel, >99 %).

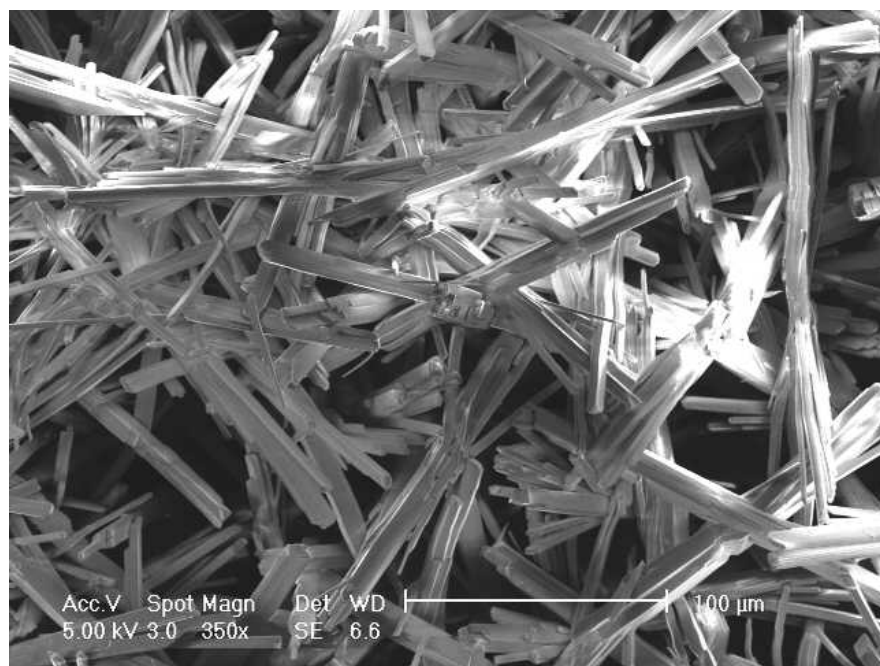
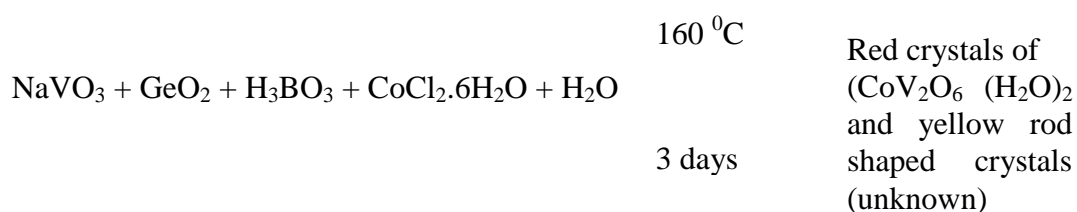
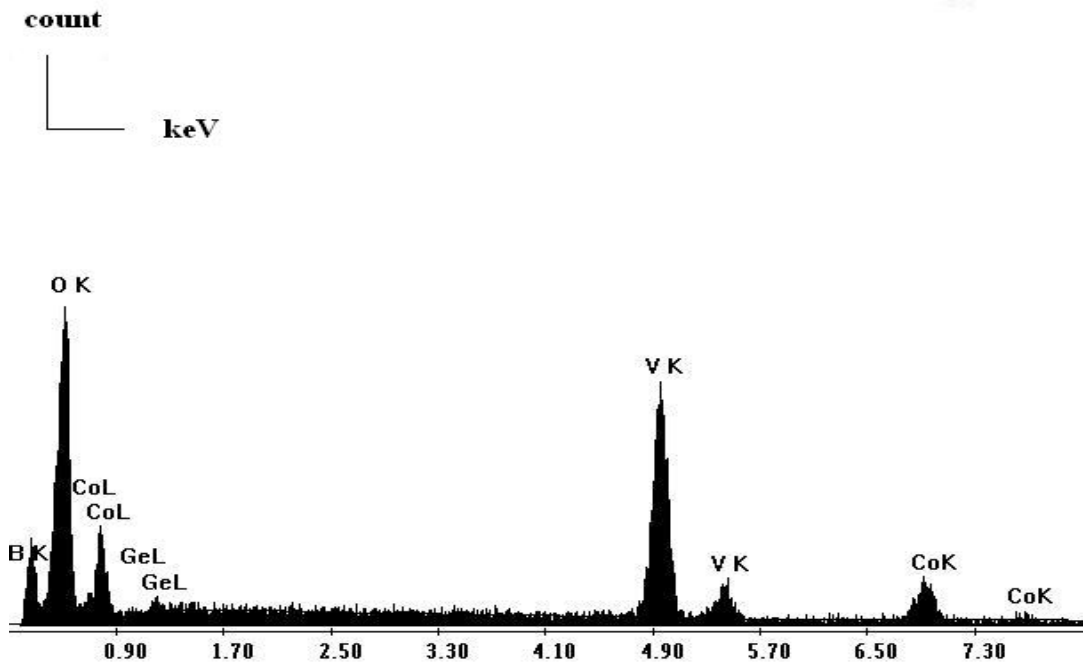


**Figure 4.12** Yellow rod shaped crystals

The reactants are in the (1: 1: 1: 1: 500) mole ratio. (9 mL water is added)



We obtained air-stable yellow crystals in the yield of 40 %. The SEM EDX results of the yellow rod shaped crystals are shown in Fig. 4.13 and their X-ray powder peaks which did not match with any compound in the XRD powder data base are shown in Fig. 4.14



Wt % B K: 11.92, O K: 38.67, V K: 32.63, Co K: 15.06, GeL: 1.72

At % B K: 24.83, O K: 54.45, V K: 14.43, Co K: 5.76, GeL: 0.54

Figure 4.13 SEM EDX graph of the yellow rod crystals

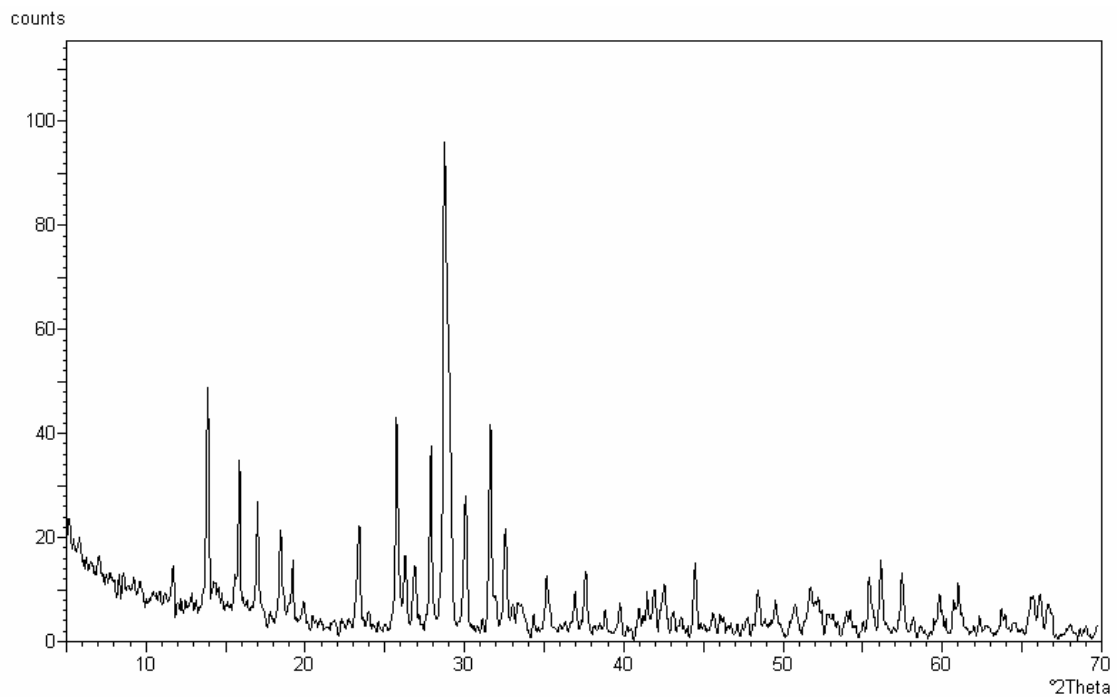
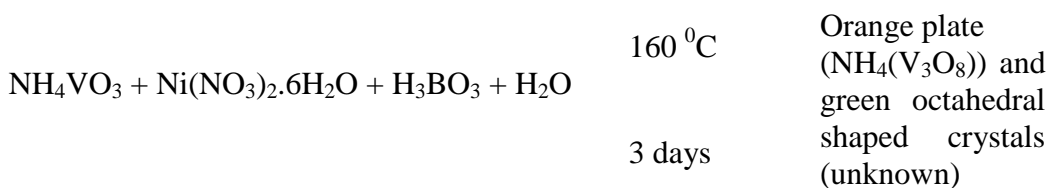


Figure 4.14 The X-ray powder peaks of the rod shaped yellow crystals

-Green octahedral shaped crystals-

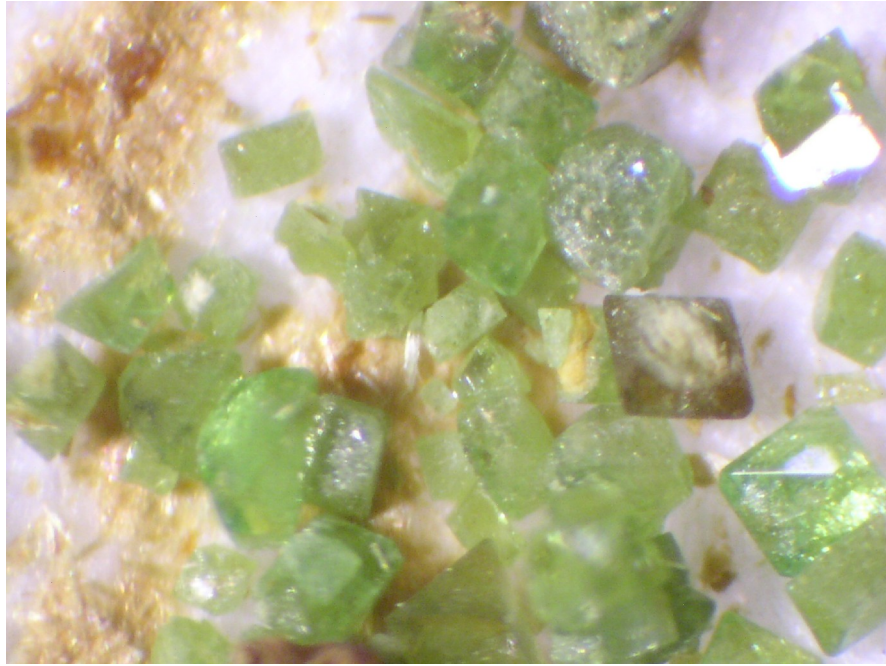
By reacting the compounds of  $\text{NH}_4\text{VO}_3$ ,  $\text{Ni}(\text{NO}_3)_2 \cdot 6\text{H}_2\text{O}$  and  $\text{H}_3\text{BO}_3$  in the water solvent green octahedral shaped crystals (Fig. 4.15) were obtained via the orange plate ones. After the SEM / EDX and X-ray single crystal results we concluded that the orange plates are ammonium vanadium oxides which have the formula of  $\text{NH}_4(\text{V}_3\text{O}_8)$ . The reaction occurred as below:

The reactants are in the (1: 1: 1: 500) mole ratio. (9 mL water is added)

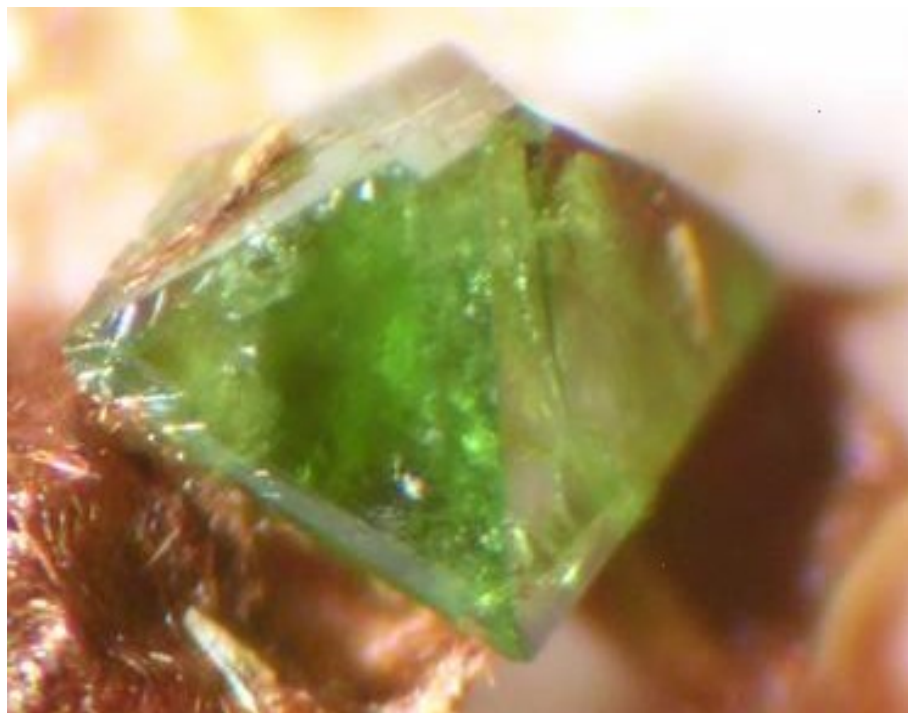


Similar reactions were tried with different ratios, such as 1: 2: 1, 1: 1: 2, 2: 1: 1, 1: 1: 1 and 1: 2: 2 with  $\text{NaVO}_3$  instead of  $\text{NH}_4\text{VO}_3$ . These different reaction ratios were applied for the aim of finding the more clear and better green octahedral crystals. It is the 1: 1: 1 ratio which we had the best ones. Also by these ratios the changing amount of the products were observed. We obtained air-stable green crystals in the size of approximately 1-2 mm with the yield of more than 30 %.

The SEM EDX results of the green octahedral shaped crystals are shown in Fig. 4.16 and their X-ray powder peaks which did not match with any compound in the XRD powder data base are shown in Fig. 4.17



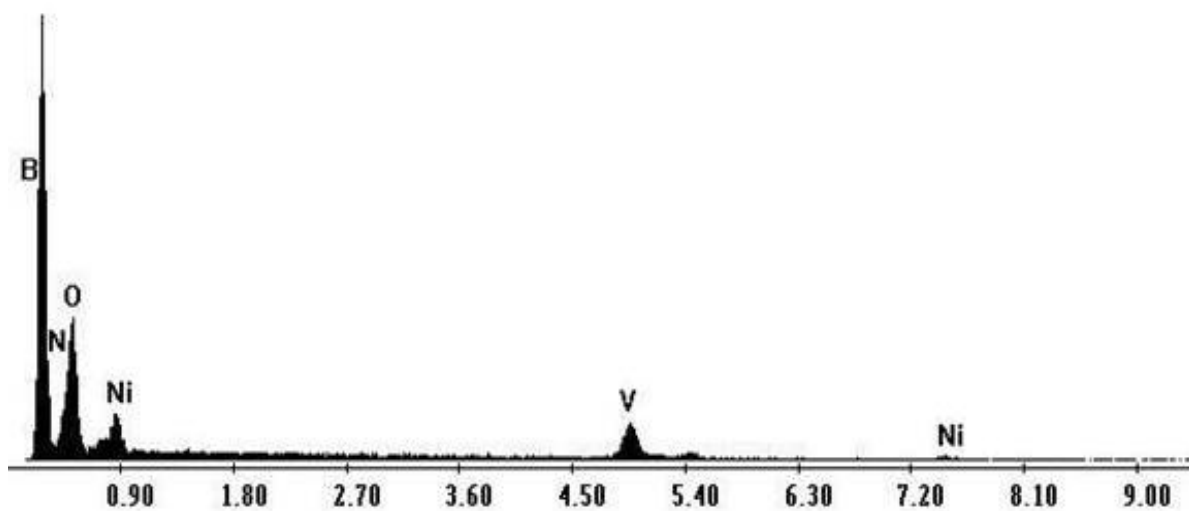
**(a)** A large view of green octahedral crystals



**(b)** One of the green octahedral crystals

Figure 4.15 Two different views of the green octahedral shaped crystals





Wt % B K: 25.25, O K: 35.38, V K: 22.60, N K: 7.46, Ni K: 9.31

At % B K: 41.10, O K: 38.93, V K: 7.81, N K: 9.37, Ni K: 2.79

Figure 4.16 SEM EDX graph of the green octahedral shaped crystals

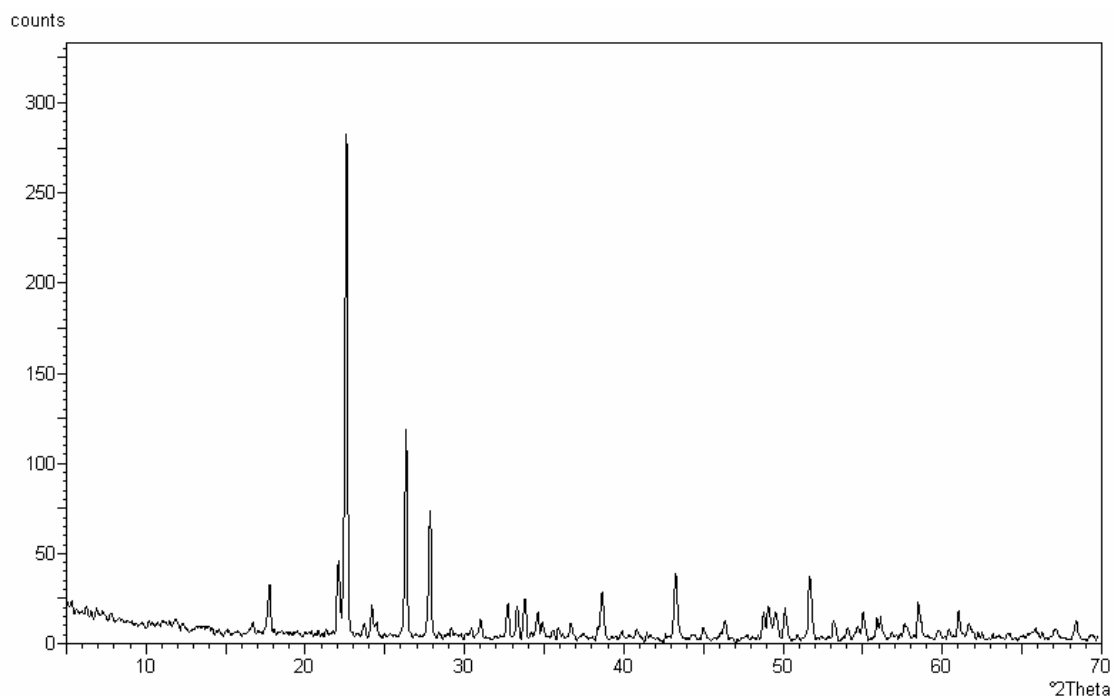
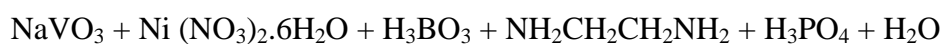


Figure 4.17 XRD peaks of the green octahedral shaped crystals

*-A bulk of green crystals-*

A bulk of attached rectangular yellowish green crystals were obtained from the reaction of  $\text{NaVO}_3$  (0.06097 g, 0.0005 mole),  $\text{Ni}(\text{NO}_3)_2 \cdot 6\text{H}_2\text{O}$  (0.1454 g, 0.0005 mole),  $\text{H}_3\text{BO}_3$  (0.0309 g, 0.0005 mole). The following reagents were used as obtained:  $\text{NaVO}_3$  (Fluka, >98 %),  $\text{Ni}(\text{NO}_3)_2 \cdot 6\text{H}_2\text{O}$  (Panreac, 98 %),  $\text{H}_3\text{BO}_3$  (Carlo Erba, 99.5-100.5 %) and  $\text{NH}_2\text{CH}_2\text{CH}_2\text{NH}_2$  (Merck, 0.9kg/L, 99%) and  $\text{H}_3\text{PO}_4$  (Kimetsan, 1.7 g/mL, 85.88%).

The reactants are in the (1: 1: 1: 20: 20: 0.96) mole ratio.(5 M, 0.2 mL of en, 5 M, 0.2 mL of phosphoric acid, 8.6 mL of water were added). The green rectangular shaped crystals are shown in Fig. 4.18. The reaction occurred as below:



160 °C

Green crystals  
(unknown)

3 days

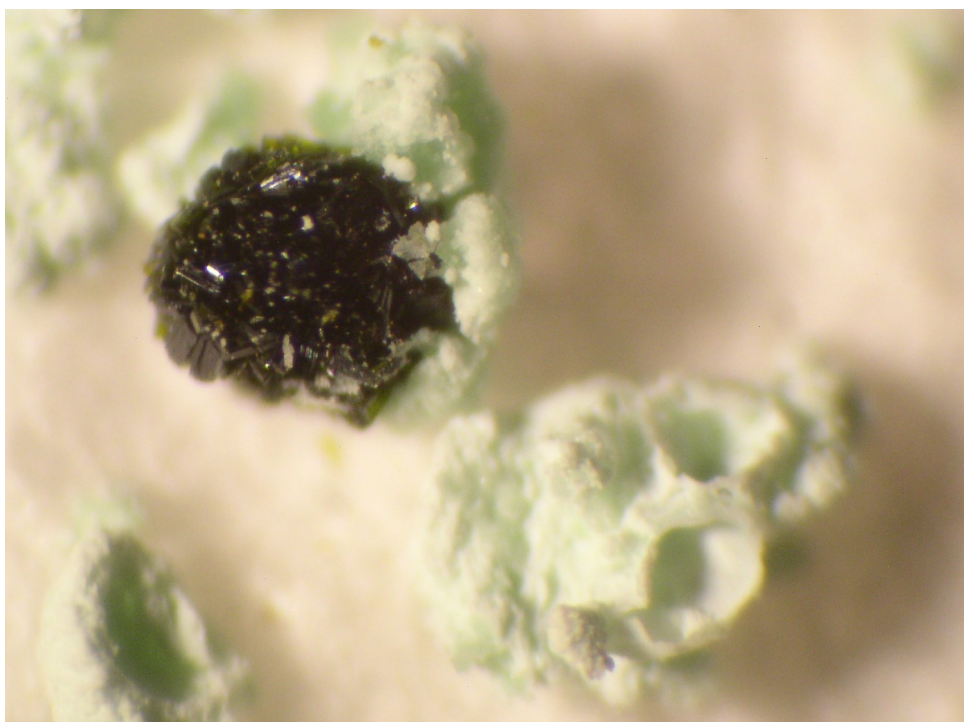
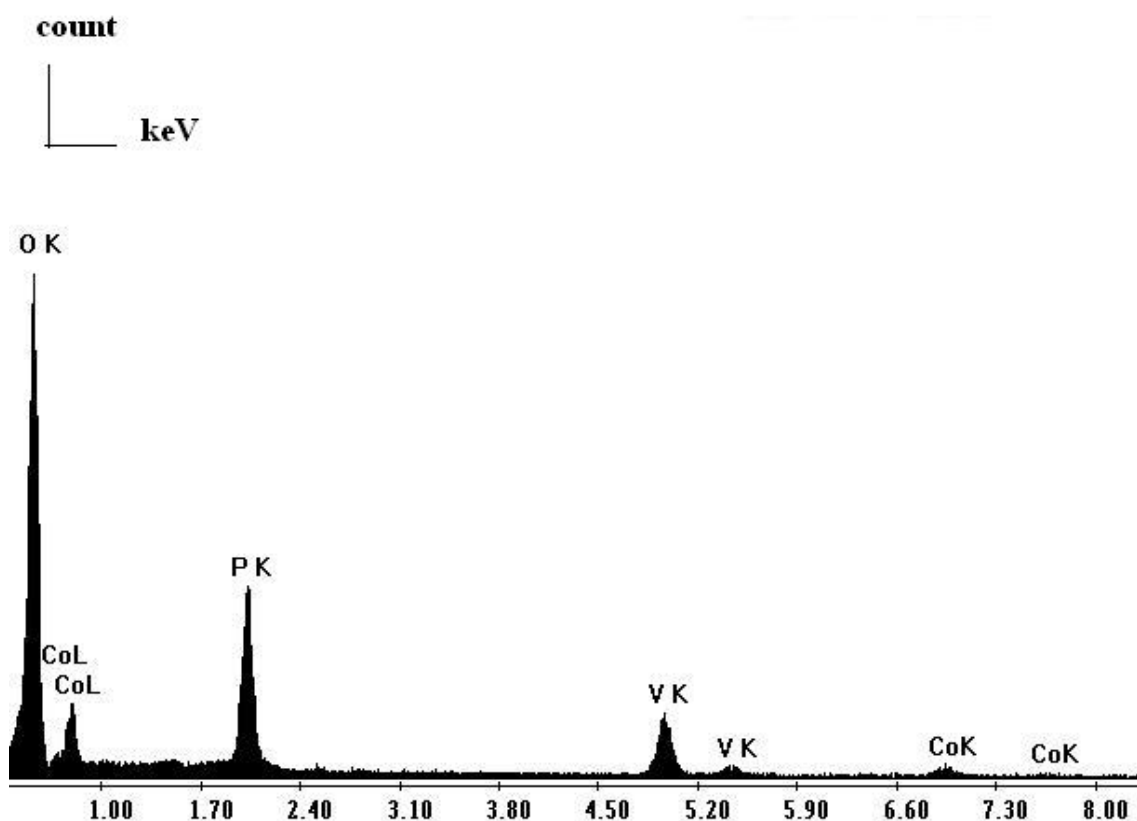


**Figure 4.18** A bulk of dark green crystals attached together in a light green pure powder

We obtained air-stable green crystals in the size of approximately 0.5-1 mm and with the yield of 30 %. The SEM EDX results of the bulk of dark green crystals are shown in Fig. 4.19 and their X-ray powder peaks which did not match with any compound in the XRD powder data base are shown in Fig. 4.20



Wt % O K: 63.79, V K: 15.23, P K: 13.78, Co K: 7.19

At % O K: 82.16, V K: 6.16, P K: 9.17, Co K: 2.51

Figure 4.19 The SEM EDX peaks of the bulk of dark green crystals

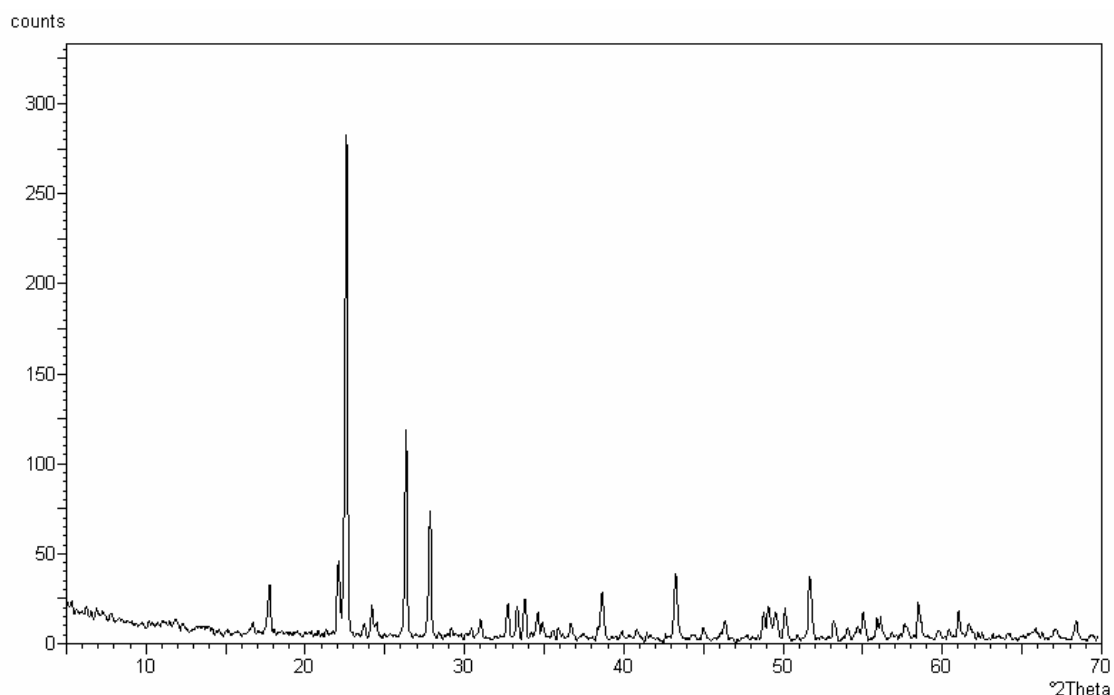


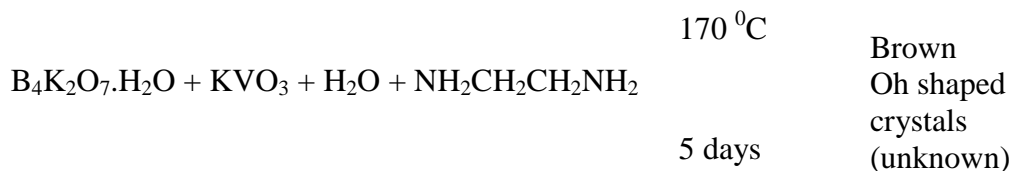
**Figure 4.20** The X-ray powder peaks of the bulk of dark green crystals

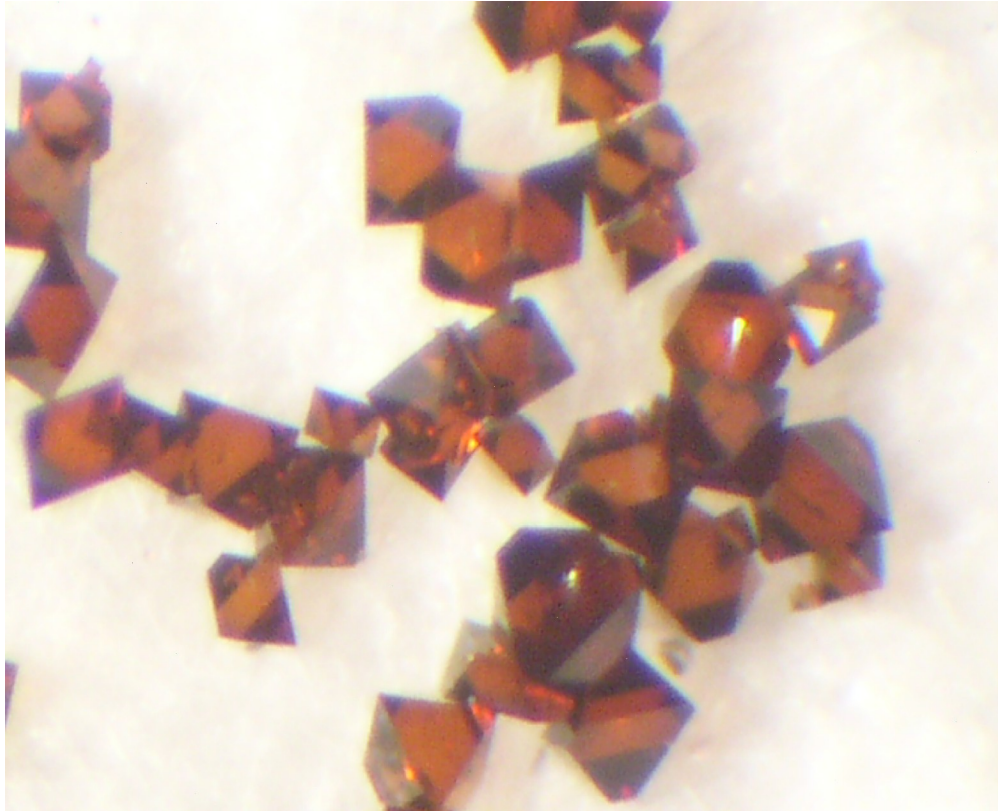
-Brown octahedral shaped crystals-

From the reaction of  $B_4K_2O_7 \cdot H_2O$  (0.9776 g, 0.0032 mole),  $KVO_3$  (0.0552 g, 0.0004 mole) brown octahedral shaped crystals were yielded. The following reagents were used as obtained:  $B_4K_2O_7 \cdot H_2O$  (Fluka, >99 %),  $KVO_3$  (Aldrich, 98 %) and  $NH_2CH_2CH_2NH_2$  (Merck, 0.9 kg/L, 99 %).

Small amount of brown octahedral shaped (Oh) crystals (Fig. 4.21) were obtained without any powder. The reaction occurred as below:

The reactants are in the (8: 1: 0.5: 2) mole ratio.





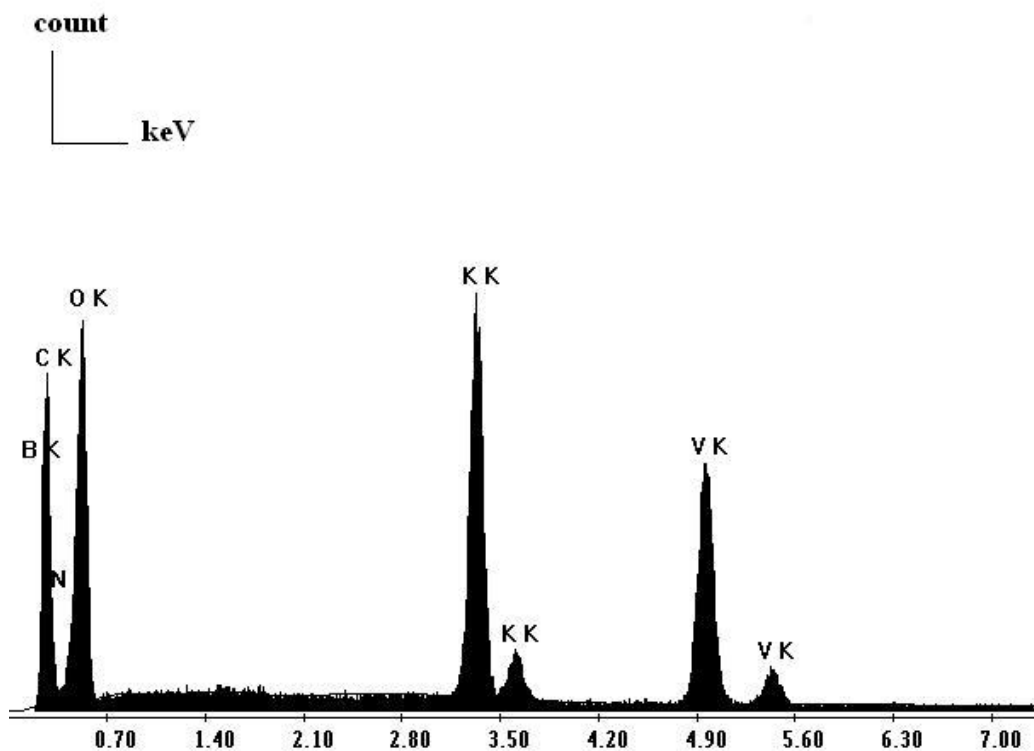
(a)



(b)

**Figure 4.21** Two different views of the brown octahedral shaped single crystals

We obtained air stable brown octahedral crystals in the size of approximately 0.5-1 mm with the yield of more than 70 %. The SEM EDX results of the brown octahedral shaped crystals are shown in Fig. 4.22.



Wt % B K: 4.96, C K: 22.65, N K: 4.71, O K: 32.16, K K: 14.97, V K: 20.54  
 At % B K: 8.38, C K: 34.43, N K: 6.14, O K: 36.70, K K: 6.99, V K: 7.36

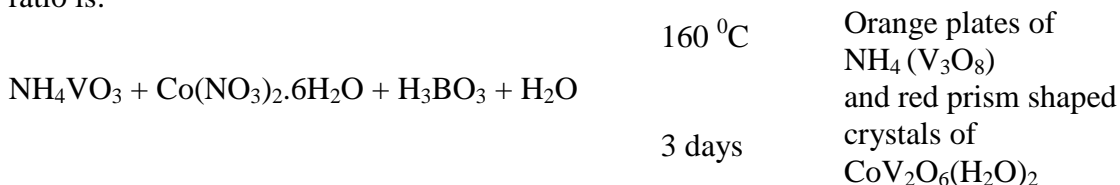
Figure 4.22 The SEM EDX results of the brown octahedral shaped crystals

## 4.5 Crystal Growth Experiments

In our laboratory, known and unknown crystals were synthesized in good size and shape by using hydrothermal method. Red prism shaped crystals (Fig.4.23) of cobalt vanadium oxide hydrate which are in the formula of  $\text{CoV}_2\text{O}_6(\text{H}_2\text{O})_2$  were prepared from the reaction of  $\text{NH}_4\text{VO}_3$  (0.1170 g, 0.001 mole),  $\text{Co}(\text{NO}_3)_2 \cdot 6\text{H}_2\text{O}$  (0.2910 g, 0.001 mole) and  $\text{H}_3\text{BO}_3$  (0.0618 g, 0.001 mole). The following reagents were used as

obtained:  $\text{NH}_4\text{VO}_3$  (Riedel, + 99.5 %),  $\text{Co}(\text{NO}_3)_2 \cdot 6\text{H}_2\text{O}$  (Carlo Erba, 99 %) and  $\text{H}_3\text{BO}_3$  (Carlo Erba, 99.5-100.5 %).

The reaction mixture was loaded into a steel autoclave. Then 9 mL of ultra pure water was added via pipette. The autoclave was sealed and heated at  $160\text{ }^\circ\text{C}$  for 3 days and then cooled to room temperature. The solid products were recovered by suction filtration, washed with water and acetone several times. The crystals were kept in mineral oil conveniently. Red prism shaped crystals of the reported materials were obtained with the orange plates in a red-orange crystalline powder. Examination of these red crystals with an Philips XL 30S FEG SEM gave results consistent with the stated compositions. The reaction in which the reactants are in the (1:1:1:500) mole ratio is:



Similar reactions were tried with a different ratio, such as 1:2:1 and also with a different temperature such as  $170\text{ }^\circ\text{C}$ . By changing one of these two parameters each time red columns which have the same formula with the red prism shaped crystals were obtained.

We obtained some orange plate shaped crystals of ammonium vanadium oxide which has the formula of  $\text{NH}_4(\text{V}_3\text{O}_8)$  besides red crystals (Fig. 4.24).

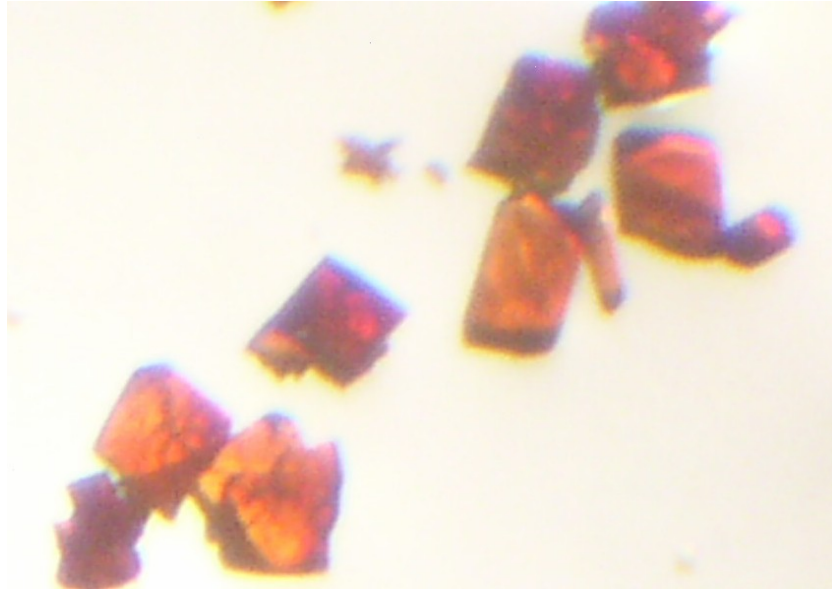


**Figure 4.23** Red prism shaped crystals

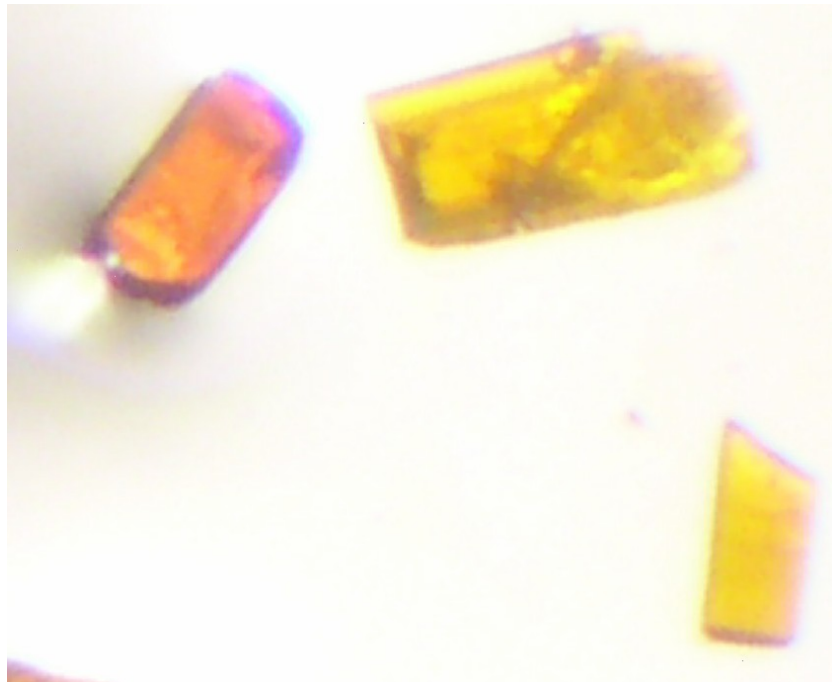


**Figure 4.24** Orange plate shaped crystals



Green square shaped crystals (Fig 4.25) of cobalt vanadyl phosphate hydrate which are in the formula of  $\text{Co}(\text{VO})_2(\text{PO}_4)_2(\text{H}_2\text{O})_4$  were obtained from the reaction of  $\text{V}_2\text{O}_5$  (0.09094 g, 0.0005 mole),  $\text{H}_2\text{C}_2\text{O}_4 \cdot 2\text{H}_2\text{O}$  (0.12607g, 0.001 mole),  $\text{CoCl}_2 \cdot 6\text{H}_2\text{O}$  (0.2739g, 0.001 mole). The following reagents were used as obtained:  $\text{V}_2\text{O}_5$  (Alfa Aesar, 99.2 %),  $\text{H}_2\text{C}_2\text{O}_4 \cdot 2\text{H}_2\text{O}$  (Carlo Erba, 99.8 %),  $\text{CoCl}_2 \cdot 6\text{H}_2\text{O}$  (Riedel, >99 %) and  $\text{H}_3\text{PO}_4$  (Kimetsan, 1.7 g/mL, 85.88 %).

A reaction mixture was loaded into a steel autoclave. Then 0.1141 mL of  $\text{H}_3\text{PO}_4$  and 9 mL ultra pure water were added via pipette. The autoclave was sealed and heated at  $160^\circ\text{C}$  for 3 days and then cooled to room temperature. The color of the resulting solution was purple. The solid products were recovered by suction filtration, washed with water and acetone several times. Dark green crystals which are strictly attached to each other were examined under microscope. Then they were kept in mineral oil conveniently. Philips XL 30S FEG SEM gave results consistent with the stated compositions. The reaction occurred as below:

The reactants are in the (1:2:2:2.92:1000) mole ratio.

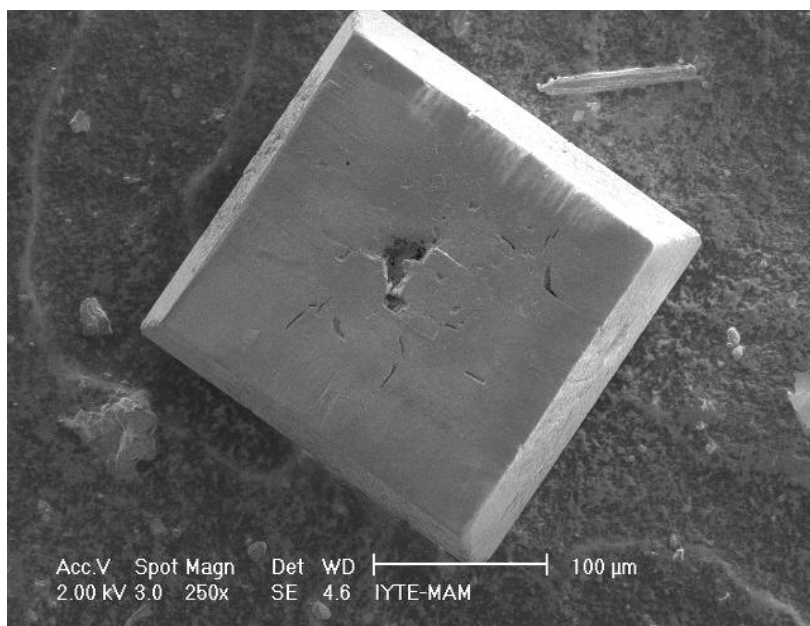
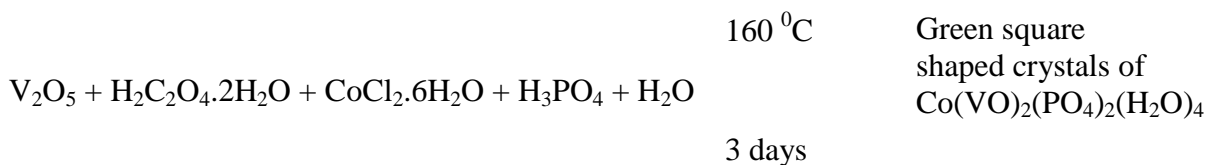


**Figure 4.25** A green square shaped crystal

## CHAPTER 5

### CONCLUSION

Our research has focused on the structure solution of the single-crystal of mixed valence polyoxovanadium  $[V_{16}O_{31}(OH)_7]Cl \cdot 15H_2O$  compound resulting from hydrothermal synthesis. To our knowledge this is the second example of cationic polyoxometalate after Zhuang's  $[(VO_4)Mo_{12}O_{36}(VO)_6][(OH)_9] \cdot 11H_2O$  [63]. The  $[V_{16}O_{31}(OH)_7]^+$  core has not yet been seen before and it has a truly unique host lattice.

The inorganic framework is composed of a vanadium oxygen cluster encapsulating a  $Cl^-$  anion. There are similar frameworks as in  $[V_{15}O_{36}Cl]^{6-}$  and  $[V_{16}O_{36}Cl]^{10-}$  as first described by Muller et al. and by Shao et al., respectively [64-65]. In addition  $[V_{15}O_{37}Cl]^{6-}$  and  $[V_{15}O_{36}Cl]^{5-}$  were synthesized by Ganne et al [36].

By using hydrothermal method we synthesized the single crystals of known compounds in appropriate (0.1-0.3 mm) sizes. Red prism shaped crystals of cobalt vanadium oxide hydrate which are in the formula of  $CoV_2O_6(H_2O)_2$  and orange plate shaped crystals of ammonium vanadium oxide which has the formula of  $NH_4(V_3O_8)$  and green square shaped crystals of cobalt vanadyl phosphate hydrate which are in the formula of  $Co(VO)_2(PO_4)_2(H_2O)_4$  were grown. The crystals of  $NH_4(V_3O_8)$  are approximately in the length of 120  $\mu m$  and in the width of 45  $\mu m$ , and the crystals of  $Co(VO)_2(PO_4)_2(H_2O)_4$  are approximately in the length of 225  $\mu m$  with the thickness of 17.18  $\mu m$ .

Vanadium oxide chemistry has several characteristic families as binary oxides, bronzes, and molecular polyanions. The chemistry of polyanions has been reviewed recently [22, 38, 39]. Apart from their interesting structural variety, polyoxovanadates show remarkable redox processes so that the species can exist with quite different electron populations [38].

We have synthesized the compound of  $[Ni(en)_3(VO_3)_2]$  in the pink hexagonal shaped single crystals by hydrothermal method. The reactants are  $NaVO_3$ ,  $Ni(NO_3)_2 \cdot 6H_2O$ ,  $H_3BO_3$  and  $NH_2CH_2CH_2NH_2$  in the (1: 1: 2: 45) mole ratios. 5 M, 9

mL of ethylenediamine was added as the solvent. The pink hexagonal shaped single crystals were obtained at 160 °C for 3 days.  $[\text{Ni}(\text{en})_3(\text{VO}_3)_2]$  compound is in the crystal system of hexagonal and in the space group  $P6_1$ . The structure is composed of  $\text{VO}_4$  tetrahedras which joined with others by sharing corners into infinite chains running along the c axis. The complex cation  $[\text{Ni}(\text{en})_3]^{2+}$  are located between the chains. The chain in the compound has a repetitive sequence of 12-nuclear corner-sharing tetrahedras.

We also synthesized other vanadium compounds whose structures are not known yet. They are yellow rod shaped crystals which were obtained from the reaction of  $\text{NaVO}_3$ ,  $\text{GeO}_2$ ,  $\text{H}_3\text{BO}_3$ ,  $\text{CoCl}_2 \cdot 6\text{H}_2\text{O}$  and  $\text{H}_2\text{O}$  as the solvent. The reactants were in the (1: 1: 1: 1: 500) mole ratio while 9 mL of water was added. The reaction was done at 160 °C for 3 days. According to the SEM / EDX results it is proved that in this compound we have boron, oxygen, germanium, vanadium and cobalt in the atomic percentages of 24.83 %, 54.45 %, and 0.54 %, 14.43 % and 5.76 % respectively.

The green octahedral shaped crystals were obtained from the reaction of reactants  $\text{NH}_4\text{VO}_3$ ,  $\text{Ni}(\text{NO}_3)_2 \cdot 6\text{H}_2\text{O}$ ,  $\text{H}_3\text{BO}_3$  and  $\text{H}_2\text{O}$  in the (1: 1: 1: 500) mole ratios while 9 mL of water was added. The reaction was done at 160 °C for 3 days. SEM / EDX results prove that in this compound we have boron, nitrogen, oxygen, vanadium and nickel in the atomic percentages 41.10 %, 9.37 %, 38.93 %, 7.81 % and 2.79 % respectively.

A bulk of attached rectangular yellowish green crystals were obtained by the reactants  $\text{NaVO}_3$ ,  $\text{Ni}(\text{NO}_3)_2 \cdot 6\text{H}_2\text{O}$ ,  $\text{H}_3\text{BO}_3$ ,  $\text{NH}_2\text{CH}_2\text{CH}_2\text{NH}_2$ ,  $\text{H}_3\text{PO}_4$  and  $\text{H}_2\text{O}$ . The reactants are in the (1: 1: 1: 20: 20: 0.96) mole ratios and 5 M, 0.2 mL en, 5 M, 0.2 mL phosphoric acid, 8.6 mL water were added as solvents. The reaction was done at 160 °C for 3 days. SEM / EDX results prove that in this compound we have oxygen, phosphorus, vanadium and cobalt elements in the atomic percentages of 82.16 %, 9.17 %, 6.16 %, 2.51 % respectively.

Brown octahedral shaped crystals were yielded from the reaction of reactants  $\text{B}_4\text{K}_2\text{O}_7 \cdot \text{H}_2\text{O}$ ,  $\text{KVO}_3$ ,  $\text{H}_2\text{O}$  and  $\text{NH}_2\text{CH}_2\text{CH}_2\text{NH}_2$  which were in the (8: 1: 0.5: 2) mole ratios. The reaction was done at 170 °C for 5 days. The SEM EDX results of the brown octahedral shaped crystals prove that in this compound we have boron, carbon, nitrogen, oxygen, potassium and vanadium elements in the atomic percentages of 8.38 %, 34.43 %, 6.14 %, 36.70 %, 6.99 % and 7.36 % respectively.

Ethylenediamine has proven to be excellent medium to synthesize novel compounds under the hydrothermal conditions.

We studied vanadium chemistry with different solvents such as water, ethylenediamine, phosphoric acid. By slightly varying the reaction conditions, we found the more suitable one to produce good quality crystals. Also learned the SEM and XRD analyzes of these synthesized compounds.

As a future work we should investigate titanium chemistry and also try to change Co and Ni with other transition metals.

## REFERENCES

- [1] Schubert, U.; Hüsing, N.; "Synthesis of Inorganic Materials"; 5; 2000; 181-184
- [2] West, A. R.; "Solid State Chemistry and Its Applications"; John Wiley and Sons, New York; 1996
- [3] Kanatzidis, M.G.; "Molten alkali-metal polychalcogenides as reagents and solvents for the synthesis of new chalcogenide materials"; Chem. Mater.; 2; 1990; 353
- [4] Jessop, P.G.; Leitner, W.; "Chemical Synthesis Using Supercritical Fluids"; Wiley-Vch; 1998
- [5] Laudise, R.A.; Ballman A.A.; Kirk-Othmer Encyclopedia of Chemical Technology 2nd Ed.; John Wiley and Sons; New York; 18; 1969; 105
- [6] Beuhler, E.; Walker, A.C.; "Growing Large Quartz Crystals"; Ind. Eng. Chem.; 42; 1950; 1369
- [7] Liao, J.-H.; Kanatzidis, M.G.; Inorg. Chem.; 31; 1992; 631
- [8] Khan, M.I. et al.; "Inorganic-organic hybrid materials; synthesis and crystal structures of the layered solids [ $\{M(H_2O)(2,2'$ -bipy) $\}V_2O_6$ ] (M = Co, Ni) "; Journal of Molecular Structure; 656; 2003; 45-53
- [9] Rabenau, A.; Angew. Chem. Int. Ed. Engl.; 26; 1985; 1026
- [10] Loy, D.A.; "Direct Formation of Aerogels by Sol-Gel Polymerizations of Alkoxysilanes in Supercritical Carbon Dioxide"; Chem. Mater.; 9; 1997; 2264
- [11] Ikornikova, N.Y.; Lobchev (ed.), E.A.; "In Hydrothermal Synthesis of Crystals"; Consultants Bureau; New York; 1971; 80
- [12] Rabenau, A.; "Crystal growth: An Introduction", Hartman, P.(Ed.); North-Holland Press, Amsterdam; 1973; 198
- [13] Pope, M.T.; Müller, A.M.; "Polyoxometalate chemistry From Topology via Self-Assembly to Applications"; Dordrecht / Boston / London; 2001
- [14] Hoffmann, M.R.; Martin, S.T.; Choi, W.; Bahnemann, D.; "Environmental Applications of Semiconductor Photocatalysis", Chem. Rev.; 95; 1995; 69
- [15] Dunitz, J.D.; Acta. Cryst; 17; 1964; 1299
- [16] Stout, G.H.; Jensen, L.H.; "X-ray Structure Determination"; John Wiley and Sons; 1989; USA

- [17] Byrappa, K.; Yoshimura M.; "Handbook of Hydrothermal Technology"; Noyes Publications; New Jersey; 2000
- [18] West, A.R.; "Solid State Chemistry and its Applications"; John Wiley and Sons; 1984
- [19] Tanaka J.; Suib S. L.; "Experimental Methods in Inorganic Chemistry"; Practice Hall; Upper Saddle River; New Jersey 07458; 1999
- [20] Müller, A.; Peters, F.; Pope, M.T.; Gatteschi, D.; "Polyoxometalates: Very Large Clusters-Nanoscale Magnets"; Chem. Rev.; 98; 1998; 239
- [21] Katsoulis, D.E.; "A Survey of Applications of Polyoxometalates"; Chem. Rev.; 98 (1); 1998; 359-388
- [22] Pope, M.T.; Müller, A.; "Polyoxometalate Chemistry: An Old Field with New Dimensions in Several Disciplines"; Angew. Chem. Int.Ed. Engl; 30; 1991; 34
- [23] Klemperer, W.G.; Marquart, T.A.; Yaghi, O.M.; "New Directions in Polyvanadate Chemistry: From Cages and Clusters to Baskets, Belts, Bowls, and Barrels"; Angew.Chem.Int.Ed.Engl.31; 1992; 49-51
- [24] Khan, M.I.; "Novel Extended Solids Composed of Transition Metal Oxide Clusters"; J. Solid State Chem.; 152; 2000; 105-112
- [25] Pope, M.T.; "Heteropoly and Isopoly Oxometalates"; Springer; Berlin; 1983
- [26] Hawthorne, F.C.; Calvo, C.; "The crystal chemistry of the  $M^+VO_3$  ( $M^+ = Li, Na, K, NH_4, Tl, Rb, \text{ and } Cs$ ) pyroxenes"; J. Solid State Chem.; 22; 1977; 157-170
- [27] Baudrin, E.; Touboul, M.; Nowogrocki, G.; "Synthesis and Crystal Structure of  $Ni(VO_3)_2 \cdot 4H_2O$  and  $\square Ni(VO_3)_2 \cdot 2H_2O$ "; J. Solid State Chem.; 152; 2002; 511
- [28] Chen, Q.; Zubieta, J.; "Coordination Chemistry of Soluble Metal Oxides of Molybdenum and Vanadium"; Coord. Chem. Rev.; 114; 1992; 107-167
- [29] Coronado, E.; Gomez-Garcia, C.J.; "Polyoxometalate-Based Molecular Materials"; Chem. Rev.; 98; 1998; 273-296
- [30] Desiraju, G.R.; "Supramolecular Synthons in Crystal Engineering - A New Organic Synthesis"; Angew.Chem.Int. Ed. Engl.; 34; 1995; 2311-2328
- [31] Mizuno, N.; Misono, M.; "Heterogeneous Catalysis"; Chem. Rev.; 98 (1); 1998; 199-218
- [32] Coronado, E.; Gomez-Garcia, C.J.; Comments Inorg. Chem.; 17; 1995; 255

- [33] Bruker SMART Version 5.054 Data Collection and SAINT-Plus Version 6.2.2 Data Processing Software for the SMART system, Bruker Analytical X-Ray Instruments; Inc.; Madison; WI; USA; 2000
- [34] Sheldrick G.M., SHELXTL Dos / Windows / NT Version 6.12, Bruker Analytical X-Ray instruments; Inc.; Madison; WI; USA; 2000.
- [35] Muller, A.; Penk, P.; Rohlfing, R.; Krickemeyer, E.; Doring; "Topologically Interesting Cages for Negative Ions with Extremely High "Coordination Number": An Unusual Property of V-O Clusters"; J. Angew. Chem. Int. Ed. Engl.; 29; 1990; 926-927
- [36] Drezen, T.; Ganne, M.; "A New Vanadium Oxide Bronze:  $[\text{NH}_3(\text{CH}_2)_6\text{NH}_3]_{10}[\text{V}_{15}\text{O}_{37}(\text{Cl})]_2[\text{V}_{15}\text{O}_{36}(\text{Cl})](\text{OH})_3(\text{H}_2\text{O})_3$  with Clusters  $[\text{V}_{15}\text{O}_{36}(\text{Cl})]^{5-}$  and  $[\text{V}_{15}\text{O}_{37}(\text{Cl})]^{6-}$  Textured by Diaminohexane"; J. Solid State Chem.; 147; 1999; 552-560
- [37] Brown, I.D.; Altermatt, D. Acta. Cryst.; B41; 1985; 244-247
- [38] Hangrman, P.J.; Finn, R. C.; Zubieta, J.; "Molecular manipulation of solid state structure: influences of organic components on vanadium oxide architectures"; Solid State Sciences; 3; 2001; 745-774
- [39] Muller, A.; Reuter, H.; Dillinger, S.; "Supramolecular Inorganic Chemistry: Small Guests in Small and Large Hosts", Angew. Chem. Int. Ed.Engl.; 34; 1995; 2328
- [40] Day, V.W.; Fredrich, M.F.; Klemperer, W.G.; Shum, W.; "Synthesis and characterization of the dimolybdate ion,  $\text{Mo}_2\text{O}_7^{2-}$ "; J. Am. Chem. Soc.; 99; 1977; 6146
- [41] Fuchs, J.; Mahjour, S.; Pickard; "Structure of the "True" Metavanadate Ion"; J. Angew. Chem., Int. Ed. Engl.; 15; 1976; 374
- [42] Evans, Jr.H.T.; "The Molecular Structure of the Isopoly Complex Ion, Decavanadate ( $\text{V}_{10}\text{O}_{28}^{6-}$ )"; Inorg. Chem. 5; 1966; 967
- [43] Oka, Y.; Yao, T.; Yamamoto, N.; "Powder X-ray crystal structure of  $\text{VO}_2(\text{A})$ "; J. Solid State Chem.; 86; 1990; 116
- [44] Li, M.; Wong, K.K.W.; Mann, S.; "Organization of Inorganic Nanoparticles Using Biotin-Streptavidin Connectors"; Chem. Mater.; 11; 1999; 23
- [45] Zaremba, C.M.; Belcher, A.M.; Fritz, M.; Le, Y.; Mann, S.; Hansma, P.K.; Morse, D.E.; Speck, J.S.; Stucky, G.D.; "Critical Transitions in the Biofabrication of Abalone Shells and Flat Pearls"; Chem. Mater.; 8; 1996; 679

- [46] Vejiux, A.; Courtini, P.; "TEM study of interfacial relationships in the  $V_2O_5$ - $TiO_2$  (anatase) system"; *J. Solid State Chem.*; 63; 1986; 179
- [47] Ueda, Y.; "Vanadate Family as Spin-Gap Systems"; *Chem. Mater.*; 10; 1998; 2653
- [48] Davis, M.E.; Katz, A.; Ahmad, W.R.; "Rational Catalyst Design via Imprinted Nanostructured Materials"; *Chem. Mater.*; 8; 1996; 1820
- [49] Gopalakrishnan, J.; "Chimie Douce Approaches to the Synthesis of Metastable Oxide Materials"; *Chem. Mater.*; 7; 1995; 1265
- [50] Huan, G.; Johnson, J.W.; Jacobson, A.J.; Merola, J.S.; "Hydrothermal synthesis and single-crystal structural characterization of  $VO(VO_3)_6(VO(C_{10}H_8N_2)_2)_2$ "; *J. Solid State Chem.*; 91; 1991; 385
- [51] Kolb, E.D.; Caporaso, A. J.; Laudise, R. A.; "Hydrothermal growth of hematite and magnetite"; *J. Crystal Growth*; 19; 1973; 242
- [52] Hibst, H.; "Hexagonal Ferrites from Melts and Aqueous Solutions, Magnetic Recording Materials"; *Angew. Chem. Int. Ed. Engl.*; 21; 1982; 270
- [53] Okamoto, S.; Sekizawa, H.; Okamoto, S. I.; "Hydrothermal synthesis, structure and magnetic properties of barium diferrite"; *J. Phys. Chem. Solids*; 36; 1975; 591
- [54] Okamoto, S.; Okamoto, S. I.; Ito, T.; "The crystal structure of a new hexagonal phase of  $AgFeO_2$ "; *Acta. Cryst. B28*; 1774; 1972
- [55] Hirano, S.; Ismail, M. G. M. U.; Somiya, S.; "Crystal growth of sodium iron titanium bronze compounds under hydrothermal conditions"; *Mat. Res. Bull.*; 11; 1976; 1023
- [56] Endo, T.; Kume, S.; Shimada, M.; Koizumi, M.; *Miner. Mag.*; 39; 1974; 559
- [57] Kolb, E.D.; Laudise, R.A.; "Phase equilibria of  $Y_3Al_5O_{12}$ , hydrothermal growth of  $Gd_3Ga_5O_{12}$  and hydrothermal epitaxy of magnetic garnets"; *J. Crystal Growth*; 29; 1975; 29
- [58] Laudise, R.A.; "Single crystals for bubble domain memories"; *J. Crystal Growth*; 13/14; 1972; 27
- [59] Lencka, M.M.; Riman, R.E.; "Thermodynamics of the Hydrothermal Synthesis of Calcium Titanate with Reference to Other Alkaline-Earth Titanates"; *Chem. Mater.*; 7; 1995; 18
- [60] Laudise, R.A.; Ballman, A.A.; "Hydrothermal Synthesis of Sapphire"; *J. Am. Chem. Soc.*; 80; 1958; 2655



- [61] TEXSAN: Single Crystal Structure Analyses software, Version 1.6 b, 1993. Molecular Structure Corporation, the Woodlands, TX 77381
- [62] SHELXTL-PLUS: Sheldrick, G.M. Siemens Analytical X-Ray Instruments, Inc., Madison, WI 53719
- [63] Yang, W; Lu, C.; Zhan, X.; Zhuang, H.; “Hydrothermal Synthesis of the First Vanadomolybdenum Polyoxocation with a ‘Metal-Bonded’ Spherical Framework”; *Inorg. Chem.*; 41; 2002; 4621-4623
- [64] Müller, A.; Sessoli, R.; Krickemeyer, E.; Bögge, H.; Meyer, J.; Gatteschi, D.; Pardi, Luca; Westphal, J.; Hovemeier, K.; Rohlfing, R.; Döring, J.; Hellweg, F.; Beugholt, C.; Schmidtman, M.; “Polyoxovanadates: High-Nuclearity Spin Clusters with Interesting Host-Guest Systems and Different Electron Populations. Synthesis, Spin Organization, Magnetochemistry, and Spectroscopic Studies.”; *Inorganic Chemistry*; 36; 1997; 23
- [65] Shao, M.; Leng, J.; Pan, Z.; Zeng, H.; Tang, Y.; *Gaogeng Xuexiao Huaxue Xuebao KTHPD.*; 11; 1990; 280